CHARACTERIZATION OF THE SUMO PATHWAY IN REGULATING MITOTIC PROGRESSION

By Christine Lee

A dissertation submitted to Johns Hopkins University in conformity with the requirements for the degree of Doctor of Philosophy

Baltimore, Maryland
December 2017

ABSTRACT

Progression through the mitotic stage of the cell cycle is regulated by several checkpoint mechanisms to ensure equal chromosomal segregation. Abnormalities during mitosis can result in the gain or loss of chromosomes, a condition known as aneuploidy. The ability to proliferate despite abnormal chromosomal copy number is a key hallmark of human cancers, and how cancer cells override cellular checkpoints is a key area of interest. Post-translational protein modifications such as phosphorylation drive mitotic entry and progression, while the ubiquitin-mediated targeting of proteins facilitates exit from mitosis. Here we present the functional requirement of another post-translational modification known as the Small Ubiquitin-related Modifier (SUMO). While the history of SUMO discovery is tied to functions in regulating mitotic progression, here we present a novel role for SUMO modification in regulating the activity of an E3 ubiquitin ligase known as the Anaphase Promoting Complex/Cyclosome during the metaphase-anaphase transition. Further characterization on the SUMO isopeptidase SENP1 during different stages of the cell cycle is also presented herein. Taken together, this thesis provides additional insights to the regulatory roles of how a small protein can have profound effects on cellular function.

Thesis Advisor:

Dr. Michael J. Matunis

Thesis Readers:

Dr. Daniela Drummond-Barbosa

Dr. Andrew Holland

Dr. Andrew Pekosz

Alternate Thesis Readers:

Dr. Steven An

Dr. Valeria Culotta

ACKNOWLEDGEMENTS

Graduate school can be compared to marathon training in many ways. In the beginning, the steep gradients ahead seem insurmountable (like the backroads of Druid Hill Park, imposing vertical challenges) or your body negatively reacting to the heat or cold (there is nothing like the dread of finding your protein precipitated out after a careful purification scheme—the chill of the cold room adding a sharp pang to your already shivering heart). But through persistence and patience, sparks of wonder are revealed: the connection of a new roadway to a familiar, well-beaten path, or the covalent modification of a substrate by a small, but powerful protein.

Luckily, Mike Matunis is a coach with multitudes of insights. Thank you, Mike, for your unrelenting support and guidance during my graduate studies. I am pretty sure you've never said "no" to any of my ideas, whether whimsical or just wrong. With patience and careful instruction, you've taught me to consider all of the caveats and proper controls so that every experiment, even with "negative" data, reveals important scientific truths. I have enjoyed the fullest training available to graduate students, with multiple opportunities to learn new techniques in other labs, to travel and present at meetings, and to communicate science through several outlets and to various

audiences. Truly, I feel that no indulgence was spared, and cannot imagine a more supportive or nurtured environment in which to develop as a scientist.

Several adages of wisdom will henceforth guide my approaches in science and in life, ones that all Matunis Lab alum have canonized: *The control for the experiment you performed last week cannot be the control for the one you perform today*; *if you don't have time to fully do the right experiment today, when will you have time to repeat it?* and the excited battle cry *to go for the jugular!* Perfecting the Matunis Code of Aesthetics (Ariel bold font, centered straight lines, and "beautiful" immunoblotting) has appealed to my neuroses. In the pursuit of these standards, I have experienced the private delight inside the film developing room, underneath the dim red glow of an unexpected result, and learned the value of clarity in presenting both oral and written work. *Thank you, for* all *of the opportunities*.

I would also like to thank the core members of my Thesis Advisory Committee, Dr. Andrew Holland, Dr. Phil Jordan, and Dr. Daniela Drummond-Barbosa. We had the great fortune in initiating a project concerning the mitotic stage of the cell cycle coincidentally with the arrival of two energetic experts in their respective fields, Andrew and Phil. Your perspectives and recommendations, and share of reagents and tools, have

driven the depth and rigor of our studies from the very beginning. I am also grateful to Daniela for careful reading of this thesis, for always centering my focus to a strong biological context, and her thoughtful and careful guidance both professional and personally. Furthermore, I want to acknowledge and thank members of the Hopkins Ubiquitin Club and the PJAMMa meetings for teaching me scientific findings that are fascinating, exciting, and fun.

I also want to thank the members of the Matunis Lab – near and far, former and current. Thank you all for your patience in instruction of techniques and also for your warmth in friendship. To my classmates and the BMB department as a whole – thank you all for your words of encouragement, advice, and generosity. To the administrate and house staff, including Sharon Warner, Shannon Gaston, Mystee Edmonds, Kear Wright, Erika Vaitekunas, Jackie and Karen – thank you for all of your work behind-the-scenes so that each day runs smoothly and cleanly. I have enjoyed the great privilege of having a truly collaborative department where colleagues are more like extended family. One of these days I will remember to make my own stock of Kanamycin-selection agar plates.

Finally, I want to thank my parents and family for their commitment in supporting my education at every level. None of my achievements would

have been possible without your countless and continual sacrifices. And to Bing – I'm sorry for all that I've said when I was hungry.

> *See enough and write it down, and then some morning when the world seems drained of wonder, there it will all be, a forgotten account with accumulated interest, paid passage back to the world out there.*
> - Joan Didion, *On Keeping a Notebook*, 1966

TABLE OF CONTENTS

LIST OF TABLES

LIST OF FIGURES

ABBREVIATIONS

6xHis	polyhistidine-tag
APC/C	Anaphase Promoting Complex/Cyclosome
ATP	Adenosine triphosphate
BCA	bicinchoninic assay
BioID	proximity-dependent biotin identification
BSA	bovine serum albumin
C. elegans	*Caenorhabditis elegans*
CDK	cyclin-dependent kinase
CO2	carbon dioxide
CPC	chromosome passenger complex
CREST	antibody from Calcinosis, Raynaud phenomenon, esophageal dysmotility, sclerodactyly, and telangiectasia syndrome patients
Cryo-EM	cryo-electron microscopy
D. mealogaster	*Drosophila melanogaster*
DAPI	4',6-diamidino-2-phenylindole
DeSI	desumoylating isopeptidase
DNA	deoxyribonucleic acid
Dox	doxycylcine

DUB	de-ubiquitinating enzymes
E. coli	*Escherichia coli*
E1	ubiquitin or SUMO activating enzyme
E2	ubiquitin or SUMO conjugating enzyme
E3	ubiquitin or SUMO ligating enzyme
EDTA	ethylenediaminetetraacetic acid
FEB	FKBP-rapamycin -associated protein
FKBP	FK5066 binding protein
GAPDH	glyceraldehyde 3-phosphate dehydrogenase
GFP	green florescent protein
GST	glutathione S-transferase
HCl	hydrogen chloride
HEPES	4-(2-hydroxyethyl)piperazine-1-ethanesulfonic acid
kDa	kiloDalton
M	molar
MBP	maltose binding protein
MCC	mitotic checkpoint complex
mCherry	mCherry fluorescence protein
mL	milliliter
mRNA	messenger RNA

NaN3	sodium azide
NEBD	nuclear envelope breakdown
NEDD8	neural precursor cell expressed, developmentally down-regulated 8
NEM	N-ethylmaleimide
NES	nuclear export signal
NLS	nuclear localization signal
NP-40	nonyl phenoxypolyethoxylethanol
NPC	nuclear pore complex
P. falciparum	*Plasmodium falciparum*
PBS	phosphate-buffered saline
PDSM	phosphorylation dependent SUMO motif
PIAS	protein inhibitor of activated STAT
PML	promyelocytic leukemia
PMSF	phenylmethanesulfonylfluoride
PTM	post-translational modification
PVDF	polyvinylidene fluoride
RING	really interesting new gene
RNA	ribonucleic acid
RNAi	RNA interference

RT	room temperature
S. cerevisiae	*Saccharomyces cerevisiae*
S. pombe	*Saccharomyces pombe*
SAC	spindle assembly checkpoint
SDS-PAGE	sodium dodecyl sulfate-polyacrylamide gel electrophoresis
SENP	sentrin-specific protease
SIM	SUMO interaction motif
siRNA	short, interfering RNA
Ska	spindle and kinetochore associated
SP-RING	Six/PIAS-RING
Strep	streptavidin
STUbL	SUMO-targeted ubiquitin ligase
SUMO	Small Ubiquitin-related Modifier
TDG	thymidine DNA glycosylase
TNX-100	triton-X 100
TopoIIα	Topoisomerase IIα
Tris	tris-(hydroxymethyl)-aminomethane
TS-T	tris-buffered saline-tween
Ulp1	UBL-specific protease 1

USPL1	ubiquitin-specific protease-like protein 1
WHB	winged helix binding
μL	microliter
μg	microgram
μm	micrometer

CHAPTER 1:
INTRODUCTION

The SUMO Protein and Pathway

The Small Ubiquitin-related Modifier, or SUMO, is a ~12 kDa protein that is post-translationally added to substrates. Components of the SUMO pathway are well conserved from yeast to humans, with essential roles in a variety of cellular processes including transcription, chromatin remodeling, ribosome biogenesis, and DNA damage repair[1]. While thousands of SUMO substrates have been identified through proteomic studies, the steady state level of a SUMO modified protein is relatively low due to the dynamic activity of conjugating and deconjugating enzymes. Nonetheless, SUMO modification can abrogate or cooperate with other post-translation modifications such as acetylation and ubiquitylation to affect downstream cellular processes. Functionally, sumoylation can direct localization of substrates or generate novel non-covalent interactions with proteins containing SUMO Interacting Motifs (SIMs)[2]. This thesis will discuss one of the conserved roles for SUMO modification in regulating cell cycle regulation, as perturbations to components of the SUMO pathway in all eukaryotes cause aberrations in mitosis.

Analogous to other members of the ubiquitin-like family of proteins, SUMO is translated as an immature precursor, and must be processed by

isopeptidases to expose a C-terminal di-glycine used for conjugation to the ε-amine of the substrate lysine[3,4]. In yeast[3,5,6], *C. elegans*[7], *D. melanogaster*[8], and even *P. falciparum*[9], a single SUMO gene is expressed, while vertebrates express three functional SUMO isoforms, SUMO1, SUMO2 and SUMO3[4]. SUMO1 is ~45% identical to SUMO2 and SUMO3, while SUMO2 and SUMO3 share ~96% sequence homology and are collectively referred to as SUMO2/3 (Figure 1-1). SUMO proteins can also be post-translationally modified by phosphorylation, ubiquitylation, and acetetylation, thus generating diverse signals[10] (Figure 1-1). Furthermore, SUMO2/3 contain a SUMO consensus site motif enabling the formation of polymeric SUMO chains (Figure 1-1) with potentially unique signaling properties.

SUMO modification occurs through an ATP-dependent enzymatic cascade involving the sequential activity of an E1 activating (expressed as the heterodimer Aos1/Uba2 in humans), an E2 conjugating (Ubc9), and several E3 ligating enzymes (Figure 1-2, Table 1-1). Compared to the ubiquitin system, SUMO conjugating machinery is relatively limited. While the ubiquitin system has ~40 E2 conjugating enzymes and over 600 identified E3 ligases which function to specify substrate selectivity, the catalog of enzymes in the SUMO system is comparatively small[11]. SUMO

modification is nonetheless an essential process and produces profound effects on protein function.

A majority of SUMO substrates are modified at lysine residues within the consensus site ψ-K-x-E/D motif, whereby ψ represents a hydrophobic residue, K is the substrate lysine, x is any amino acid, followed by an acidic residue, either glutamic or aspartic acid[4,12]. An additional SUMO consensus site motif incorporating post-translational modification by kinase activity is defined as a phosphorylation-dependent SUMO motif (PDSM), with an amino acid sequence ψ-K-x-E/D-x-x-S-P[13].

SUMO in Eukaryotes

The single SUMO gene in *S. cerevisiae* was first identified in a genetic screen for mutants that suppress MIF2 (Mitotic fidelity of chromosome transmission), which is an ortholog of the human centromere protein CENP-C[4]. *MIF2* results in mitotic delays and defects in chromosome segregation and microtubule morphology, while the temperature-sensitive *mif2-3* strain stabilized mitotic and structural stability[5]. Several groups simultaneously cloned the mouse and human homologs of *SMT3* with variable nomenclature[12]. UBL1 (ubiquitin-like protein 1) and Sentrin were identified through two-hybrid screens for interactors of Rad51 and Rad52

and “death domains” in Fas/APO-1 and TNF receptor 1 as baits[14,15], while PIC1 (PML interacting protein 1) was shown to co-localize in PD10 nuclear bodies[16]. The GTPase-activating protein RanGAP1 was the first bona fide substrate shown to be modified by a novel ubiquitin-related modifier, named GMP1 (GAP-modifying protein 1)[17] and SUMO1 (small ubiquitin-related modifier)[18]. Sumoylation of RanGAP1 directs targeting to the nuclear pore complex (NPC) and localization to the cytoplasmic face of the NPC facilitates nucleocytoplasmic transport[17,18]. While the single SUMO gene in lower eukaryotes is essential, genetic knockouts of the three different SUMO paralogs in mice suggest some degree of functional redundancy. SUMO1 knockout mice are viable but not without defects, suggesting that SUMO2/3 in part can compensate for SUMO1[19–22]. Furthermore, SUMO2 knockout mice are embryonic lethal while SUMO3 knockout mice are viable—further suggesting the compensatory capabilities and underscoring the functional importance of SUMO2[23]. Paralog selectivity in response to different cellular stresses have also been implicated, as high molecular weight SUMO2/3 conjugates are stimulated under conditions of heat shock or oxidative stress while SUMO1 levels remain relatively unchanged[24]. While drugs that selectively inhibit the formation of the E1-SUMO intermediate have been in development[25,26], compounds directed towards the conjugation of distinct

SUMO paralogs will provide insights into the functional redundancy and cellular requirements of SUMO1, 2, and 3.

SUMO Isopeptidases

Regulation of SUMO modification at the level of deconjugation is a critical axis of the SUMO pathway. SUMO isopeptidases cleave at the C-terminal glycine of SUMO and the substrate lysine. Several classes of SUMO isopeptidases have been identified, beginning with the discovery of Ulp1 (UBL-specific protease 1) in *S. cerevisiae*[27]. Like deubiquitinating enzymes, SUMO isopeptidases are cysteine proteases but are unrelated in sequence. Interestingly, Ulp1 was found to have sequence homology and catalytic mechanisms similar to viral proteases[27]. The second family member was discovered shortly thereafter, and Ulp2 was characterized in *S. cerevisiae* as having important but non-essential roles in maintaining chromosomal stability and cell morphology[28]. Functionally, Ulp1 is an essential gene required for normal mitotic progression, as temperature-sensitive mutants arrest during the G2/M stage of the cell cycle[27]. The amino terminus of Ulp1 is non-essential for catalysis, but directs localization that is functionally important for activity[29]. Similarly, the SUMO isopeptidases in humans, first identified as SENPs (sentrin-specific isopeptidase)[30], contain conserved C-terminal catalytic domains and divergent N-terminal sequences

that are important for directing sub-cellular localization and activity[31]. The identification and characterization of the SENP family members demonstrate distinct roles for desumoylation. SENP1 and SENP2 regulate mitotic regulation[32,33], SENP3 regulates transcriptional activity, SENP3 and SENP5 coordinate ribosome biogenesis, while SENP6 and SENP7 have functions in editing polymeric SUMO chains[34]. Genetic knockouts of different SENP paralogs demonstrate the essential requirement of SUMO isopeptidase activity. Both SENP1 and SENP2 knockout mice are embryonic lethal at mid-gestation due to aberrations in cardiac development and function[35,36]. Additional classes of SUMO isopeptidases have also been identified[37,38], and future classification on how these enzymes affect the catalog of thousands of SUMO substrates is of particular interest. Whether SENPs have SUMO paralog specificity *in vivo* or if substrate recognition is mediated by another mechanism is also a question that remains unanswered.

SUMO Interacting Motifs (SIMs)

SUMO modification can generate novel protein-protein interactions between a sumoylated substrate and another protein containing a SUMO Interacting Motif (SIM)[2]. A consensus sequence for SIM binding is defined as a stretch of hydrophobic amino acids (V/I)-x-(V/I)-(V/I) flanked by an

acidic residue. The hydrophobic amino acids in SIMs interact non-covalently with a hydrophobic pocket situated in the β_2 strand on the surface of SUMO, creating a parallel or antiparallel β-strand conformation[39,40] (Figure 1-3). SIM motifs can facilitate efficient SUMO conjugation, as in the case of SIM motifs present in select SUMO E3 ligases[41,42]. SUMO-SIM interactions can also reorient structural conformations, as demonstrated in *in vitro* studies of thymidine DNA glycosylase (TDG)[43]. Additionally, SUMO-SIM interactions can additively assemble protein complexes, as in the case of the PML (promyelocytic leukemia) protein, whereby SUMO-modified PML interacts with SIMs in other PML proteins to form PML nuclear bodies[44,45]. SIMs can also facilitate the recruitment of SUMO Targeted Ubiquitin Ligases (STUbLs)[46,47] and mediate substrate targeting to the proteasome. In one example, SUMO is recognized by SIMs in Rap80 (Figure 1-3), which also contains ubiquitin interacting motifs (UIMs). A SUMO-ubiquitin hybrid chain is assembled through the activity of RNF4, an E3 ubiquitin ligase that facilitates proteasomal degradation[48]. In addition, a variation on the SIM motif includes a phosphorylation site in close proximity to the hydrophobic residues[40], which functions to specify interactions with substrates and enhance SIM recognition. Furthermore, a "code of specificity" for SIM binding partners to SUMO1 and SUMO2/3

provides a level of paralog selection due to differences in amino acid composition in the β_2 strand where SIM binding occurs[40]. Taken together, the functional consequences of SUMO-SIM interactions are a feature of the SUMO system that facilitates functional diversity in regulating cellular processes.

SUMO and Mitotic Regulation

This thesis will cover how components of the SUMO pathway coordinate mitotic progression. While there are many excellent reviews on several components of mitotic regulation[49–54], a brief historical overview and current models will be described herein.

Cell Cycle Progression is Coordinated by CDK/Cyclins and the Ubiquitin-Proteasome System

The discovery of cyclin launched a series of compelling questions that have shaped our current understanding of how eukaryotic cells grow and divide. Cyclins were first observed in sea urchin eggs and named based on the observation that protein levels rise and fall in a pattern concomitant with cell divisions[55]. Thus, the search for regulatory controls of an intrinsic cell "autonomous oscillator"[56] led to the discovery of cell cycle checkpoints[57], coordinated by what is now known to be the activity of Cyclin-Dependent

Kinases (CDKs)[58]. A complete characterization of the Cyclin-CDK partners has been described[59] (Figure 1-4), and discovery of cyclins as the regulatory factors driving cell cycle progression, especially in the context of mitotic exit, has been shown. In a landmark experiment, *in vitro* transcribed cyclin B1 mRNA added to egg extracts depleted of endogenous mRNA was sufficient to drive mitosis[60].

In roughly the same timeframe, the study of proteolysis also broadened in scope to what we now understand to be an essential and equally complex system. The discovery of the lysosome as a "proteolytic apparatus" could only explain in part how proteins are degraded. Hydrolysis of peptide bonds is an ATP-dependent process and an energy requirement for protein degradation in prokaryotes lacking lysosomes obviated a singular pathway of proteolysis[61]. This outstanding discrepancy, together with the observation that lysosomal degradation is not a substrate-specific or temporally controlled process, prompted the search for an ATP-dependent system for protein degradation. This search lead to the discovery of ubiquitin[62,63]. Enzymes in the ubiquitin pathway, including E1, E2, E3, and de-ubiquitinating (DUBs) enzymes, and the functional connection to proteasomal degradation have since been characterized[64–66] (Figure 1-5). The discovery of ubiquitin-mediated cyclin degradation[67] linked these two

cellular processes together, and the identification of the E3 ubiquitin ligase known as the Anaphase Promoting Complex/Cyclosome[68] laid the groundwork for the continued investigation of mitotic regulation, including the studies in this thesis.

The Spindle Assembly Checkpoint and Anaphase Promoting Complex/Cyclosome

Phosphorylation events by Cdk1 regulate mitotic progression. Cdk1-mediated phosphorylation of the nuclear lamina and components of the nuclear pore complex initiate prophase, benchmarked by nuclear envelope breakdown (NEBD) and depolymerization of the lamins[69]. Of note, the Nup358-RanGAP1-Ubc9 complex and the Nup107-160 complex both re-localize from the nuclear pore complexes during interphase to the mitotic spindle and kinetochores during mitosis[70,71]. During mitosis, Nup358 functions as a SUMO E3 ligase, and regulates the SUMO modification of Topoisomerase IIα[72] at kinetochores. As chromosomes decondense, centromereic regions in the DNA, specified by regions containing the histone variant CENP-A, become recruitment centers for the Chromosome Passenger Complex (CPC)[73]. Structural proteins like Ndc80 and signaling kinases like Aurora B contribute to kinetochore formation and mediate

amphitelic microtubule attachment. Kinetochores that have not yet come under proper attachment with the mitotic spindle generate the Spindle Assembly Checkpoint (SAC)[51,53] (Figure 1-6). One of the first steps in SAC signaling is the recruitment of Mad1 to kinetochores. Recruitment and conversion to the "closed" conformation of Mad2 facilitates Cdc20 capture, and the Mad2-Cdc20 complex can diffuse from the kinetochore to bind with BubR1 and Bub3 to complete the formation of the Mitotic Checkpoint Complex (MCC)[74]. The MCC binds to and inhibits the activity of the Anaphase Promoting Complex/Cyclosome (APC/C) (Figure 1-6). SAC mediated inhibition of APC/C activity is not a binary "toggle switch" but a "rheostat" in which timing of mitotic exit is regulated by multiple inputs so that chromosomes segregate equally and genome integrity is maintained[75].

Generally, when sister chromosomes have appropriately aligned along the metaphase plate and kinetochores have come under proper bi-orientation and tension with the mitotic spindle, dynein motor proteins "strip" the checkpoint signal from kinetochores, effectively "silencing" the checkpoint[76–78] (Figure 1-6). Interestingly, landmark laser ablation studies whereby a single microtubule was detached from a kinetochore proved to be sufficient to relaunch robust checkpoint signaling and inhibit anaphase onset[79]. Precisely how the SAC signal can be rapidly and robustly generated

is yet a mystery. Subsequent activation of the APC/C towards Cyclin B1 and securin are the final steps leading to mitotic exit (Figure 1-6). The APC/C is a RING (Really Interesting New Gene) family E3 ubiquitin ligase and is a multi-subunit molecular machine that facilitates the ubiquitylation of several mitotic substrates[50]. Ubiquitylation and subsequent degradation of Cyclin B1 inactivates the mitotic Cdk1 kinase, while securin degradation results in the activation of separase, an enzyme that cleaves the cohesin ring holding sister chromosomes together[54]. The premature degradation of Cyclin B1 and securin may result in precocious mitotic exit. Thus, the APC/C must be carefully regulated to prevent premature sister chromosome segregation.

As a RING E3, the APC/C catalyzes the direct transfer of ubiquitin from the E2~Ub thiolester intermediate to generate a stable isopeptide linkage between the substrate lysine and the C-terminus of ubiquitin[80] (Figure 1-4). To date, two ubiquitin E2 enzymes have been characterized, including UbcH10, which binds to the cullin-like WHB (winged helix binding) and RING domains on the catalytic module of the APC/C, comprised of the APC2 and APC11 subunits, respectively[81,82]. Ube2S was identified as a chain elongating enzyme[83] of the APC/C, and has since been shown to generate branched ubiquitin chains for efficient targeting to the proteasome following E3-mediated transfer[84–87]. Appropriate localization of

the APC/C at kinetochores has also been an important regulatory role for efficient APC/C activity and mitotic exit[88–91]. Whether UbcH10 and Ube2S localization at kinetochores is an important determinant of ubiquitin transfer is unknown.

Analysis of MCC-bound APC/C[92,93] compared to substrate-bound structures demonstrates that the APC/C has conformational flexibility, especially in the APC2/11 catalytic module. Whether MCC release contributes to this structural change or if the APC/C is post-translationally modified to adopt a more stable conformation, as in the case of the ubiquitin-like modification of NEDD8 on the RING E3 ligase Rbx1[94], is yet unknown. Furthermore, the mechanism of release of the inhibitory MCC from the APC/C is still an outstanding question, while the requirement of APC15 subunit and the activity of AAA-ATPases have been implicated in this process[95,96].

Phosphorylation of the APC/C complex has been known to be an important regulatory factor[97], and the recruitment of coactivators, including Cdc20 and Cdh1, to the complex has also been known to be critical for activity[98]. Recent structural studies from three independent groups have detailed a molecular mechanism for how coactivator recruitment is regulated by mitotic phosphorylation. Phosphorylation of the APC1 subunit by Cdk1

relieves an autoinhibitory loop, allowing subsequent binding of the coactivator Cdc20 through its C-terminal IR (isoleucine, asparagine) tail domain and results in APC/C activity towards select substrates[99–101]. An additional coactivator, Cdh1 associates with the APC/C and is also known to selectively ubiquitylate late mitotic substrates[102,103]. However, how the switch from Cdc20 to Cdh1 occurs is yet an outstanding question. Finally, the recruitment of substrates to the APC/C is an area of particular interest, as selection is mediated by short linear sequence motifs, or degron motifs[104]. Notable degrons recognized by the APC/C are KEN boxes, D boxes, the ABBA motif, and a CRY motif[104]. Whether the degrons themselves contribute towards ordered substrate turnover or if other mechanisms coordinate degron recognition will provide add addition insights towards understanding how this major molecular machine is regulated.

Thesis Rationale

Since the discovery of SUMO, a variety of SUMO substrates have been characterized as important regulators of mitosis (Table 2). Previous work in *S. cerevisiae* demonstrated that *smt-3* and *ubc-9* mutants arrest in mitosis, resulting in a large budded phenotype and failed to properly degrade the APC/C substrates Clb-3 and Pds1, homologs of human Cyclin B1 and

securin[104]. Chapter 2 describes a novel molecular mechanism of how SUMO modification is also required for stimulating the activity of the APC/C and timely degradation of CyclinB1 and securin in human cells. A follow up to a previously characterized requirement of SENP1 activity in regulating the metaphase-anaphase transition[30] is presented in Chapter 3. Inquiry on the basic principles governing cell cycle progression have important implications for developing cancer therapeutics, as all of the current first line chemotherapies target rapidly dividing cells. A comprehensive understanding of how the SUMO pathway regulates mitotic progression provides a tractable approach towards the future development of treatment.

Figure 1-1

Human SUMO Paralogs & Post-Translational Modifications of SUMO

Three functional SUMO isoforms are expressed in human cells, including SUMO1, SUMO2, and SUMO3. SUMO2 and SUMO3 share ~96% sequence homology, and are collectively referred as SUMO2/3. Current techniques cannot distinguish between the SUMO2 and SUMO3. SUMO1 shares ~45% sequence homology with SUMO2/3. All SUMO paralogs can be post-translationally modified by phosphorylation, ubiquitylation, acetylation, and SUMO2/3 contain
SUMO consensus site motifs that result in the generation of poly-SUMO chains.

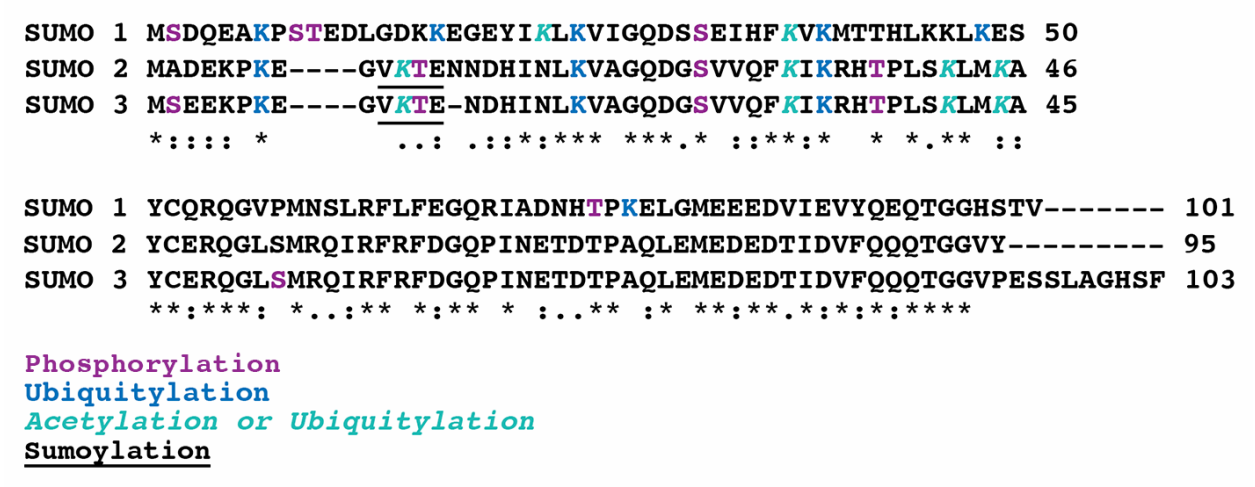
SUMO 1 MSDQEAKPSTEDLGDKKEGEYIKLKVIGQDSSEIHFKVKMTTHLKKLKES 50
SUMO 2 MADEKPKE----GVKTENNDHINLKVAGQDGSVVQFKIKRHTPLSKLMKA 46
SUMO 3 MSEEKPKE----GVKTE-NDHINLKVAGQDGSVVQFKIKRHTPLSKLMKA 45
SUMO 1 YCQRQGVPMNSLRFLFEGQRIADNHTPKELGMEEEDVIEVYQEQTGGHSTV------- 101
SUMO 2 YCERQGLSMRQIRFRFDGQPINETDTPAQLEMEDEDTIDVFQQQTGGVY--------- 95
SUMO 3 YCERQGLSMRQIRFRFDGQPINETDTPAQLEMEDEDTIDVFQQQTGGVPESSLAGHSF 103
Phosphorylation
Ubiquitylation
Acetylation or Ubiquitylation
Sumoylation

Figure 1-2

The SUMO Pathway

The Small Ubiquitin-related Modifier (SUMO) is first processed by SUMO isopeptidases (SENPs) to expose a C-terminal di-glycine motif. SUMO modification generally occurs at consensus site sequences, beginning with a hydrophobic amino acid (φ), conjugation at lysine (K), followed by any amino acid (x), and either glutamic or aspartic acid (E/D). Covalent SUMO conjugation occurs through an enzymatic cascade involving E1, E2, and E3 enzymes. Functionally, SUMO modification results in the generation of novel non-covalent protein-protein interactions through recognition of a SUMO Interacting Motif (SIM); interactions with other post-translational modifications, such as ubiquitylation and subsequent substrate degradation; and localization of proteins to distinct sub-cellular compartments. SUMO modification is reversed by the activity of SENPs.

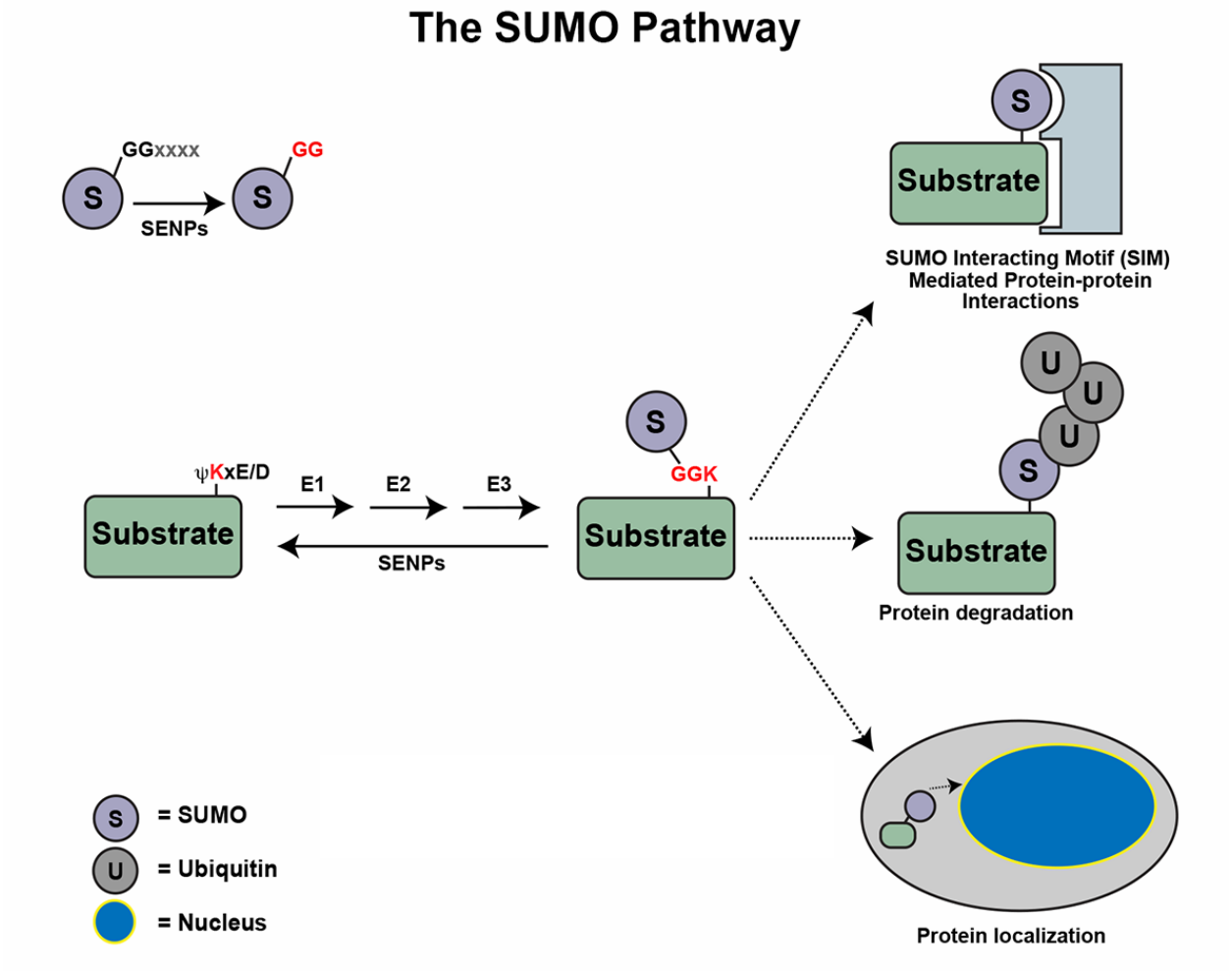
The SUMO Pathway
GGxxxx
GG
S
S
SENPs
S
Substrate
SUMO Interacting Motif (SIM)
Mediated Protein-protein
Interactions
ψKxE/D
E1
E2
E3
S
GGK
Substrate
Substrate
SENPs
U
U
U
S
Substrate
Protein degradation
Protein localization
S = SUMO
U = Ubiquitin
= Nucleus

Figure 1-3

Structure of SUMO Interacting Motif (SIM) in Rap80 with SUMO2

Non-covalent interactions between SUMO-modified proteins and proteins containing SUMO Interacting Motifs (SIMs) occur between amino acid residues Q35 (glutamine), F36 (phenylalanine), and I38 (isoleucine) of SUMO2 and proteins containing a hydrophobic SIM consensus sequence V/I-V/-x-V/I (V is valine, I is isoleucine, x is any amino acid). Rap80 contains a SIM that interacts non-covalently with the β_2 strand in SUMO2.

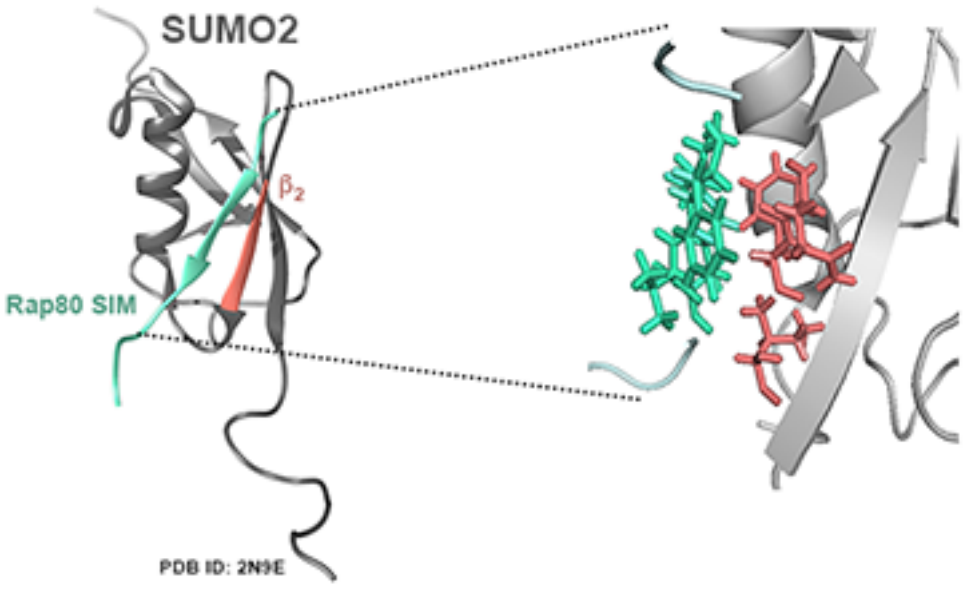

Figure 1-4

The Cell Cycle is Regulated by Cyclin/CDKs

Cyclins and Cyclin Dependent Kinsases (CDKs) regulate progression through the cell cycle. During the G1 phase of the cell cycle, Cyclin E interacts with CDK2, Cyclin A interacts with CDK1 and CDK2 between S and G2 phases, while Cyclin B interacts with CDK1 during M phase (mitosis). Cyclin expression increases at the beginning of each phase of the cell cycle and is degraded by the activity of the ubiquitin-proteasome system.

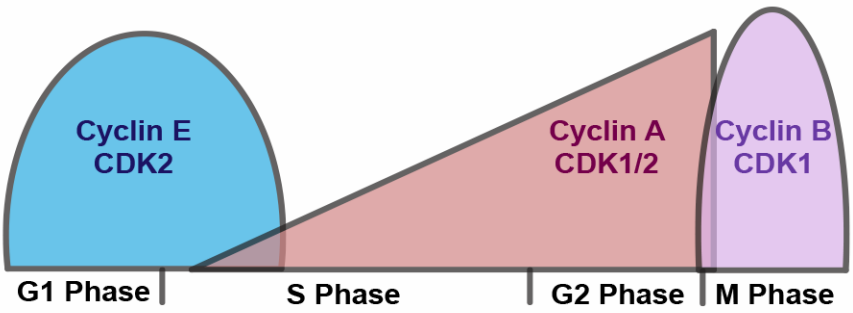

Figure 1-5

The Ubiquitin-Proteasome Pathway

Ubiquitin is a post-translational modification that is covalently added to substrates through the sequential activity of E1, E2, and E3 enzymes. Modification occurs at lysine residues, and can be reversibly removed by the activity of de-ubiquitinating enzymes (DUBs). Poly-ubiquitin chains target substrates to the 26S proteasome, whereby proteins are degraded so that amino acids can be recycled.

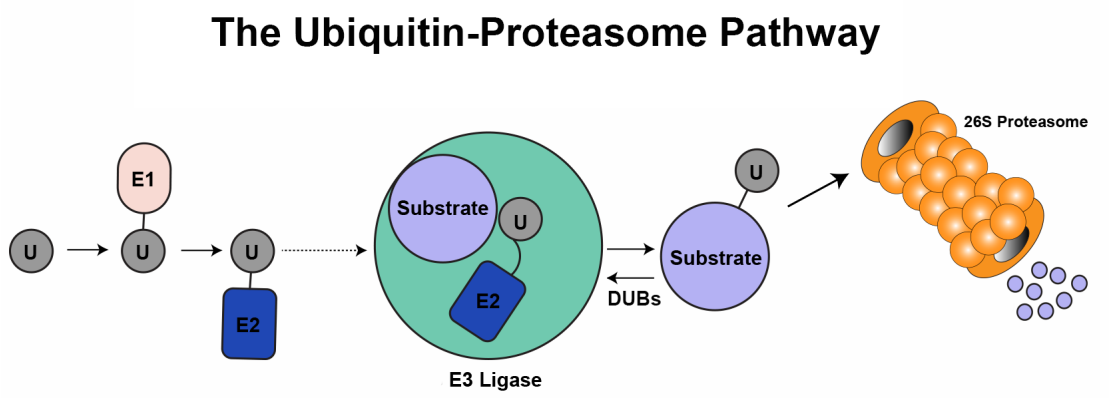

Figure 1-6

Mitosis is Regulated by the Spindle Assembly Checkpoint and the Anaphase Promoting Complex/Cyclosome (APC/C)

At the onset of mitosis, kinetochores that have yet aligned with the mitotic spindle generate an inhibitory signal, known as the Spindle Assembly Checkpoint. Checkpoint signaling contributes to the formation and assembly of the Mitotic Checkpoint Complex (MCC), which binds to an inhibits the activity of the Anaphase Promoting Complex/Cyclosome (APC/C). The APC/C is a multi-subunit complex that functions as an E3 ubiquitin ligase. Throughout mitosis, the APC/C ubiquitylates specific substrates. Importantly, the substrates Cyclin B1 and Securin are ubiquitylated during the metaphase-anaphase transition. The APC2 and APC11 subunits are the cullin and RING domains of the APC/C and function as the catalytic arm of this ligase. APC4 is a subunit described in this thesis that is SUMO-modified during mitosis. Depending on whether the MCC or a substrate is bound to the APC/C, Cryo-EM images show that the APC2/11 module adopts different conformations, which may be an important regulatory feature of ligase activity.

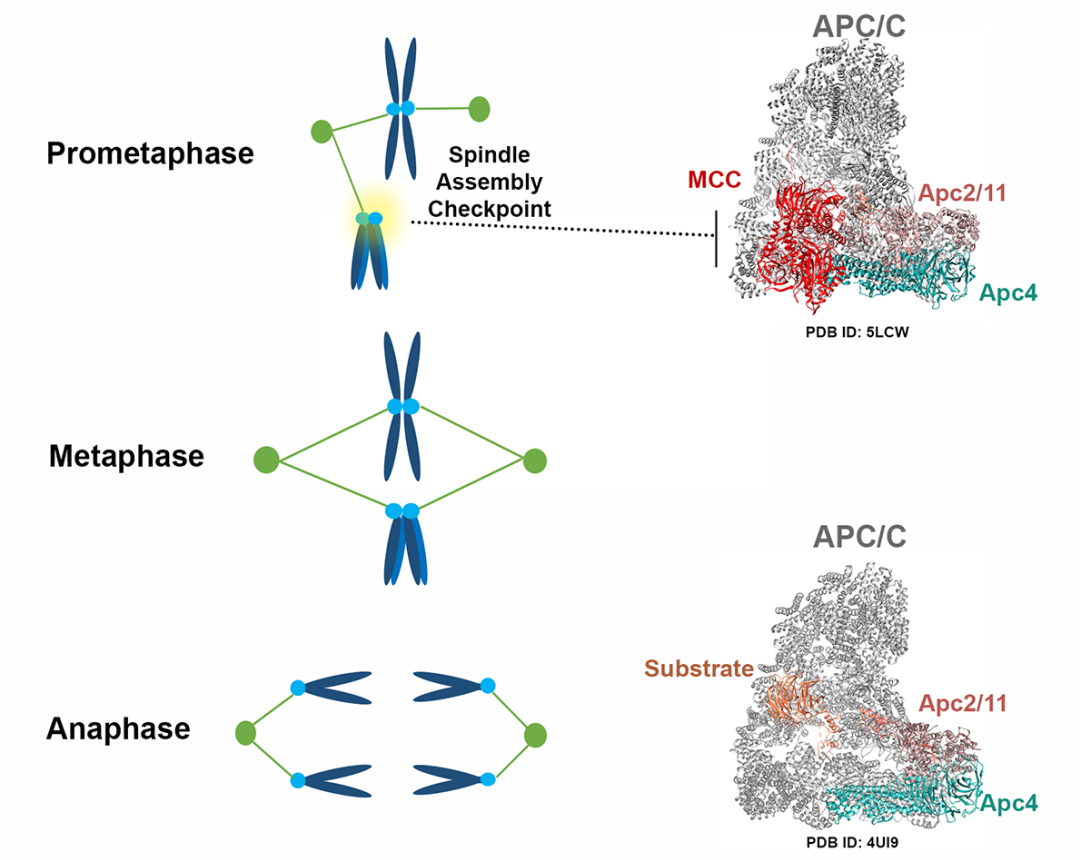
Prometaphase
Spindle
Assembly
Checkpoint
APC/C
MCC
Apc2/11
Apc4
PDB ID: 5LCW
Metaphase
Anaphase
APC/C
Substrate
Apc2/11
Apc4
PDB ID: 4UI9

Table 1-1

SUMO Pathway Enzymes

SUMO paralogs SUMO1, SUMO2, and SUMO 3 are covalently conjugated to substrates through the activity of activating E1, conjugating E2, and ligating E3 enzymes, and reversibly removed by the activity of SUMO Isopeptidases.

Enzyme	Vertebrate	*S. cerevisiae*
SUMO Paralogs	SUMO1	Smt3
	SUMO2	
	SUMO3	
Activating Enzyme (E1)	Aos1/SAEI + Uba2/SAE2	Aos1+Uba2
Conjugating Enzyme (E2)	Ubc9	Ubc9
SP-RING SUMO ligases (E3)	PIAS1	Siz1
	PIAS3	Siz2/Nfi
	PIASxα	
	PIASxβ	
	PIASγ	
	Mms21	Mms21
Other SUMO ligases (E3)	BanBP2	
	Pc2	
SUMO Isopeptidase	SENP1	Ulp1
	SENP2	Ulp2 (Smt4)
	SENP3	
	SENP5	
	SENP6	
	SENP7	
	DESI1	
	DESI2	
	USPL1	

Table 1-2

Validated mitotic SUMO substrates

Associated Mitotic Function	Protein	Reference(s)
Chromosome Passenger Complex	Aurora B	106
	Bir1 (survivin)	107
	Borealin	108
Spindle Assembly Checkpoint	Mps1	109,110
	BubR1	111,112
Centromere/ Kinetochore Structure	CENP-E	112
	CENP-H/I/K	33
	Cep3	107
	Ndc10	107
	Ndc80	107
	Nuf2	112
	Kif18A	113
Cohesin/ Condensin	Pds5	114,115
	Scc1	116
Chromosome Decatenation	Topoisomerase IIα	72,117,118
	PICH	119
Other	Psmd1	120
	RanGAP1	17,18
	APC4	121–123

REFERENCES

1. Flotho & Melchior. Sumoylation: A Regulatory Protein Modification in Health and Disease. Annual Review of Biochemistry 82, 357–385 (2013).

2. Kerscher. SUMO junction-what's your function? New insights through SUMO-interacting motifs. EMBO reports 8, 550–5 (2007).

3. Johnson, Schwienhorst, Dohmen & Blobel. The ubiquitin- like protein Smt3p is activated for conjugation to other proteins by an Aos1p/Uba2p heterodimer. The EMBO Journal 16, 5509–5519 (1997).

4. Gareau & Lima. The SUMO pathway: emerging mechanisms that shape specificity, conjugation and recognition. Nature Reviews Molecular Cell Biology 11, nrm3011 (2010).

5. Meluh & Koshland. Evidence that the MIF2 gene of Saccharomyces cerevisiae encodes a centromere protein with homology to the mammalian centromere protein CENP-C. Molecular Biology of the Cell 6, 793–807 (1995).

6. Tanaka et al. Characterization of a Fission Yeast SUMO-1 Homologue, Pmt3p, Required for Multiple Nuclear Events, Including the Control of Telomere Length and Chromosome Segregation. Molecular and Cellular Biology 19, 8660–8672 (1999).

7. Surana, Gowda, Tripathi, Broday & Das. Structural and functional analysis of SMO-1, the SUMO homolog in Caenorhabditis elegans. PLOS ONE 12, e0186622 (2017).

8. Nie, Xie, Loo & Courey. Genetic and Proteomic Evidence for Roles of Drosophila SUMO in Cell Cycle Control, Ras Signaling, and Early Pattern Formation. PLoS ONE 4, e5905 (2009).

9. Reiter et al. Identification of Biochemically Distinct Properties of the Small Ubiquitin-related Modifier (SUMO) Conjugation Pathway in Plasmodium falciparum. Journal of Biological Chemistry 288, 27724–27736 (2013).

10. Hendriks & Vertegaal. A comprehensive compilation of SUMO

proteomics. Nature Reviews Molecular Cell Biology 17, nrm.2016.81 (2016).

11. Clague, Heride & Urbé. The demographics of the ubiquitin system. Trends in Cell Biology 25, 417–426 (2015).

12. Melchior & Melchior. SUMO-NONCLASSICAL UBIQUITIN. annual (2000). doi:10.1146/annurev.cellbio.16.1.591

13. Hietakangas et al. PDSM, a motif for phosphorylation-dependent SUMO modification. Proceedings of the National Academy of Sciences of the United States of America 103, 45–50 (2006).

14. Shen, Pardington-Purtymun, Comeaux, Moyzis & Chen. UBL1, a Human Ubiquitin-like Protein Associating with Human RAD51/RAD52 Proteins. Genomics 271–279 (1996). doi:10.1006/geno.1996.0462

15. Okura et al. Protection against Fas/APO-1- and tumor necrosis factor-mediated cell death by a novel protein, sentrin. Journal of immunology (Baltimore, Md. : 1950) 4277–81 (1996).

16. Boddy, Howe, Etkin, Solomon & Freemont. PIC 1, a novel ubiquitin-like protein which interacts with the PML component of a multiprotein complex that is disrupted in acute promyelocytic leukaemia. Oncogene 971–82 (1996).

17. Matunis, Coutavas & Blobel. A novel ubiquitin-like modification modulates the partitioning of the Ran-GTPase-activating protein RanGAP1 between the cytosol and the nuclear pore complex. The Journal of Cell Biology 135, 1457–1470 (1996).

18. Mahajan, Delphin, Guan, Gerace & Melchior. A Small Ubiquitin-Related Polypeptide Involved in Targeting RanGAP1 to Nuclear Pore Complex Protein RanBP2. Cell 88, 97–107 (1997).

19. Zhang et al. Sumo-1 Function Is Dispensable in Normal Mouse Development. Molecular and Cellular Biology 5381–5390 (2008). doi:10.1128/MCB.00651-08

20. Alkuraya et al. SUMO1 Haploinsufficiency Leads to Cleft Lip and

Palate. Science 1751–1751 (2006). doi:10.1126/science.1128406

21. Wang et al. Defective sumoylation pathway directs congenital heart disease. Birth Defects Research Part A: Clinical and Molecular Teratology 468–476 (2011). doi:10.1002/bdra.20816

22. Evdokimov, Sharma, Lockett, Lualdi & Kuehn. Loss of SUMO1 in mice affects RanGAP1 localization and formation of PML nuclear bodies, but is not lethal as it can be compensated by SUMO2 or SUMO3. J Cell Sci 4106–4113 (2008). doi:10.1242/jcs.038570

23. Wang et al. SUMO2 is essential while SUMO3 is dispensable for mouse embryonic development. EMBO reports 878–885 (2014). doi:10.15252/embr.201438534

24. Saitoh & Hinchey. Functional Heterogeneity of Small Ubiquitin-related Protein Modifiers SUMO-1 versus SUMO-2/3. Journal of Biological Chemistry 275, 6252–6258 (2000).

25. Fukuda et al. Ginkgolic Acid Inhibits Protein SUMOylation by Blocking Formation of the E1-SUMO Intermediate. Chemistry & Biology 16, 133–140 (2009).

26. He et al. Probing the roles of SUMOylation in cancer cell biology by using a selective SAE inhibitor. Nature Chemical Biology 13, nchembio.2463 (2017).

27. Li & Hochstrasser. A new protease required for cell-cycle progression in yeast. Nature 398, 18457 (1999).

28. Li & Hochstrasser. The Yeast ULP2 (SMT4) Gene Encodes a Novel Protease Specific for the Ubiquitin-Like Smt3 Protein. Molecular and Cellular Biology 20, 2367–2377 (2000).

29. Li & Hochstrasser. The Ulp1 SUMO isopeptidase. The Journal of Cell Biology 160, 1069–1082 (2003).

30. Gong, Kamitani, Millas & ETH, Y. Identification of a Novel Isopeptidase with Dual Specificity for Ubiquitin- and NEDD8-conjugated Proteins. Journal of Biological Chemistry 275, 14212–14216 (2000).

31. Mukhopadhyay & Dasso. Modification in reverse: the SUMO proteases. Trends in Biochemical Sciences 32, 286–295 (2007).

32. Cubeñas-Potts, Goeres & Matunis. SENP1 and SENP2 affect spatial and temporal control of sumoylation in mitosis. Molecular biology of the cell 24, 3483–95 (2013).

33. Mukhopadhyay, Arnaoutov & Dasso. The SUMO protease SENP6 is essential for inner kinetochore assembly. The Journal of Cell Biology 188, 681–692 (2010).

34. Nayak, A. & Müller, S. SUMO-specific proteases/isopeptidases: SENPs and beyond. Genome Biology 15, 1–7 (2014).

35. Era et al. The SUMO protease SENP1 is required for cohesion maintenance and mitotic arrest following spindle poison treatment. Biochemical and Biophysical Research Communications 426, 310–316 (2012).

36. Kang et al. SUMO-Specific Protease 2 Is Essential for Suppression of Polycomb Group Protein-Mediated Gene Silencing during Embryonic Development. Molecular Cell (2010). doi:10.1016/j.molcel.2010.03.005

37. Shin et al. DeSUMOylating isopeptidase: a second class of SUMO protease. EMBO reports 13, 339–346 (2012).

38. Schulz et al. Ubiquitin- specific protease- like 1 (USPL1) is a SUMO isopeptidase with essential, non- catalytic functions. EMBO reports 13, 930–938 (2012).

39. Song, Zhang, Hu & Chen. Small ubiquitin-like modifier (SUMO) recognition of a SUMO binding motif: a reversal of the bound orientation. The Journal of biological chemistry 280, 40122–9 (2005).

40. Hecker, Rabiller, Haglund, Bayer & Dikic. Specification of SUMO1- and SUMO2-interacting Motifs. Journal of Biological Chemistry 281, 16117–16127 (2006).

41. Stehmeier & Muller. Phospho-regulated SUMO interaction modules

connect the SUMO system to CK2 signaling. Molecular cell 33, 400–9 (2009).

42. Yunus & Lima. Structure of the Siz/PIAS SUMO E3 ligase Siz1 and determinants required for SUMO modification of PCNA. Molecular cell 35, 669–82 (2009).

43. Baba et al. Crystal structure of thymine DNA glycosylase conjugated to SUMO-1. Nature 435, nature03634 (2005).

44. Shen, Lin, Scaglioni, Yung & Pandolfi. The Mechanisms of PML-Nuclear Body Formation. Molecular Cell 24, 331–339 (2006).

45. Matunis, Zhang & Ellis. SUMO: The Glue that Binds. Developmental Cell 11, 596–597 (2006).

46. Westerbeck et al. A SUMO-targeted ubiquitin ligase is involved in the degradation of the nuclear pool of the SUMO E3 ligase Siz1. Molecular Biology of the Cell 25, 1–16 (2014).

47. Prudden et al. SUMO- targeted ubiquitin ligases in genome stability. The EMBO Journal 26, 4089–4101 (2007).

48. Guzzo et al. RNF4-Dependent Hybrid SUMO-Ubiquitin Chains Are Signals for RAP80 and Thereby Mediate the Recruitment of BRCA1 to Sites of DNA Damage. Sci. Signal. (2012). doi:10.1126/scisignal.2003485

49. Lara-Gonzalez, Kim & Desai. Taming the Beast: Control of APC/C Cdc20 -Dependent Destruction. Cold Spring Harbor Symposia on Quantitative Biology 033712 (2017). doi:10.1101/sqb.2017.82.033712

50. Musacchio. The Molecular Biology of Spindle Assembly Checkpoint Signaling Dynamics. Current Biology 25, R1002–R1018 (2015).

51. Lara-Gonzalez, Westhorpe & Taylor. The Spindle Assembly Checkpoint. Current Biology 22, R966–R980 (2012).

52. Pines. Cubism and the cell cycle: the many faces of the APC/C. Nature Reviews Molecular Cell Biology 12, nrm3132 (2011).

53. Foley & Kapoor. Microtubule attachment and spindle assembly checkpoint signalling at the kinetochore. Nature Reviews Molecular Cell Biology 14, nrm3494 (2012).

54. Musacchio & Salmon. The spindle-assembly checkpoint in space and time. Nature Reviews Molecular Cell Biology 8, 379–393 (2007).

55. Evans, Rosenthal, Youngblom, Distel & Cell. Cyclin: a protein specified by maternal mRNA in sea urchin eggs that is destroyed at each cleavage division. (1983).

56. Murray. Recycling the Cell Cycle Cyclins Revisited. Cell 116, 221–234 (2004).

57. Weinert & Hartwell. The RAD9 gene controls the cell cycle response to DNA damage in Saccharomyces cerevisiae. Science (New York, N.Y.) 241, 317–22 (1988).

58. Nurse. Genetic control of cell size at cell division in yeast. Nature 256, 547–551 (1975).

59. Bloom & Cross. Multiple levels of cyclin specificity in cell-cycle control. Nature Reviews Molecular Cell Biology nrm2105 (2007). doi:10.1038/nrm2105

60. Murray, Solomon & Nature. The role of cyclin synthesis and degradation in the control of maturation promoting factor activity. (1989).

61. Ciechanover. The unravelling of the ubiquitin system. Nature Reviews Molecular Cell Biology 16, 322–324 (2015).

62. Ciehanover, Hod & Hershko. A heat-stable polypeptide component of an ATP-dependent proteolytic system from reticulocytes. Biochemical and Biophysical Research Communications 81, 1100–1105 (1978).

63. Hershko, Ciechanover, Heller, Haas & Rose. Proposed role of ATP in protein breakdown: conjugation of protein with multiple chains of the polypeptide of ATP-dependent proteolysis. Proceedings of the National Academy of Sciences of the United States of America 77, 1783–6 (1980).

64. Hershko, Heller, Elias & Ciechanover. Components of ubiquitin-protein ligase system. Resolution, affinity purification, and role in protein breakdown. The Journal of biological chemistry 258, 8206–14 (1983).

65. Waxman, Fagan & Goldberg. Demonstration of two distinct high molecular weight proteases in rabbit reticulocytes, one of which degrades ubiquitin conjugates. The Journal of biological chemistry 262, 2451–7 (1987).

66. Hough, Pratt & Rechsteiner. Ubiquitin-lysozyme conjugates. Identification and characterization of an ATP-dependent protease from rabbit reticulocyte lysates. The Journal of biological chemistry 261, 2400–8 (1986).

67. Hershko, Ganoth, Pehrson, Palazzo & Cohen. Methylated ubiquitin inhibits cyclin degradation in clam embryo extracts. The Journal of biological chemistry 266, 16376–9 (1991).

68. Peters. The anaphase promoting complex/cyclosome: a machine designed to destroy. Nature Reviews Molecular Cell Biology 7, nrm1988 (2006).

69. Gerace & Blobel. The nuclear envelope lamina is reversibly depolymerized during mitosis. Cell 19, 277–87 (1980).

70. Ritterhoff et al. The RanBP2/RanGAP1*SUMO1/Ubc9 SUMO E3 ligase is a disassembly machine for Crm1-dependent nuclear export complexes. Nature Communications 7, 11482 (2016).

71. Zuccolo et al. The human Nup107–160 nuclear pore subcomplex contributes to proper kinetochore functions. The EMBO Journal 26, 1853–1864 (2007).

72. Azuma, Arnaoutov & Dasso. SUMO-2/3 regulates topoisomerase II in mitosis. The Journal of Cell Biology 163, 477–487 (2003).

73. Ruchaud, Carmena & Earnshaw. Chromosomal passengers: conducting cell division. Nature Reviews Molecular Cell Biology 8, 798–812 (2007).

74. Sudakin, Chan & Yen. Checkpoint inhibition of the APC/C in HeLa cells is mediated by a complex of BUBR1, BUB3, CDC20, and MAD2. The Journal of Cell Biology 154, 925–936 (2001).

75. Collin, Nashchekina, Walker & Pines. The spindle assembly checkpoint works like a rheostat rather than a toggle switch. Nature Cell Biology 15, 1378–1385 (2013).

76. Howell et al. Cytoplasmic dynein/dynactin drives kinetochore protein transport to the spindle poles and has a role in mitotic spindle checkpoint inactivation. The Journal of Cell Biology 155, 1159–1172 (2001).

77. Griffis, Stuurman & Vale. Spindly, a novel protein essential for silencing the spindle assembly checkpoint, recruits dynein to the kinetochore. The Journal of Cell Biology 177, 1005–1015 (2007).

78. Wojcik et al. Kinetochore dynein: its dynamics and role in the transport of the Rough deal checkpoint protein. Nature Cell Biology 3, 1001–1007 (2001).

79. Rieder, Cole, Khodjakov & Sluder. The checkpoint delaying anaphase in response to chromosome monoorientation is mediated by an inhibitory signal produced by unattached kinetochores. The Journal of Cell Biology 130, 941–948 (1995).

80. Metzger, Pruneda, Klevit & Weissman. RING-type E3 ligases: Master manipulators of E2 ubiquitin-conjugating enzymes and ubiquitination. Biochimica et Biophysica Acta (BBA) - Molecular Cell Research 1843, 47–60 (2014).

81. Brown et al. RING E3 mechanism for ubiquitin ligation to a disordered substrate visualized for human anaphase-promoting complex. Proceedings of the National Academy of Sciences 112, 5272–5279 (2015).

82. Chang, Zhang, Yang, McLaughlin & Barford. Atomic structure of the APC/C and its mechanism of protein ubiquitination. Nature 522, 450–454 (2015).

83. Wu et al. UBE2S drives elongation of K11-linked ubiquitin chains by the Anaphase-Promoting Complex. Proceedings of the National Academy of

Sciences 107, 1355–1360 (2010).

84. Kelly, Wickliffe, Song, Fedrigo & Rape. Ubiquitin Chain Elongation Requires E3-Dependent Tracking of the Emerging Conjugate. Molecular Cell 56, 232–245 (2014).

85. Meyer & Rape. Enhanced Protein Degradation by Branched Ubiquitin Chains. Cell 157, 910–921 (2014).

86. Williamson et al. Identification of a physiological E2 module for the human anaphase-promoting complex. Proceedings of the National Academy of Sciences 106, 18213–18218 (2009).

87. Wickliffe, Williamson, Meyer, Kelly & Rape. K11-linked ubiquitin chains as novel regulators of cell division. Trends in Cell Biology 21, 656–663 (2011).

88. Acquaviva, Herzog, Kraft & Pines. The anaphase promoting complex/cyclosome is recruited to centromeres by the spindle assembly checkpoint. Nature Cell Biology 6, ncb1167 (2004).

89. Topper et al. The Dephosphorylated Form of the Anaphase-Promoting Complex Protein Cdc27/Apc3 Concentrates on Kinetochores and Chromosome Arms in Mitosis. Cell Cycle 1, 287–297 (2002).

90. Jörgensen, Brundell, Starborg & Höög. A Subunit of the Anaphase-Promoting Complex Is a Centromere-Associated Protein in Mammalian Cells. Molecular and Cellular Biology 18, 468–476 (1998).

91. Sivakumar, Daum, Tipton, Rankin & Gorbsky. The spindle and kinetochore–associated (Ska) complex enhances binding of the anaphase-promoting complex/cyclosome (APC/C) to chromosomes and promotes mitotic exit. Molecular Biology of the Cell 25, 594–605 (2014).

92. Yamaguchi et al. Cryo-EM of Mitotic Checkpoint Complex-Bound APC/C Reveals Reciprocal and Conformational Regulation of Ubiquitin Ligation. Molecular Cell 63, 593–607 (2016).

93. Alfieri et al. Molecular basis of APC/C regulation by the spindle assembly checkpoint. Nature 536, 431–436 (2016).

94. Duda et al. Structural Insights into NEDD8 Activation of Cullin-RING Ligases: Conformational Control of Conjugation. Cell 134, 995–1006 (2008).

95. Eytan et al. Disassembly of mitotic checkpoint complexes by the joint action of the AAA-ATPase TRIP13 and p31comet. Proceedings of the National Academy of Sciences 111, 12019–12024 (2014).

96. Mansfeld, Collin, Collins, Choudhary & Pines. APC15 drives the turnover of MCC-CDC20 to make the spindle assembly checkpoint responsive to kinetochore attachment. Nature Cell Biology 13, ncb2347 (2011).

97. Kraft et al. Mitotic regulation of the human anaphase- promoting complex by phosphorylation. The EMBO Journal 22, 6598–6609 (2003).

98. Izawa & Pines. The mitotic checkpoint complex binds a second CDC20 to inhibit active APC/C. Nature 517, 631–634 (2015).

99. Qiao et al. Mechanism of APC/CCDC20 activation by mitotic phosphorylation. Proceedings of the National Academy of Sciences 113, E2570–E2578 (2016).

100. Zhang et al. Molecular mechanism of APC/C activation by mitotic phosphorylation. Nature 533, 260–264 (2016).

101. Fujimitsu, Grimaldi & Yamano. Cyclin-dependent kinase 1–dependent activation of APC/C ubiquitin ligase. Science 352, 1121–1124 (2016).

102. Hagting et al. Human securin proteolysis is controlled by the spindle checkpoint and reveals when the APC/C switches from activation by Cdc20 to Cdh1. The Journal of Cell Biology 157, 1125–1137 (2002).

103. Pfleger, Lee & Kirschner. Substrate recognition by the Cdc20 and Cdh1 components of the anaphase-promoting complex. Genes & Development 15, 2396–2407 (2001).

104. Davey & Morgan. Building a Regulatory Network with Short Linear

Sequence Motifs: Lessons from the Degrons of the Anaphase-Promoting Complex. Molecular Cell 64, 12–23 (2016).

105. Dieckhoff, Bolte, Sancak, Braus & Irniger. Smt3/SUMO and Ubc9 are required for efficient APC/C- mediated proteolysis in budding yeast. Molecular Microbiology 51, 1375–1387 (2004).

106. Ban, Nishida & Urano. Mitotic kinase Aurora- B is regulated by SUMO- 2/3 conjugation/deconjugation during mitosis. Genes to Cells 16, 652–669 (2011).

107. Montpetit, Hazbun, Fields & Hieter. Sumoylation of the budding yeast kinetochore protein Ndc10 is required for Ndc10 spindle localization and regulation of anaphase spindle elongation. The Journal of Cell Biology 174, 653–663 (2006).

108. Klein, Haindl, Nigg & Muller. RanBP2 and SENP3 Function in a Mitotic SUMO2/3 Conjugation-Deconjugation Cycle on Borealin. Molecular Biology of the Cell 20, 410–418 (2009).

109. Restuccia, Yang, Chen, Lu & Dai. Mps1 is SUMO-modified during the cell cycle. Oncotarget 7, 3158–3170 (2015).

110. Jelluma, Dansen, Sliedrecht, Kwiatkowski & Kops. Release of Mps1 from kinetochores is crucial for timely anaphase onset. The Journal of Cell Biology 191, 281–290 (2010).

111. Yang et al. BubR1 Is Modified by Sumoylation during Mitotic Progression. Journal of Biological Chemistry 287, 4875–4882 (2012).

112. Zhang et al. SUMO-2/3 Modification and Binding Regulate the Association of CENP-E with Kinetochores and Progression through Mitosis. Molecular Cell 29, 729–741 (2008).

113. Yang, Chen & Dai. Sumoylation of Kif18A plays a role in regulating mitotic progression. BMC Cancer 15, 197 (2015).

114. D'Ambrosio & Lavoie. Pds5 Prevents the PolySUMO-Dependent Separation of Sister Chromatids. Current Biology 24, 361–371 (2014).

115. Stead et al. Pds5p regulates the maintenance of sister chromatid cohesion and is sumoylated to promote the dissolution of cohesion. The Journal of Cell Biology 163, 729–741 (2003).

116. Wu et al. Scc1 sumoylation by Mms21 promotes sister chromatid recombination through counteracting Wapl. Genes & Development 26, 1473–1485 (2012).

117. Ryu, Furuta, Kirkpatrick, Gygi & Azuma. PIASy-dependent SUMOylation regulates DNA topoisomerase IIα activity. The Journal of Cell Biology 191, 783–794 (2010).

118. Dawlaty et al. Resolution of Sister Centromeres Requires RanBP2-Mediated SUMOylation of Topoisomerase IIα. Cell 133, 103–115 (2008).

119. Sridharan, Park, Ryu & Azuma. SUMOylation Regulates Polo-like Kinase 1-interacting Checkpoint Helicase (PICH) during Mitosis. Journal of Biological Chemistry 290, 3269–3276 (2015).

120. Ryu, Gygi, Azuma, Arnaoutov & Dasso. SUMOylation of Psmd1 Controls Adrm1 Interaction with the Proteasome. Cell Reports 7, 1842–1848 (2014).

121. Cubeñas-Potts et al. Identification of SUMO-2/3-modified proteins associated with mitotic chromosomes. Proteomics 15, 763–72 (2015).

122. Schou, Kelstrup, Hayward, Olsen & Nilsson. Comprehensive Identification of SUMO2/3 Targets and Their Dynamics during Mitosis. PLoS ONE 9, e100692 (2014).

123. Schimmel et al. Uncovering SUMOylation Dynamics during Cell-Cycle Progression Reveals FoxM1 as a Key Mitotic SUMO Target Protein. Molecular Cell 53, 1053–1066 (2014).

CHAPTER 2:

SUMOYLATION PROMOTES OPTIMAL APC/C ACTIVATION AND TIMELY ANAPHASE

ABSTRACT

The Anaphase Promoting Complex/Cyclosome (APC/C) is a ubiquitin ligase that functions as the gatekeeper to mitotic exit. Steps critical for APC/C activation have been identified, including silencing of the spindle assembly checkpoint. Factors that modulate APC/C following activation, however, remain poorly understood. We have identified a role for the small ubiquitin-related modifier (SUMO) in fine-tuning APC/C activity downstream of checkpoint silencing. Sumoylation of the APC4 subunit of APC/C, which peaks at the metaphase-anaphase transition, controls the timing of anaphase onset by enhancing APC/C activity. We have also identified a functionally important SUMO interacting motif in the cullin-homology domain of APC2, a domain in the APC/C catalytic core critical for E2 binding. We propose that interactions between APC2 and sumoylated APC4 stabilize a conformation of the catalytic core that is optimized for E2 recruitment and substrate ubiquitylation. Our findings reveal a novel mechanism for SUMO-mediated regulation of mitotic exit.

INTRODUCTION

Aberrations during cell division can result in abnormal chromosome number or aneuploidy, a key hallmark of human cancers[1]. Cellular mechanisms therefore exist to safeguard against chromosome missegregation, including the spindle assembly checkpoint (SAC) that functions during the mitotic stage of the cell cycle. At the onset of mitosis, mitotic kinases and microtubule motor proteins coordinate attachment of spindle microtubules to kinetochores to appropriately align sister chromatids at the metaphase plate[2]. The SAC monitors unattached kinetochores or kinetochores that have not yet developed proper tension, and produces an inhibitory signal known as the Mitotic Checkpoint Complex (MCC)[3,4]. The MCC is composed of BubR1, Bub3, Cdc20, and Mad2 and functions to inhibit the activity of the Anaphase Promoting Complex or Cyclosome (APC/C), a ubiquitin RING E3 ligase[5]. Upon appropriate chromosome alignment, SAC silencing, and activation of the APC/C, the processive ubiquitylation and subsequent degradation of Cyclin B1 and securin promotes anaphase onset[6]. The dynamics between SAC signaling and protein turnover produces a fine-tuned "rheostat"[7] responsive to multiple signals affecting APC/C activity and mitotic exit.

The multi-subunit APC/C is a member in a large family of cullin-RING E3 ligases and functions most prominently as the gatekeeper to mitotic exit. APC/C activity must be exquisitely regulated to target specific substrates for ubiquitin-mediated proteolysis during different points in the cell cycle[8]. In part, this is coordinated by co-activator binding[9], appropriate sub-cellular localization[10–12], and SAC signaling[4] during mitosis. Studies of APC/C structure[13–15], interactions with the E2 enzymes UbcH10 and Ube2S[16,17], and binding to degron motifs identified in substrates[18] are beginning to provide detailed molecular insights into APC/C function and regulation. These findings reveal that APC/C is composed of a highly dynamic catalytic core including APC2, the cullin subunit, and APC11 that contains the RING domain. The APC2-11 module must be stabilized in varying conformations to allow for co-activator, E2 enzyme, and selective substrate binding, all culminating in APC/C activation. Phosphorylation provides one molecular mechanism for fine-tuning the structure of the APC/C catalytic core and promoting co-activator binding and activation[19–22]. Here we have identified a second post-translational modification, the attachment of the small ubiquitin related modifier (SUMO), as a critical mechanism for regulating APC/C activity in mitosis.

SUMO regulates a variety of essential cellular processes, including DNA replication and repair, chromatin remodeling, and mitosis[23]. There are several paralogs of SUMO, including SUMO1, SUMO2 and SUMO3 with potentially distinct functions. SUMO2 and SUMO3 are ~96% identical and are collectively referred to as SUMO2/3, whereas SUMO1 is ~45% identical to SUMO2 and SUMO3. Analogous to the ubiquitin pathway, SUMOs are added to proteins by the sequential cascade of E1, E2, and E3 enzymes. However, the catalog of SUMO pathway enzymes in vertebrates is smaller in comparison to the ubiquitin system, with a single activating E1 (expressed as the homodimer Aos1/Uba2), a single E2 conjugating enzyme (Ubc9) and approximately a dozen E3 ligases[24]. The SUMO pathway also includes a family of cysteine proteases, known as Sentrin Isopeptidases (SENPs), that reversibly remove SUMOs from substrates[25]. Regulation at the level of deconjugation is an important axis controlling SUMO function, as demonstrated by the importance of SENP1 and SENP2 in regulating mitotic progression[26]. Although dynamic cycling between conjugation and de-conjugation can result in a relatively low steady-state level of sumoylation for many substrates, sumoylation nonetheless produces profound effects on substrate localization and function in a variety of cellular pathways.

One functional paradigm for SUMO is that it acts as "molecular Velcro" to generate non-covalent interactions between proteins and facilitate protein complex assembly[27]. Novel protein-protein interactions are generated between sumoylated proteins and proteins containing SUMO-interacting motifs (SIMs). SUMO-SIM interactions are required for the assembly of complex cellular structures, including PML nuclear bodies[28], ribosomes[29] and kinetochores[28,30–32]. Early genetic studies in *S. cerevisiae* have also identified SUMO pathway components as essential for progression through mitosis[33–35]. Yeast sumoylation mutants result in a large budded phenotype and fail to properly degrade APC/C substrates Pds1 and Clb-3, indicating an essential role for sumoylation during the metaphase-anaphase transition[36]. Precisely how sumoylation regulates the metaphase-anaphase transition in higher order eukaryotes has not yet been defined. Additional investigations in human cell lines have underscored the importance of sumoylation in early mitotic processes, including kinetochore-microtubule interactions[30,37], sister chromatid cohesion[38,39], and checkpoint signaling[40–42]. Recent proteomic studies have also identified sumoylation sites on subunits of the APC/C, suggesting novel roles for sumoylation during the metaphase-anaphase transition[43–46].

Here, we demonstrate that the APC/C subunit APC4 is sumoylated at two C-terminal residues. We show that APC4 sumoylation peaks at the metaphase-anaphase transition, enhances APC/C activity, and is required for normal anaphase onset. In addition, our findings demonstrate that the cullin-containing APC/C subunit, APC2, also contains a functional C-terminal SIM, which is in close spatial proximity to APC4 sumoylation sites. Our data show that the SUMO-SIM interaction between APC4 and APC2 is required for normal anaphase onset. We propose that interactions between SUMO-modified APC4 and the SIM in APC2 stabilize a conformation of the catalytic core that is optimal for UbcH10 recruitment and APC/C activity.

MATERIALS AND METHODS

Plasmids and cell lines

The coding sequence for APC4 was PCR-amplified from pENTR221 ANAPC4 (Ultimate Human ORF Collection, HiT Center, Johns Hopkins University) and subcloned into pJET 1.2 (ThermoFisher Scientific). The linear SUMO2 fusion (without the C-terminal di-glycine) was PCR-amplified and inserted in frame to the C-terminus of APC4 in the vector above. APC2 was sub-cloned into the pCITE vector from a plasmid (a gift from Hongtao Yu, UT Southwestern). Single N-terminal FLAG tags were inserted using PCR-amplified sequences. Single ($APC4^{K772A}$, $APC4^{K798A}$), double ($APC4^{K772/798A}$, $APC4^{K772/798R}$, $APC2^{SIM\ Mutant}$), and triple mutants ($APC4^{KR}SUMO2^{QFI}$) were generated by PCR-based QuickChange site-directed mutagenesis (Stratagene, La Jolla, CA) using the wild-type APC4, APC2, and SUMO2 vectors as a template.

293FT and YFP-H2B HeLa cells (a gift from Andrew Holland, Johns Hopkins University, Baltimore, MD) were used to generate tetracycline-inducible cell lines. Lentiviruses containing a blasticidin-resistant tetracycline inducible plasmid, in addition to hygromycin-resistant APC4 or APC2 transgenes were incorporated via lentiviral infection as described previously[47,48]. In brief, 1 μg of lentiviral DNA construct, 800 ng psPAX2

(Addgene, Cambridge, MA, USA), and 200 ng pMD2.G (Addgene) were transfected into 293FT cells using XTremeGene HP (Roche) according to manufacturer's instructions. After 48 h, the viral supernatant was filtered through a 0.44 μM PVDF membrane and transduced to YFP-H2B HeLa cells in the presence of 8 μg/mL polybrene (Santa Cruz Biotechnology). After 24 h, cells were treated with 10 μg/mL blasticidin to select for the tetracycline-inducible cells for 1 week. Selection for stable cell lines was performed with hygromycin B (Roche) at a final concentration of 200 μg/mL for an additional week concomitant with 10 μg/mL blasticidin selection. Individual blasticidin and hygromycin-resistant colonies were isolated with cloning discs (after ~2 weeks) and tested for APC4 or APC2 expression by immunoblot analysis.

Cell culture and synchronization

293FT, JW36 HeLa, YFP-H2B HeLa, U2OS, and 6xHis-SUMO2 (a gift from Mary Dasso, National Institutes of Health, Bethesda, MD) cells were maintained at 37°C in a 5% CO_2 atmosphere. Cells were grown in DMEM medium (Gibco) containing 10% fetal bovine serum (Atlanta Biologicals). Thymidine (Sigma-Aldrich) was dissolved in DMSO and used at a final concentration of 2 mM. Nocodazole (Calbiochem) was dissolved in

DMSO and used at a final concentration of 100 ng/mL or 3.3 μM as indicated. To synchronize cells into S phase, cells were cultured in the presence of 2 mM thymidine for 19 h, released in drug-free media for 6 h, and cultured in 2 mM thymidine for 19 h. For mitotic timecourse analysis, cells were released from the double thymidine block and harvested in 2x SDS-sample buffer at indicated timepoints.

To weaken SAC signaling, 50 nM of the Mps1 kinase inhibitor, Reversine (Cayman Chemical, Ann Arbor, Michigan), was used immediately before timelapse acquisition.

RNAi interference

JW36 HeLa or YFP-H2B HeLa cells were transfected using Lipofectamine RNAiMAX (Invitrogen) and siRNA oligonucleotides at a final concentration of 20 nM for 48 hours and before analysis by immunoblotting, timelapse microscopy, or immunofluorescence microscopy. Stable cell lines were treated with doxycycline to induce expression of FLAG-APC4, FLAG-APC4^{KR}, or FLAG-APC4^{KR}-SUMO-2 concomitant with siRNA depletion of endogenous APC4. Two oligonucleotides targeting the 3' UTR of APC4 were validated, but oligonucleotide 2 was used for all experiments. APC4 oligonucleotides were purchased from Dharmacon:

APC4 Oligo 1: (5' – AGCUUGCCAUUAUUGUGUGUGUAAU – 3'), APC4 Oligo 2: (5' – CAUAGGAGAUGGACUAAGAUGUCUUGG – 3'); Scramble control: (5' –CUUCCUCUCUUUCUCUCCCUUGUGA-3'), and SENP1 oligo(b): (5' GCAAAUGGCCAAUGGAGAAAUUCUA-3') and SENP2 oligo(a): (5'AUAUCUGGAUUCUAUGGGAUU-3') were used as previously described[26].

APC2 oligonucleotides were designed using the BLOCK-iT RNAi Designer (ThermoFisher Scientific) to target the 5' UTR and purchased from Integrated DNA Technologies: 5' – TGGCTGCGCGTGCAGACGTGCGTCA – 3'.

In Vitro Sumoylation

APC4 wild-type, APC4^{K772A}, APC4^{K798A}, APC4$^{K772/798A}$, and RanGAP1 were produced by *in vitro* transcription and translation in rabbit reticulocyte lysate in the presence of [^{35}S]methionine according to the manufacturer's instructions (Promega, Madison, WI). 2 μL of translation product was added to a 30 μL reaction containing 200 nM human SUMO E1 enzyme, 600 nM human Ubc9, 1.0 μM human SUMO-1 or SUMO-2 proteins, 1 mM ATP, 20 units/mL creatine phosphokinase, 5 mM phosphocreatine, 0.6 μg/ml inorganic pyrophosphatase from *E. coli*, 20 mM

HEPES-KOH (pH 7.3), 110 mM potassium acetate, 2 mM magnesium acetate, and 1 mM dithiothreitol (DTT). Reactions were incubated at 30°C for the indicated times and stopped by addition of 2x SDS-sample buffer and analyzed by SDS-PAGE followed by autoradiography.

Recombinant SUMO proteins and SUMO enzymes were purified from *E. coli* as previously described (Yunus and Lima, 2009).

Antibody and imaging techniques

For immunoblotting, proteins were separated by SDS-PAGE, transferred onto nitrocellulose membranes, blocked in 5% milk in TS-T, and then probed with the following antibodies diluted in PBS supplemented with 2% BSA and 0.05% NaN_3: APC2 (rabbit, 1:1000 a generous gift from Hongtao Yu), APC4 (rabbit, A301-176A, 1:2000, Bethyl Laboratories, Inc), BubR1 (rabbit, GeneTex, 1:1000) Cyclin B1 (mouse, GNS1: sc-245, 1:200, Santa Cruz Laboratories), Cdc20 (mouse, p55 CDC (E-7): sc-13-162, 1:250, Santa Cruz Laboratories), ECS (DDDDK, goat, 1:1000, A190-101A, Bethyl Laboratories, Inc.), GAPDH (rabbit, TAB1001, OpenBiosystems, 1:15,000), Myc (mouse, a generous gift from Hongtao Yu), SENP1 (rabbit, ab108981, 1:10,000, Abcam), SENP2 (rabbit polyclonal, produced as described previously: Goeres *et al.*, 2011, 1:500), SUMO-1 (21C7, 1:100), SUMO-2/3

(8A2, 1:800), and Tubulin (mouse, DM1A, 1:5000, Sigma-Aldrich.) Secondary antibodies conjugated to HRP (Jackson Laboratories) were used at 1:10,000 diluted in 5% milk in TS-T. Immunoblot analysis was performed using either an enzyme-linked chemiluminescent substrate (Luminata Crescendo Western HRP Substrate, EMD Millipore) and developed with film or IR Dye-labeled secondary antibodies (anti rabbit IgG IRDye 800, LI-COR 926-32211) and imaged using the Odyssey infrared imager (LI-COR). Images were processed with Adobe Photoshop CS6.

To test the localization of Flag-APC4 and Flag-APC4^{KR}, cells were depleted of endogenous APC4 using siRNA and induced with doxycycline for 48 hours on glass coverslips. Cells were permeabilized using transport buffer (200 mM HEPES pH 6.5, 110 mM potassium acetate, 20 mM magnesium acetate, 1 μg/mL leupeptin, 1 μg/mL pepstatin A, 20 μg/mL aprotinin, 1 mM phenylmethylsulfonyl fluoride (PMSF), and 20 mM N-ethylmaleimide (NEM), and 20 μg/mL digitonin) at room temperature for 15 min. Cells were then washed 1x with PBS, and fixed in 2% formaldehyde at room temperature for 20 mins. After washing with PBS, cells were immunostained at room temperature using respective antibodies.

For SAC co-localization studies using immunofluorescence microscopy, stable cell lines were induced with doxycycline to express

FLAG-APC4 or FLAG-APC4^{KR} with siRNA against APC4 for 48 hours on glass coverslips. Cells were fixed in 3.5% paraformaldehyde in PBS for 7 min and permeabilized in 0.5% Triton-X 100 in PBS for 20 min at room temperature. Immunostaining was performed with the following antibodies diluted in PBS supplemented with 2% BSA: BubR1 (rabbit, GeneTex, 1:500), Cdc20 (mouse, p55 CDC(E-7): sc13-162, 1:50), CREST (human, 15-235-0001, Antibodies Inc., 1:100), FLAG (mouse, M2, 1:300, Sigma-Aldrich), Mad1 (mouse, 1:500, Active Motif), and Mad2 (rabbit, Covance, 1:500), followed by secondary antibodies to Alexa Fluor 594 and Alexa Fluor 647 at (1:300, Life Technologies, Grand Island, NY). Images were acquired using a Zeiss Observer Z1 fluorescence microscope with a Zeiss Plan-Apochromat 63x objective (numerical aperture 1.40) and Apotome VH optical sectioning grid (Carl Zeiss, Jena, Germany). Images were obtained at room temperature with immersion oil using a Zeiss AxioCam MRm camera and processed using AxioVision Software Release 4.8.2 and Adobe Photoshop CS6.

For immunoprecipitations to detect SUMO-modified APC4, lysates of YFP-H2B HeLa cells were treated with siRNA oligonucleotides against endogenous APC4 and induced with doxycycline for FLAG-APC4 or FLAG-APC4^{KR} expression for 48 h. Cell lysates were arrested in

prometaphase with a 3.3 μM nocodazole treatment for 4 hours and harvested in RIPA lysis buffer supplemented with protease inhibitors (cOmplete ULTRA EDTA-free tablets, Roche), 1mM phenylmethylsulfonyl fluoride (PMSF), and 10 mM N-ethylmaleimide, sonicated, and centrifuged 14,000 rpm for 20 min at 4°C. Protein lysates were quantified using a bicinchoninic acid protocol (ThermoScientific) to normalize protein inputs. Cell lysates were incubated with rabbit anti-APC4 antibodies (rabbit, 2 μg antibody per mg of cell lysate, Bethyl Laboratories) immobilized on Protein-A agarose beads (sc-2001, Santa Cruz) and incubated at 4°C overnight. Beads were washed with RIPA buffer 3x and proteins were eluted directly in 2x SDS-sample buffer.

Ni-NTA Affinity Purification

To investigate APC4 sumoylation during mitosis, U2OS or 6xHis-SUMO2 U2OS cells were synchronized into S phase using 2 mM thymidine or treated with 100 ng/mL nocodazole for 16 hours for prometaphase arrest, followed by 2, 4, or 8 hours release into drug-free media. Cells were washed 1x in PBS and flash frozen in liquid nitrogen until assays were performed. Cells were lysed in 6 M guanidine HCl lysis buffer, containing: 6 M guanidine HCl, 100 mM NaCl, 10 mM imidazole, 10 mM Tris-HCl pH 8.5,

and 10 mM β-Mercaptoethanol. Cells were sonicated briefly, cleared by centrifugation, and incubated with pre-washed Ni-NTA agarose (QIAGEN) for 2 hrs at 4°C. After a series of wash steps (1x Buffer A: 6M guanidine HCl, 10 mM Tris-HCl pH 8.5, 300 mM NaCl, 20 mM imidazole, 1% TNX-100, 1x Buffer B: 8M urea, 10 mM Tris-HCl pH 8.5, 300 mM NaCl, 20 mM imidazole, 1% TNX-100, 2x Buffer C: 8M urea, 10 mM Tris-HCl pH 6.5, 300 mM NaCl, 20 mM imidazole, 1% TNX-100), proteins were eluted in 2x SDS-sample buffer and analyzed by SDS-PAGE and immunoblotting.

APC/C ubiquitination assays

For APC/C activity assays, cells were treated with doxycycline to induce APC4 or APC2 expression for 24 hours, synchronized into S phase using 2 mM thymidine in the presence of doxycycline, released into drug-free media for 6 hours, and arrested in prometaphase using 100 ng/mL nocodazole for 5 hours. Cell pellets were washed 1x with PBS and flash frozen in liquid nitrogen. Ubiquitylation reactions were performed as previously described (Ji et al. 2017). Briefly, cells were lysed using a 25G 5/8 needle (BD PrecisionGlide) in 50 mM HEPES pH 7.5, 120 mM KCl, 3mM $MgCl_2$, 0.1% NP-40, protease inhibitors (cOmplete ULTRA EDTA-free tables, Roche), phosphatase inhibitors (PhosSTOP, Sigma-Aldrich), 1

mM DTT, and turbonuclease (Sigma-Aldrich, T4330-50KU). Cleared lysates (from a 30 min spin at 14,000 rpm and 4°C) were incubated with anti-goat DDDDK-conjugated agarose beads (ECS, S190-101, Bethyl Laboratories) for 2 hours. After wash 2x with detergent-free buffer (10 mM HEPES, pH 7.5, 100 mM KCl, 0.1 mM $CaCl_2$, 1 mM $MgCl_2$) proteins were eluted directly in 2x SDS-sample buffer and analyzed by SDS-PAGE and immunoblotting for APC2. Remaining fractions of beads were incubated with 1 μg recombinant human Cdc20 (a generous gift from Hongtao Yu) for 1 h, followed by an *in vitro* ubiquitylation reaction buffer (10 mM HEPES, pH 7.5, 100 mM KCl, 0.1 mM $CaCl_2$, 1 mM $MgCl_2$) including 150 μM bovine ubiquitin (Sigma), 5 μM Uba1, 750 nM UbcH10, 3 μM Ube2S, and 5μM Myc-tagged Cyclin B1, supplemented with 1X energy mixture (7.5 mM phosphocreatine, 1 mM ATP, 100 μM EGTA, and 1 mM $MgCl_2$). After incubation at room temperature with gentle shaking for 15, 30, or 60 min, the reactions were stopped with SDS loading buffer and analyzed by Western blotting.

Timelapse microscopy

For live-cell imaging, cells were cultured in Lab-Tek Chambered #1.0 Borosilicate Coverglass slides (Nunc, Rochester, NY), doxycycline induced

and siRNA treated targeting APC4, and then imaged 48 hours post-transfection. Immediately before imaging, cells were switched to pre-warmed CO_2-independent media (Invitrogen) supplemented with 10% FBS. Cells were maintained at 37°C on a Zeiss Observer Z1 fluorescence microscope fitted with an incubation chamber. Images were acquired using a Zeiss EC Plan-Neofluar 40x objective (numerical aperture 1.3) every 5 min for 16 hours with a Zeiss AxioCam MRm camera and processed using AxioVision Software Release 4.8.2. Data analysis was performed using Prism 6 for Mac OS X (GraphPad Software, Inc.)

Statistical analysis

Statistical analyses were carried out using Prism 6 for Mac OSX (GraphPad Software, Inc.) with two-tailed student *t* tests. Data with a *P*-value < 0.05 was considered as statistically significant.

RESULTS

APC4 is sumoylated in a cell-cycle dependent manner at lysines 772 and 798

APC4 is a protein subunit at the base of the APC/C that is sumoylated in mitosis[46]. To more precisely characterize the temporal regulation of APC4 sumoylation during the cell cycle, we synchronized HeLa cells using a double thymidine block. After release from thymidine for varying lengths of time, cell lysates were analyzed by immunoblotting for APC4 and the APC/C substrates, Cyclin B1 and Cdc20 (Figure 1A). Consistent with a possible role in regulating APC/C activity in mitosis, APC4 sumoylation levels (evidenced by the detection of a predominant high molecular mass protein band migrating at 120 kDa) increased with entry into mitosis and peaked at the time of Cyclin B1 degradation. To further demonstrate that APC4 is sumoylated in a mitosis-dependent manner, we utilized a stably expressing 6xHis-SUMO2 U2OS cell line and a parent U2OS cell line as a control. Cells were synchronized at different stages of the cell cycle and SUMO-modified proteins were captured using Nickel-NTA agarose. Affinity purifications from both U2OS and 6xHis-SUMO2 U2OS cells capture the unmodified form of APC4, which migrates at ~97 kDa. Immunoblots confirm that APC4 is SUMO-modified based on the

appearance of a shift in molecular weight at ~120 kDa in nocodazole-arrested 6xHis-SUMO2 U2OS cells that does not appear in the U2OS cell line (Sup. Figure 1A). APC4 sumoylation levels peak at mitotic entry followed by a subsequent decrease during mitotic exit (Sup. Figure 1A).

Human APC4 contains two C-terminal lysine residues located within consensus sumoylation sites, at positions 772 and 798, that have previously been reported to be sumoylated in high throughput mass spectrometry studies[43–46] (Figure 1B). To characterize APC4 sumoylation and modification at K772 and K798, we expressed wild type and mutant variants of APC4 in rabbit reticulocyte lysate in the presence of [^{35}S]-methionine. Translation products were incubated in reactions containing recombinant SUMO E1 activating and E2 conjugating enzymes and SUMO2 for varying lengths of time and analyzed by SDS-PAGE and autoradiography (Figure 1C). In reactions containing wild type APC4, we observed two prominent high molecular mass bands of 120 and 135 kDa, consistent with sumoylation at two sites. In reactions containing APC4 with single amino acid substitutions at either K772A or K798A, a single high molecular mass band of 120 kDa was observed, whereas sumoylation was abolished in reactions containing the K772A/798A double mutant. Reactions were also performed in the presence of recombinant SUMO1 with comparable results but with

lower efficiency compared to SUMO2 (Sup. Figure 1A). *In vitro* reactions demonstrate that lysine 798 is more efficiently modified by either SUMO1 or SUMO2, suggesting a functionally important role for the C-terminal lysine (Figure 1C and Sup. Figure 1B). Thus, our findings are consistent with previous mass spectrometry studies indicating that APC4 is sumoylated at two C-terminal lysine residues at positions 772 and 798.

To verify that K772 and K798 are the major sites in APC4 sumoylated *in vivo*, we generated stable HeLa cell lines allowing for inducible expression of FLAG-tagged, wild type APC4 (APC4) or a K772/798R mutant, hereafter referred to as $APC4^{KR}$ (Figure 1D). These cells also constitutively expressed yellow fluorescent protein (YFP)-tagged histone H2B to facilitate live cell imaging. To investigate APC4 sumoylation using these cell lines, we depleted endogenous APC4 using siRNAs directed against the 3' UTR and induced expression of the FLAG-tagged transgenes to near endogenous levels (Figure 1E). APC4 was immunoprecipitated from cell lysates using FLAG-specific antibodies and immunoblotting analysis was performed using APC4- or SUMO2/3-specific antibodies. Two SUMO2/3-modified protein bands were detected at 120 and 135 kDa in immunoprecipitates from wild type cells (Figure 1F), but not in immunoprecipitates from cells expressing $APC4^{KR}$ (Figure 1G). We also

evaluated sumoylation by SUMO1 with comparable results (Sup. Figure 1C). These findings confirm that K772 and K798 are the major APC4 sumoylation sites *in vivo*.

We also explored the regulation of APC4 sumoylation by SUMO isopeptidases by depleting cells of SENP1 or SENP2, two isopeptidases critical for normal mitotic progression[26] (Cubeñas-Potts et al. 2013). SENP1 or SENP2 were depleted using siRNAs as previously described[26], and cells were synchronized at metaphase using a nocodazole block followed by a 2-hour release into media containing the proteasome inhibitor MG132[49]. Immunoblot analysis of cell lysates revealed that APC4 sumoylation is specifically enhanced in SENP1-depleted cells compared to control or SENP2-depleted cells (Sup. Figure 1D), implicating SENP1 as a regulator of APC4 sumoylation in mitosis.

Sumoylation of APC4 is required for timely metaphase to anaphase transition

As a subunit of the APC/C, APC4 is predicted to be essential for normal cell cycle progression. To test this prediction, we depleted cells of endogenous APC4 by siRNA knockdown and analyzed cells after 48 hours using timelapse microscopy. This analysis revealed that ~88% of cells die as

a result of defects in mitosis (Figure 2A). Specifically, 20% of cells undergo a prolonged metaphase as defined as >60 min, and 69% undergo an abnormal mitosis—including defects in chromosome congression and inability to maintain a metaphase plate—resulting in cell death as depicted in single frame images (Figure 2B). These observations are consistent with defects observed in cells depleted of other essential APC/C subunits[50].

Having established that APC4 is an essential APC/C subunit required for mitotic progression, we next sought to investigate the function of APC4 sumoylation with knockdown and rescue experiments using the inducible cell lines described above. Cells were depleted of endogenous APC4 by an siRNA targeting the 3' UTR and concomitant induction of APC4 or APC4^{KR} for 48 hours. Progression through mitosis was analyzed after 16 hours of timelapse acquisition beginning with nuclear envelope breakdown (NEBD) and ending with anaphase onset. Induction of the APC4^{KR} mutant was not as effective as wild type APC4 in rescuing the APC4 knockdown defects, as cells exhibited a significant metaphase to anaphase delay before mitotic exit (Figure 2A, 2C-E). On average, APC4 cells spent 35.35 min to transition from NEBD-metaphase and APC4^{KR} cells spent 37.94 min. Further analysis revealed that cells expressing APC4 or APC4^{KR} do not have statistically significant differences ($p = 0.38$) in the time from NEBD to metaphase, but

have significant differences ($p < 0.0001$) in the time between metaphase and anaphase onset (Figure 2C-D). On average, APC4 cells spent 23.04 min from metaphase to anaphase and $APC4^{KR}$ cells spent 86.49 min. Despite the observed metaphase delay, $APC4^{KR}$ expressing cells ultimately progressed to anaphase and exited mitosis normally.

Sequence homology in higher eukaryotes reveals well-conserved sumoylation consensus sites at lysines 772 and 798 in the C-terminus of APC4 (Sup. Figure 1A). To determine if individual SUMO mutants affect mitotic progression, we generated stable inducible cell lines with a single N-terminal FLAG tag and lysine to arginine substitutions at either lysine 772 or 798 (Sup. Figure 1B). Single clones were depleted of endogenous APC4 using siRNA, and FLAG-$APC4^{772R}$ ($APC4^{772R}$) or FLAG-$APC4^{798R}$ ($APC4^{798R}$) expression was induced using doxycycline for 48 hrs prior to timelapse acquisition (Sup. Figure 1C). Single APC4 sumoylation mutants result in a metaphase-anaphase delay intermediate between APC4 wild type and the double APC4 sumoylation mutant (Sup. Figure 1D). These data suggest that both APC4 sumoylation mutants are necessary for prolonged metaphase delay and that a single sumoylation site is sufficient for mitotic exit. Furthermore, cells expressing single APC4 mutations exit mitosis normally without obvious chromosomal abnormalities. On average,

APC4^{772R} cells and APC4^{K798R} cells take 30 minutes and 38 minutes to progress from NEBD-metaphase, respectively, compared to 26 minutes in control cells (Sup. Figure 1E). These differences are not statistically significant (Control vs. APC4^{772R} p = 0.16, Control vs. APC4^{798R} p = 0.07). On average, APC4^{772R} cells took 40 minutes to transition from metaphase-anaphase, and APC4^{798R} took 66 minutes. Compared to control cells, which spent 27 minutes in metaphase-anaphase, both APC4^{772R} and APC4^{798R} cells have statistically significant differences (p = 0.03 and p = 0.03, respectively) (Sup. Figure 1F). However, both single mutants partially rescue the prolonged delay observed in the double mutant, which comparatively spends an average of 86 minutes in the metaphase-anaphase transition.

To explore the molecular basis of the metaphase to anaphase delay observed in APC4^{KR} expressing cells, we monitored the degradation of the APC/C substrates, Cyclin B1 and Cdc20. Following depletion of endogenous APC4 and induction of APC4 or APC4^{KR}, cells were synchronized using a double thymidine block and released in drug-free media. In APC4 expressing cells, APC4 sumoylation peaked concomitantly with declines in Cyclin B1 and Cdc20 protein levels, beginning at ~12 hours following thymidine release (Figure 2F). As expected, APC4 sumoylation was not observed in APC4^{KR} expressing cells (Figure 2G). In addition, the

rate of decline in Cyclin B1 and Cdc20 protein levels was substantially reduced compared to wild type APC4 expressing cells. Specifically, Cyclin B1 levels in APC4 cells are degraded ~12 h following thymidine release, while $APC4^{KR}$ cells show comparable Cyclin B1 turnover at ~15 h following thymidine release (Fig. 2F-G). CyclinB1 protein levels from three independent experiments were normalized and quantified (Figure 2H). On average, the rate of CyclinB1 turnover is attenuated in $APC4^{KR}$ expressing cells. CyclinB1 levels reach 50% of peak at approximately 12 hours following double thymidine release in APC4 expressing cells whereas $APC4^{KR}$ expressing cells reach similar levels at ~14 hours following release (Figure 2H). This observation indicates that the delay in anaphase onset detected in $APC4^{KR}$ expressing cells correlates with a deficiency in the turnover of APC/C-dependent target proteins. Taken together, our findings suggest that APC4 sumoylation is required for optimal APC/C function.

APC4 sumoylation does not affect APC/C or MCC localization at kinetochores

Sumoylation is known to affect protein localization, including targeting to kinetochores in mitosis[32,51]. In addition, spindle checkpoint signaling is important for recruiting APC/C to kinetochores, suggesting

localization as a critical factor affecting APC/C function[10–12]. To test whether the metaphase delay observed in APC4^{KR} expressing cells was due to defects in APC/C localization, we performed immunofluorescence microscopy on FLAG-tagged APC4 and APC4^{KR} expressing cells. Cells were co-stained with anti-FLAG and CREST (a kinetochore marker) antibodies. Both APC4 and APC4^{KR} were detected at kinetochores in prometaphase and metaphase cells at similar levels (Figure 3A). In addition, kinetochore localization dissipated similarly in wild type and APC4^{KR} expressing cells upon anaphase onset (Figure 3A-B).

We also performed immunofluorescence microscopy to investigate how the kinetochore recruitment and turnover of SAC proteins is affected in APC4^{KR} expressing cells. Mitotic cells were analyzed using antibodies specific for SAC proteins including Mad1, Mad2, BubR1, and Cdc20 (Figure 2C-F). As expected, APC4 expressing cells accumulate each of these SAC proteins at high levels in prometaphase and these levels decrease significantly at metaphase and through anaphase. Comparable results were obtained using APC4^{KR} expressing cells. These findings indicate that neither the localization of APC/C to kinetochores nor the recruitment and release of MCC proteins are regulated by APC4 sumoylation.

APC4 sumoylation is critical downstream of spindle assembly checkpoint inactivation

To directly test if APC4 sumoylation is required for APC/C activation independent of spindle assembly checkpoint (SAC) signaling, we weakened the SAC using reversine, an inhibitor of the Mps1 kinase[52]. APC4 and APC4^{KR} cells were depleted of endogenous APC4 by siRNA and transgene expression was induced with doxycycline for 48 hours prior to drug treatment, which was administered at the start of timelapse imaging (Sup. Figure 3A). Progression through mitosis beginning with nuclear envelope breakdown (NEBD) to anaphase onset was analyzed after 4 hours of timelapse acquisition. On average, APC4 cells spent 48.65 minutes in mitosis (NEBD to anaphase onset, SD = 15.99 min) and 34.87 minutes (SD = 11.00 min) when treated with reversine (Sup. Fig. 3B). This difference was statistically significant ($p = 0.0014$). APC4^{KR} cells spent 81.48 minutes (SD = 30.78 min) in mitosis while reversine treated APC4^{KR} cells averaged 78.78 minutes (SD = 21.41 min). Fixed images from timelapse microscopy analyses demonstrate that reversine treatment weakens checkpoint signaling in APC4 cells, resulting in premature anaphase and a precocious mitotic exit in APC4 expressing cells (Sup. Figure 3C-D) while APC4^{KR} cells treated with reversine still undergo a prolonged mitosis (Sup. Figure 3E-F). This

difference in total mitotic timing was not statistically significant in between $APC4^{KR}$ and $APC4^{KR}$ cells treated with reversine ($p = 0.73$), supportive of a functional role for APC4 sumoylation downstream of checkpoint inactivation.

SUMO fusion to APC4 bypasses the need for its sumoylation in mitotic progression

Having established that a defect in APC4 sumoylation affects timely Cyclin B1 degradation and anaphase onset, we next sought to investigate the consequences of constitutive APC4 sumoylation. Towards this end, we generated a stable cell line allowing for inducible expression of a FLAG-tagged linear APC4-SUMO2 fusion protein (Figure 4A). Linear SUMO fusions have successfully mimicked conjugation at internal lysines in multiple other proteins[53,54]. Our rationale for utilizing SUMO2 was based on *in vitro* analysis demonstrating that SUMO2 is conjugated to APC4 more efficiently (Fig. 1C, Sup. Fig. 1B) in addition to the finding that SUMO2/3 plays a dominant role during mitosis compared to SUMO1[30]. A single SUMO2 was fused to the APC4 K772/798A mutant protein, which allowed us to assess functionality, as discussed below.

To investigate the consequences of constitutive APC4 sumoylation, endogenous APC4 was depleted using siRNA knockdown and the $APC4^{KR}$-SUMO2 fusion protein ($APC4^{KR-S2}$ or KR-S2) was induced to near endogenous expression levels (Figure 4B). Following 48 hours of siRNA depletion and transgene expression, cell cycle progression was analyzed by timelapse microscopy (Figure 4C). Time course analysis revealed no measurable differences between control and $APC4^{KR-S2}$ expressing cells. No defects in the timing from NEBD to chromosome alignment at the metaphase plate were observed, and importantly, the timing from metaphase alignment to anaphase onset was normal (Figure 4D-E). On average, control cells took 22.83 minutes to progress from NEBD-metaphase and 27.42 minutes from metaphase to anaphase, while $APC4^{KR-S2}$ cells took 24.58 minutes to progress from NEBD-metaphase and 25.08 minutes from metaphase to anaphase. Thus, fusing SUMO2 to the C-terminus of $APC4^{KR}$ rescues the requirement for sumoylation at K772 and K798, a demonstration of the functionality of the linear fusion protein. The absence of any overt consequences on cell cycle progression reveals that forced sumoylation of APC4 alone does not cause untimely APC/C activation.

APC4 sumoylation enhances APC/C ubiquitin E3 ligase activity

Collectively, our findings suggest that sumoylation of APC4 may function downstream of spindle checkpoint inactivation to enhance APC/C activity and the degradation of Cyclin B1 and other target proteins. To directly measure the effects of APC4 sumoylation on APC/C activity, we performed *in vitro* ubiquitylation assays using APC/C complexes immunopurified from our stable, inducible cell lines and recombinant N-terminal fragment of Cyclin B1 as a substrate. APC/C was immunopurified from FLAG-tagged APC4 and APC4^{KR-S2} cell lysates using anti-FLAG antibodies conjugated to Affi-Prep beads under conditions where sumoylation of the wild type protein was undetectable (Figure 4F). Immunoblot analysis using antibodies for APC2 demonstrated that equivalent levels in intact complexes were isolated under each condition (Figure 4G). The ubiquitylation of Cyclin B1 was monitored by immunoblot analysis after 15, 30, and 60 min reaction times (Figure 4H). Consistent with our *in vivo* evidence suggesting that APC4 sumoylation enhances rates of Cyclin B1 turnover (Figure 2F), this assay revealed that APC4^{KR-S2} complexes more efficiently ubiquitylate Cyclin B1 compared to wild-type APC4 complexes (Figure 4H and I). Relatively modest ubiquitylation in our hands may be due to close proximity of FLAG-APC4 to the catalytic center

of the APC/C, but our assays nonetheless demonstrate the laddering typical of *in vitro* ubiquitylation reactions.

APC2 contains a conserved C-terminal SIM critical for APC/C function

To investigate the underlying mechanism of how APC4 sumoylation stimulates APC/C activity, we analyzed previously published high-resolution Cryo-EM structures of the APC/C from the Barford, Schulman, and Yamano groups[17,19,20,55–57]. While the extreme C-terminal residues of APC4 (residues 757-808) containing the sumoylation sites are disordered and not visible in these structures, the location of the visible C-terminus (residue 756) suggests that sumoylated APC4 residues are in close proximity (within ~35 Å) to the C-terminus of APC2 (Figure 5A). Notably, APC2 is part of the structurally dynamic catalytic core of APC/C and critical for E2 binding and positioning[56,57]. Sequence analysis of APC2 revealed a potential SIM in the C-terminus that is conserved across mammals (Figure 5B, 6A). The SIM consists of a stretch of hydrophobic residues followed by negatively charged aspartic acid residues from 727-738, just prior to the winged helix B domain that is critical for APC/C activity[57,58].

To determine whether this predicted SIM mediates interactions between APC2 and SUMO, we expressed wild type APC2 and a SIM

mutant, containing alanine substitutions at residues 728 and 729 (Figure 5B), in rabbit reticulocyte lysate supplemented with [^{35}S]-methionine. Translated proteins were pulled down with immobilized recombinant GST or a recombinant GST-SUMO fusion protein (GST-SUMO2x3), and binding was evaluated by SDS-PAGE and autoradiography as well as scintillation counting. This analysis revealed specific interactions between APC2 and SUMO2 that was dependent on the predicted C-terminal SIM (Figures 5C-E). Binding assays performed using deletion mutants verified the presence of this single functional SIM in the C-terminus of APC2 (Sup. Figure A-D).

Based on its predicted proximity to sumoylated APC4 residues, we hypothesized that non-covalent interactions between the C-terminus of APC2 and SUMO may contribute to the observed effects of APC4 sumoylation on APC/C activity. To test this hypothesis, we generated stable cell lines allowing for inducible expression of FLAG-tagged wild type APC2 or the APC2 SIM mutant defective (APC2^{SM}) in SUMO binding. Endogenous APC2 was depleted by siRNA knockdown in the presence and absence of concomitant transgene expression (Figure 6B) and effects on cell cycle progression were evaluated by timelapse microscopy. As expected, depletion of APC2 resulted in severe mitotic defects comparable to those observed in APC4-depleted cells, although defects were only observed in

~50% of cells, presumably due to incomplete knockdown (Figure 6B and C). Expression of FLAG-APC2 SIM mutant was much less effective than expression of wild type FLAG-APC2 in rescuing APC2 depletion defects. In particular, although all cells progressed from NEBD to metaphase normally, a significant fraction exhibited prolonged metaphase delays comparable to those observed in APC4^{KR} expressing cells (Figure 6D-G). On average, APC2 cells spent 24.53 minutes to progress from NEBD-metaphase and 18.3 minutes from metaphase to anaphase, while APC2^{SM} cells spent 24.43 minutes to progress from NEBD-metaphase and 35.07 minutes from metaphase to anaphase. These findings support the notion that APC2 SUMO binding promotes APC/C activity and anaphase onset. Because the C-terminal domain of APC2 plays a critical role in recruiting and positioning UbcH10~Ub for catalysis and is flexible[56,57], we propose that APC4 sumoylation stabilizes a conformation that is optimal for UbcH10 binding and substrate modification (Figure 7).

SIM binding is required for APC/C function

To evaluate if SUMO recognition by the SIM in APC2 is functionally important, we generated mutations in the second β-strand of SUMO2 critical for SIM binding[59–61]. A stable cell line expressing a SIM binding mutant was

expressed, wherein alanine substitutions at glutamine 35, phenylalanine 36, and isoleucine 38 (SUMO2-QFI or $SUMO2^{QFI}$) were made to the linear FLAG-$APC4^{KR\text{-}S2}$ transgene (Figure 7A). Following endogenous APC4 depletion and doxycycline-induced expression (Figure 7C), cells were imaged using timelapse microscopy. On average, control cells spent 28.59 minutes from NEBD-metaphase, while $APC4^{KR}SUMO2^{QFI}$ expressing cells spent 34.89 minutes. This difference is not statistically significant difference ($p = 0.097$). However, control cells spent 18.28 minutes on average transitioning from metaphase-anaphase, while $APC4^{KR}SUMO2^{QFI}$ cells spent 53.15 minutes, a statistically significant difference ($p = 0.0011$). These data rule out the possibility that APC4 sumoylation has steric effects on APC/C activity and demonstrate that SIM recognition of sumoylated APC4 is functionally important for normal mitotic progression.

DISCUSSION

During early stages of mitosis, the SAC generates well characterized inhibitory signals to block APC/C activity and anaphase onset[2,4–6]. Signals and mechanisms acting downstream of SAC silencing that function to regulate APC/C activity and specificity, however, are less well understood. Here, we have shown that sumoylation is required for optimal activation of APC/C following chromosome alignment and checkpoint silencing. We have identified sumoylation sites in the C-terminus of APC4 and a SIM in the cullin-homology domain of APC2 that are both critical for optimal APC/C function at the metaphase-anaphase transition. Based on our findings, we propose that interactions between sumoylated APC4 and APC2 stabilize a conformation of the APC/C catalytic core that enhances E2 binding and substrate ubiquitylation.

APC4 Sumoylation Stimulates the APC/C

Several lines of evidence indicate that sumoylation is required for APC/C activity after SAC is satisfied. First, cells expressing sumoylation deficient APC4^{KR}, SUMO-binding deficient APC2^{SM}, and SIM-binding deficient APC4^{KR}SUMO2^{QFI} undergo normal progression from NEBD to metaphase plate alignment, but exhibit delays during the metaphase-

anaphase transition, accompanied by delays in Cyclin B1 degradation. Second, mimicking constitutive APC4 sumoylation through expression of $APC4^{KR\text{-}S2}$ had no adverse effects on progression through mitosis, demonstrating that APC4 sumoylation alone is insufficient to affect APC/C activation prior to SAC silencing. Furthermore, $APC4^{KR\text{-}S2}$ rescued the metaphase delay observed in $APC4^{KR}$ cells, further suggesting that sumoylation functions downstream of checkpoint silencing to stimulate APC/C activity. Additional analysis of kinetochore localization of SAC proteins in APC4 and $APC4^{KR}$-expressing metaphase cells indicated that sumoylation is not required to downregulate MCC assembly at kinetochores. Finally, weakening the SAC with the Mps1 kinase inhibitor reversine significantly reduced total mitotic timing and precocious anaphase in APC4 cells but not in $APC4^{KR}$ cells. Importantly, whether APC4 sumoylation affects MCC disassembly from the APC/C is yet unknown.

Metaphase delays downstream of SAC inactivation like those observed in $APC4^{KR}$-, $APC2^{SM}$-, and $APC4^{KR}SUMO2^{QFI}$ expressing cells are unusual and have only been observed in a limited number of cases. In one example, the spindle and kinetochore-associated (Ska) complex has been proposed to promote APC/C localization to chromosomes with the effect of stimulating Cyclin B1 and securin degradation[62]. Although it is unclear how

chromosomal localization affects APC/C activity, it is interesting to speculate that this may involve sumoylation of APC4 by one of the known chromosome-associated SUMO E3 ligases, RanBP2/Nup358 or PIASγ[63,64]. Additionally, mutations that inactivate Ube2S, the ubiquitin E2 conjugating enzyme responsible for elongating K11-linked polyubiquitin chains on APC/C substrates, also lead to delays in anaphase onset[65]. This defect is due in part to inefficient turnover of inhibitory MCC proteins, and is thus checkpoint dependent[16]. While we have ruled out a dependence on SAC signaling using the Mps1 kinase inhibitor reversine, APC4^{KR}- and APC4^{SM}-expressing cells may similarly be affected by reduced turnover of MCC proteins.

Temporal regulation of APC4 sumoylation

APC4 sumoylation is detectable in all other stages of the cell cycle, but peaks during the metaphase-anaphase transition. The factors controlling APC4 sumoylation levels remain largely uncharacterized, but may include SUMO E3 ligases. For example, RanBP2 and PIASγ control sumoylation of topoisomerase I I α (Topo IIα) during mitosis. In mouse embryonic fibroblasts, RanBP2 mediates SUMO1 modification of Topo IIα resulting in appropriate localization to inner centromeres and promoting DNA

decatenation[63]. Furthermore, in Xenopus egg extracts, PIASγ mediates SUMO2/3 modification of Topo IIα, regulating appropriate disjunction of sister chromatids before anaphase[64]. Both RanBP2 and PIASγ localize to centromeres during mitosis, and may also regulate APC4 sumoylation in a spatiotemporal manner, as APC/C also localizes to centromeres during mitosis. Further characterization of SUMO E3 ligases affecting APC4 modification will deepen our current understanding of SUMO-dependent APC/C activation.

Another possible regulator of APC4 sumoylation during mitosis is the SUMO isopeptidase, SENP1. SENP1 is a critical for timely progression during the metaphase-anaphase transition[26]. Notably, SENP1 depletion leads to elevated levels of APC4 sumoylation, suggesting that APC4 is a bona fide substrate (Sup. Figure 1C). APC4 sumoylation levels increase specifically during the metaphase-anaphase transition, followed by a subsequent decrease coinciding with Cyclin B1 degradation. These collective findings suggest that the dynamic regulation of APC4 sumoylation may be under the spatiotemporal control of SENP1 activity. How SENP1 function or recognition of APC4 may be temporally regulated throughout the cell cycle remains to be determined. Furthermore, the C-terminus of APC4 is phosphorylated at residues S777 and S779 during mitosis[19] that lie in close

proximity to the APC4 sumoylation sites. Previous evidence for phosphorylation-dependent sumoylation has been described[24,66], leaving an additional possibility that APC4 sumoylation may also be under the regulatory control of mitotic kinases.

Sumoylation as a modulator of the catalytic core

Canonical cullin-RING ligases include cullin and RING proteins, and the catalytic center of the APC/C is composed of APC2 and APC11, which contain cullin and RING homology domains, respectively. Domains within the C-terminus of APC2, including the cullin homology domain, facilitate cooperative interactions with APC11 and a partner E2, UbcH10 (Figure 5B). Specifically, a C-terminal α/β domain is essential for binding APC11-RING, and a distal winged helix B (WHB) domain makes direct contacts with UbcH10[55,57]. Substrate ubiquitylation is thus dependent on the coordination of the cullin-RING-E2 module, which forms the active site of the APC/C. APC2-11 is known to adopt multiple conformations that are responsive to MCC binding and release, Cdc20 co-activator binding, and the recruitment of ubiquitin-charged UbcH10[14,55–57]. How dynamics of the catalytic center are regulated and how specific conformations of the catalytic center are stabilized are yet unknown. Recent structural studies have shown that

UbcH10 binding is one factor that limits the degrees of freedom of APC2-11[57]. Functional studies have shown that binding and stabilizing interactions between APC2 and UbcH10 are required for optimal substrate ubiquitylation[17]. Therefore, subtle changes in conformation and stability induced by UbcH10 binding have significant effects on activity. Our studies have identified sumoylation as another mechanism for affecting conformation and stability of the catalytic core.

We have identified a functionally important SIM, located within the cullin homology domain of APC2 and linking the α/β and WHB domains (Figure 5B). The position of this SIM suggests that SUMO binding stabilizes a conformation of the catalytic core optimal for UbcH10 recruitment, APC/C catalysis and substrate ubiquitylation. Both the APC4 SUMO modification sites and the APC2 SIM are conserved in mammals (Sup. Figure 1A, Figure 5B), consistent with a functional connection between these domains in higher eukaryotes. Notably, both the APC4 sumoylation sites and the SIM are located within domains that are unstructured in current structures. We propose that sumoylation stabilizes these flexible domains and importantly, the catalytic core of the APC/C. Consistently, our *in vivo* studies show that both APC4 SUMO and APC2 SIM mutants result in metaphase-anaphase delays, indicative of defects in APC/C activity. The linear APC4^{KR}SUMO2

fusion rescues the metaphase-anaphase delay observed in the APC4^{KR} mutant, while mutations in SUMO2 that disrupt SIM recognition does not. Taken together, these data establish a functional relationship between APC2 SIM recognition and APC4 sumoylation during the metaphase-anaphase transition. Finally, *in vitro* studies demonstrate that APC4 sumoylation stimulates APC/C-mediated Cyclin B1 ubiquitylation. A formal test of our model will benefit from structural studies of sumoylated APC/C.

There is precedence for ubiquitin-like modifications of other cullin-RING E3s that influence catalysis. For example, NEDD8 modifies a lysine residue in the cullin of Rbx1 that leads to conformational changes and prevents binding of the Rbx1 inhibitor, CAND1[67]. NEDDylation releases the cullin-RING domain of Rbx1 from conformational constraints, which results in enhanced catalysis and substrate ubiquitylation[67]. In contrast, we propose that sumoylation of APC4 stabilizes a conformation that limits the geometries of the cullin-RING-E2 catalytic module, resulting in APC/C activation. NEDDylation of APC/C subunits have yet to be characterized. However, NEDDylation likely regulates cullin-RING E3 ligases through mechanisms distinct from sumoylation, and it is unlikely that sumoylation replaces the functional role of NEDDylation in the context of the APC/C or other cullin-RING E3 ligases.

SUMO has been previously found to affect multiple other enzymatic processes. For example, sumoylation has been proposed to promote the turnover of thymidine DNA glycosylase (TDG) during base excision repair. Structural studies suggest that sumoylated TDG adopts different conformations mediated by intramolecular SIM interactions, reducing affinity to DNA *in vitro*[68,69]. However, it remains to be determined if this model holds true *in vivo*[70]. In addition, SUMO modification is important for other cellular processes such as transcription, chromatin remodeling, and DNA damage repair[23]. Furthermore, ribosomes[29], PML nuclear bodies[27,28,71], and kinetochores[30–32] require SUMO modification for assembly and activity. In these examples, SUMO functions by enhancing protein-protein interactions through non-covalent SIM binding to promote assembly of functional complexes. In contrast to these previously characterized examples, we propose that APC4 SUMO modification is a stabilizing factor mediating intermolecular interactions of a pre-assembled molecular machine. This novel role for sumoylation may also function to stabilize and coordinate SUMO-SIM interactions across proteins within other pre-assembled complexes, thereby regulating protein conformation and modulating function.

In summary, we have shown that both covalent SUMO modification and non-covalent SIM-mediated binding play important roles in regulating APC/C activity and mitotic exit. We propose that SUMO-SIM interactions function to stabilize the cullin-RING-E2 module of the multi-subunit APC/C in an active conformation, thereby stimulating catalytic activity. While additional molecular mechanisms affecting APC/C activity downstream of checkpoint silencing have yet to be determined, here we identify sumoylation as a critical post-translational regulator of the metaphase-anaphase transition. Importantly, inhibitors to the SUMO pathway are currently being developed for chemotherapeutic use, and our studies provide molecular insights into how these inhibitors may function to inhibit cell division.

REFERENCES

1. Kops, Weaver & Cleveland. On the road to cancer: aneuploidy and the mitotic checkpoint. Nature Reviews Cancer 5, 773–785 (2005).

2. Foley & Kapoor. Microtubule attachment and spindle assembly checkpoint signalling at the kinetochore. Nature Reviews Molecular Cell Biology 14, nrm3494 (2012).

3. Lara-Gonzalez, Westhorpe & Taylor. The Spindle Assembly Checkpoint. Current Biology 22, R966–R980 (2012).

4. Musacchio & Salmon. The spindle-assembly checkpoint in space and time. Nature Reviews Molecular Cell Biology 8, 379–393 (2007).

5. Musacchio. The Molecular Biology of Spindle Assembly Checkpoint Signaling Dynamics. Current Biology 25, R1002–R1018 (2015).

6. Sivakumar & Gorbsky. Spatiotemporal regulation of the anaphase-promoting complex in mitosis. Nature Reviews Molecular Cell Biology 16, nrm3934 (2015).

7. Collin, Nashchekina, Walker & Pines. The spindle assembly checkpoint works like a rheostat rather than a toggle switch. Nature Cell Biology 15, 1378–1385 (2013).

8. Pines. Cubism and the cell cycle: the many faces of the APC/C. Nature Reviews Molecular Cell Biology 12, nrm3132 (2011).

9. Matyskiela & Morgan. Analysis of Activator-Binding Sites on the APC/C Supports a Cooperative Substrate-Binding Mechanism. Molecular Cell 34, 68–80 (2009).

10. Acquaviva, Herzog, Kraft & Pines. The anaphase promoting complex/cyclosome is recruited to centromeres by the spindle assembly checkpoint. Nature Cell Biology 6, ncb1167 (2004).

11. Jörgensen, Brundell, Starborg & Höög. A Subunit of the Anaphase-Promoting Complex Is a Centromere-Associated Protein in Mammalian Cells. Molecular and Cellular Biology 18, 468–476 (1998).

12. Topper et al. The Dephosphorylated Form of the Anaphase-Promoting Complex Protein Cdc27/Apc3 Concentrates on Kinetochores and Chromosome Arms in Mitosis. Cell Cycle 1, 287–297 (2002).

13. Herzog et al. Structure of the Anaphase-Promoting Complex/Cyclosome Interacting with a Mitotic Checkpoint Complex. Science (New York, N.Y.) 323, 1477 (2009).

14. Chang, Zhang, Yang, McLaughlin & Barford. Molecular architecture and mechanism of the anaphase-promoting complex. Nature 513, nature13543 (2014).

15. Brown et al. Mechanism of Polyubiquitination by Human Anaphase-Promoting Complex: RING Repurposing for Ubiquitin Chain Assembly. Molecular Cell 56, 246–260 (2014).

16. Kelly, Wickliffe, Song, Fedrigo & Rape. Ubiquitin Chain Elongation Requires E3-Dependent Tracking of the Emerging Conjugate. Molecular Cell 56, 232–245 (2014).

17. Brown et al. Dual RING E3 Architectures Regulate Multiubiquitination and Ubiquitin Chain Elongation by APC/C. Cell 165, 1440–1453 (2016).

18. Davey & Morgan. Building a Regulatory Network with Short Linear Sequence Motifs: Lessons from the Degrons of the Anaphase-Promoting Complex. Molecular Cell 64, 12–23 (2016).

19. Zhang et al. Molecular mechanism of APC/C activation by mitotic phosphorylation. Nature 533, 260–264 (2016).

20. Qiao et al. Mechanism of APC/CCDC20 activation by mitotic phosphorylation. Proceedings of the National Academy of Sciences 113, E2570–E2578 (2016).

21. Fujimitsu, Grimaldi & Yamano. Cyclin-dependent kinase 1–dependent activation of APC/C ubiquitin ligase. Science 352, 1121–1124 (2016).

22. Kraft et al. Mitotic regulation of the human anaphase- promoting complex by phosphorylation. The EMBO Journal 22, 6598–6609 (2003).

23. Flotho & Melchior. Sumoylation: A Regulatory Protein Modification in Health and Disease. Annual Review of Biochemistry 82, 357–385 (2013).

24. Gareau & Lima. The SUMO pathway: emerging mechanisms that shape specificity, conjugation and recognition. Nature Reviews Molecular Cell Biology 11, nrm3011 (2010).

25. Mukhopadhyay & Dasso. Modification in reverse: the SUMO proteases. Trends in Biochemical Sciences 32, 286–295 (2007).

26. Cubeñas-Potts, Goeres & Matunis. SENP1 and SENP2 affect spatial and temporal control of sumoylation in mitosis. Molecular biology of the cell 24, 3483–95 (2013).

27. Jentsch & Psakhye. Control of Nuclear Activities by Substrate-Selective and Protein-Group SUMOylation. Annual Review of Genetics 47, 167–186 (2013).

28. Shen, Lin, Scaglioni, Yung & Pandolfi. The Mechanisms of PML-Nuclear Body Formation. Molecular Cell 24, 331–339 (2006).

29. Finkbeiner, Haindl, Raman & Muller. SUMO routes ribosome maturation. Nucleus 2, 527–532 (2011).

30. Zhang et al. SUMO-2/3 Modification and Binding Regulate the Association of CENP-E with Kinetochores and Progression through Mitosis. Molecular Cell 29, 729–741 (2008).

31. Werner, Flotho & Melchior. The RanBP2/RanGAP1∗ SUMO1/Ubc9 Complex Is a Multisubunit SUMO E3 Ligase. Molecular Cell 46, 287–298 (2012).

32. Joseph, Tan, Karpova, McNally & Dasso. SUMO-1 targets RanGAP1 to kinetochores and mitotic spindles. The Journal of Cell Biology 156, 595–602 (2002).

33. Meluh & Koshland. Evidence that the MIF2 gene of Saccharomyces

cerevisiae encodes a centromere protein with homology to the mammalian centromere protein CENP-C. Molecular Biology of the Cell 6, 793–807 (1995).

34. Biggins, Bhalla, Chang, Smith & Murray. Genes involved in sister chromatid separation and segregation in the budding yeast Saccharomyces cerevisiae. Genetics 159, 453–70 (2001).

35. Seufert, Futcher & Jentsch. Role of a ubiquitin-conjugating enzyme in degradation of S- and M-phase cyclins. Nature 373, 78–81 (1995).

36. Dieckhoff, Bolte, Sancak, Braus & Irniger. Smt3/SUMO and Ubc9 are required for efficient APC/C- mediated proteolysis in budding yeast. Molecular Microbiology 51, 1375–1387 (2004).

37. Li et al. SUMOylated NKAP is essential for chromosome alignment by anchoring CENP-E to kinetochores. Nature Communications 7, 12969 (2016).

38. Azuma, Arnaoutov & Dasso. SUMO-2/3 regulates topoisomerase II in mitosis. The Journal of Cell Biology 163, 477–487 (2003).

39. dharan, Park, Ryu & Azuma. SUMOylation Regulates Polo-like Kinase 1-interacting Checkpoint Helicase (PICH) during Mitosis. Journal of Biological Chemistry 290, 3269–3276 (2015).

40. Yang et al. BubR1 Is Modified by Sumoylation during Mitotic Progression. Journal of Biological Chemistry 287, 4875–4882 (2012).

41. Fernández-Miranda et al. SUMOylation modulates the function of Aurora-B kinase. Journal of Cell Science 123, 2823–2833 (2010).

42. Ban, Nishida & Urano. Mitotic kinase Aurora- B is regulated by SUMO- 2/3 conjugation/deconjugation during mitosis. Genes to Cells 16, 652–669 (2011).

43. Matic et al. Site-Specific Identification of SUMO-2 Targets in Cells Reveals an Inverted SUMOylation Motif and a Hydrophobic Cluster SUMOylation Motif. Molecular Cell 39, 641–652 (2010).

44. Schou, Kelstrup, Hayward, Olsen & Nilsson. Comprehensive Identification of SUMO2/3 Targets and Their Dynamics during Mitosis. PLoS ONE 9, e100692 (2014).

45. Schimmel et al. Uncovering SUMOylation Dynamics during Cell-Cycle Progression Reveals FoxM1 as a Key Mitotic SUMO Target Protein. Molecular Cell 53, 1053–1066 (2014).

46. Cubeñas-Potts et al. Identification of SUMO-2/3-modified proteins associated with mitotic chromosomes. Proteomics 15, 763–72 (2015).

47. Chang et al. Structural and Functional Roles of Daxx SIM Phosphorylation in SUMO Paralog-Selective Binding and Apoptosis Modulation. Molecular Cell 42, 62–74 (2011).

48. Yang & Shih. The deubiquitinating enzyme USP37 regulates the oncogenic fusion protein PLZF/RARA stability. Oncogene 32, onc2012537 (2012).

49. Meyer & Rape. Enhanced Protein Degradation by Branched Ubiquitin Chains. Cell 157, 910–921 (2014).

50. Lange et al. Defective sister chromatid cohesion is synthetically lethal with impaired APC/C function. Nature Communications 6, 8399 (2015).

51. Joseph, Liu, Jablonski, Yen & Dasso. The RanGAP1-RanBP2 Complex Is Essential for Microtubule-Kinetochore Interactions In Vivo. Current Biology 14, 611–617 (2004).

52. Santaguida, Tighe, D'Alise, Taylor & Musacchio. Dissecting the role of MPS1 in chromosome biorientation and the spindle checkpoint through the small molecule inhibitor reversine. The Journal of Cell Biology 190, 73–87 (2010).

53. Holmstrom, Antwerp & Iñiguez-Lluhí. Direct and distinguishable inhibitory roles for SUMO isoforms in the control of transcriptional synergy. Proceedings of the National Academy of Sciences 100, 15758–15763 (2003).

54. Yurchenko, Xue & Sadofsky. SUMO Modification of Human XRCC4

Regulates Its Localization and Function in DNA Double-Strand Break Repair. Molecular and Cellular Biology 26, 1786–1794 (2006).

55. Alfieri et al. Molecular basis of APC/C regulation by the spindle assembly checkpoint. Nature 536, 431–436 (2016).

56. Yamaguchi et al. Cryo-EM of Mitotic Checkpoint Complex-Bound APC/C Reveals Reciprocal and Conformational Regulation of Ubiquitin Ligation. Molecular Cell 63, 593–607 (2016).

57. Brown et al. RING E3 mechanism for ubiquitin ligation to a disordered substrate visualized for human anaphase-promoting complex. Proceedings of the National Academy of Sciences 112, 5272–5279 (2015).

58. Tang et al. APC2 Cullin Protein and APC11 RING Protein Comprise the Minimal Ubiquitin Ligase Module of the Anaphase-promoting Complex. Molecular Biology of the Cell 12, 3839–3851 (2001).

59. Huang, Ko, Li & Wang. Crystal structures of the human SUMO- 2 protein at 1.6 Å and 1.2 Å resolution. European Journal of Biochemistry 271, 4114–4122 (2004).

60. Sun, Leverson & Hunter. Conserved function of RNF4 family proteins in eukaryotes: targeting a ubiquitin ligase to SUMOylated proteins. The EMBO Journal 26, 4102–4112 (2007).

61. Zhu et al. Small Ubiquitin-related Modifier (SUMO) Binding Determines Substrate Recognition and Paralog-selective SUMO Modification. Journal of Biological Chemistry 283, 29405–29415 (2008).

62. Sivakumar, Daum, Tipton, Rankin & Gorbsky. The spindle and kinetochore–associated (Ska) complex enhances binding of the anaphase-promoting complex/cyclosome (APC/C) to chromosomes and promotes mitotic exit. Molecular Biology of the Cell 25, 594–605 (2014).

63. Dawlaty et al. Resolution of Sister Centromeres Requires RanBP2-Mediated SUMOylation of Topoisomerase IIα. Cell 133, 103–115 (2008).

64. Ryu, Furuta, Kirkpatrick, Gygi & Azuma. PIASy-dependent SUMOylation regulates DNA topoisomerase IIα activity. The Journal of

Cell Biology 191, 783–794 (2010).

65. Williamson et al. Identification of a physiological E2 module for the human anaphase-promoting complex. Proceedings of the National Academy of Sciences 106, 18213–18218 (2009).

66. Hietakangas et al. PDSM, a motif for phosphorylation-dependent SUMO modification. Proceedings of the National Academy of Sciences of the United States of America 103, 45–50 (2006).

67. Duda et al. Structural Insights into NEDD8 Activation of Cullin-RING Ligases: Conformational Control of Conjugation. Cell 134, 995–1006 (2008).

68. Baba et al. Crystal structure of thymine DNA glycosylase conjugated to SUMO-1. Nature 435, nature03634 (2005).

69. Hardeland, Steinacher, Jiricny & Schär. Modification of the human thymine- DNA glycosylase by ubiquitin- like proteins facilitates enzymatic turnover. The EMBO Journal 21, 1456–1464 (2002).

70. McLaughlin, Coey, Yang, Drohat & Matunis. Characterizing Requirements for Small Ubiquitin-like Modifier (SUMO) Modification and Binding on Base Excision Repair Activity of Thymine-DNA Glycosylase in Vivo. Journal of Biological Chemistry 291, 9014–9024 (2016).

71. Matunis, Zhang & Ellis. SUMO: The Glue that Binds. Developmental Cell 11, 596–597 (2006).

Figure 2-1

APC4 is sumoylated in a cell-cycle dependent manner at two C-terminal lysines.

(A) HeLa cells were synchronized in S-phase using a double-thymidine arrest and released for varying time points. Whole cell lysates were analyzed by immunoblotting for APC4, Cyclin B1, Cdc20, and glyceraldehyde 3-phosphate dehydrogenase (GAPDH) as a loading control. Asterisks indicate sumoylated forms of APC4. (B) APC4 contains two C-terminal SUMO consensus site lysines at 772 and 798. (C) Full length wild type APC4 or the indicated lysine to alanine substitution mutants were expressed in rabbit reticulocyte lysate in the presence of [^{35}S]-methionine and incubated for the indicated times in modification reactions containing SUMO E1 and E2 enzymes and SUMO2. Proteins were detected by SDS-PAGE and autoradiography. Asterisks indicate sumoylated forms of APC4. (D) Constructs coding for FLAG-tagged versions of wild type APC4 or a sumoylation-deficient mutant containing arginine substitutions at lysines 772 and 798 (APC4^{KR}) were used to generate stable inducible cell lines in YFP-H2B HeLa cells. (E) Endogenous APC4 was depleted by siRNA, and FLAG-APC4 or FLAG-APC4^{KR} stable cell lines were induced by doxycycline for 48 h. Immunoblot analysis using APC4 and tubulin specific

antibodies reveals that FLAG-APC4 and FLAG-APC4^{KR} are expressed at near endogenous levels. (F-G) Co-immunoprecipitations were performed with an antibody against APC4, followed by immunoblotting for APC4 or SUMO2. FLAG-APC4 is sumoylated *in vivo* while FLAG-APC4^{KR} is not. Asterisks indicate sumoylated APC4.

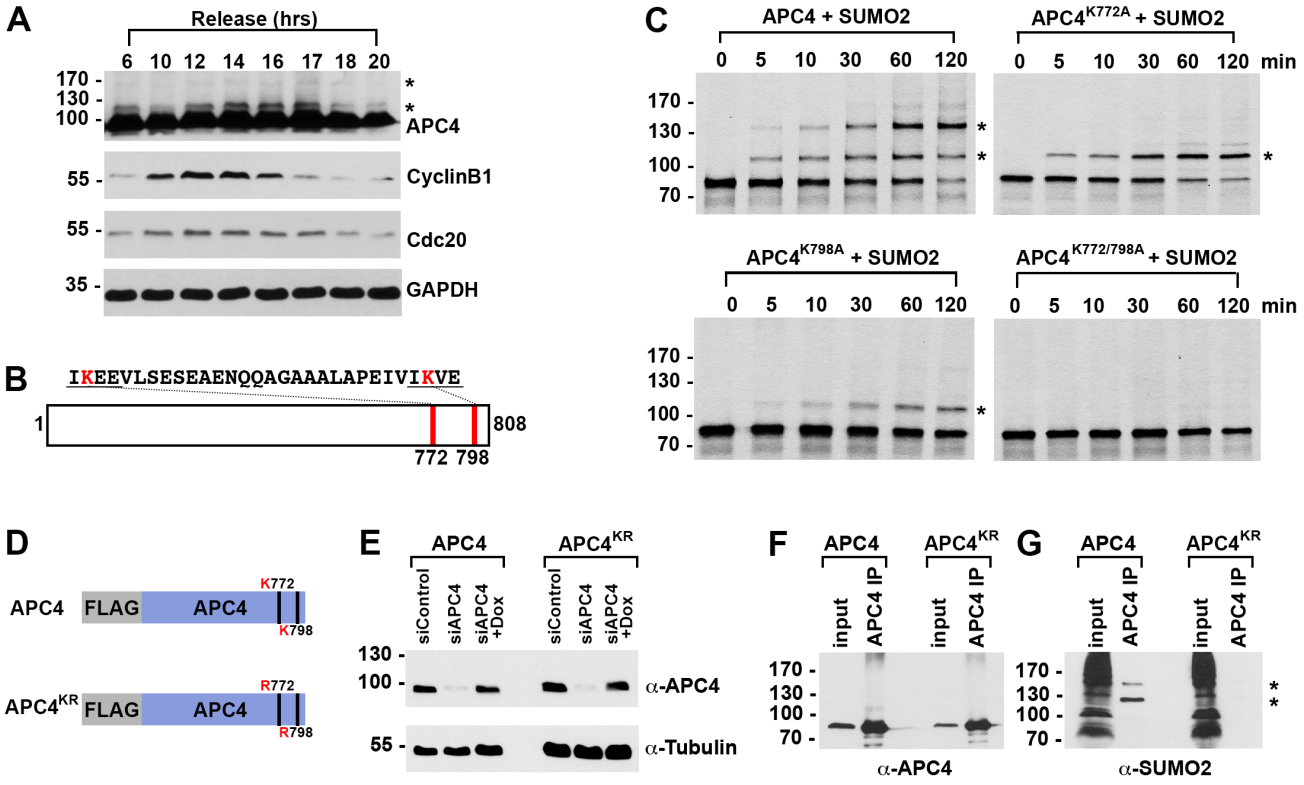
A
Release (hrs)
6 10 12 14 16 17 18 20
170 -
130 -
100 -
APC4
55 -
CyclinB1
55 -
Cdc20
35 -
GAPDH
B
IKEEVLSESEAENQQAGAAALAPEIVIKVE
1
808
772 798
C
APC4 + SUMO2
APC4K772A + SUMO2
0 5 10 30 60 120 min
170 -
130 -
100 -
70 -
APC4K798A + SUMO2
APC4K772/798A + SUMO2
D
APC4
FLAG
APC4
K772
K798
APC4KR
R772
R798
E
APC4
APC4KR
siControl
siAPC4
siAPC4 +Dox
130 -
100 -
α-APC4
55 -
α-Tubulin
F
APC4
APC4KR
input
APC4 IP
170 -
130 -
100 -
70 -
α-APC4
G
APC4
APC4KR
input
APC4 IP
α-SUMO2

FIGURE 2-2

APC4 is sumoylated *in vivo* and *in vitro* at two C-terminal lysine residues; APC4 sumoylation is regulated by SENP1.

(A) U2OS or 6xHis-SUMO2 U2OS cells were synchronized in different stages of the cell cycle. Cells were lysed in 6M guanidine HCl lysis buffer, immunopurified with Ni-NTA agarose, washed in buffers containing 8M urea, and analyzed by SDS-PAGE and immunoblotting with antibodies against APC4 or SUMO2/3. Single asterisks (*) indicates SUMO modified forms of APC4. A double asterisk (**) indicates unconjugated 6xHis-SUMO2. (B) Full length APC4 was expressed *in vitro* and incubated for the indicated times in modification reactions containing SUMO E1 and E2 enzymes and SUMO1. Proteins were detected by autoradiography. APC4 lysine to alanine single mutant ($APC4^{K772A}$ and $APC4^{K798A}$) and a double mutant ($APC4^{K772/798A}$) were expressed *in vitro* and incubated with recombinant SUMO1. Asterisks (*) indicate sumoylated forms of APC4. (C) Endogenous APC4 was depleted by siRNA, and APC4 WT or $APC4^{KR}$ were induced by doxycycline for 48 h. Co-immunoprecipitations were performed with an antibody against APC4, followed by immunoblotting for APC4 or SUMO1. APC4 WT cells are sumoylated *in vivo* while $APC4^{KR}$ is not. Asterisks indicate sumoylated APC4. (D) HeLa cells were treated siRNA

oligos targeting a control, SENP1, or SENP2 as previously described (Cubeñas-Potts et al. 2013b). 36 h following siRNA depletion, cells were arrested into S phase with 2mM thymidine for 19 hours, released for 6 h using a 100 ng/mL nocodazole treatment, followed by a 2 hr treatment with MG132 to synchronize into metaphase. Whole cell lysates were immunoblotted with antibodies specific for APC4, SENP1, SENP2, and GAPDH. Arrows indicate sumoylated forms of APC4.

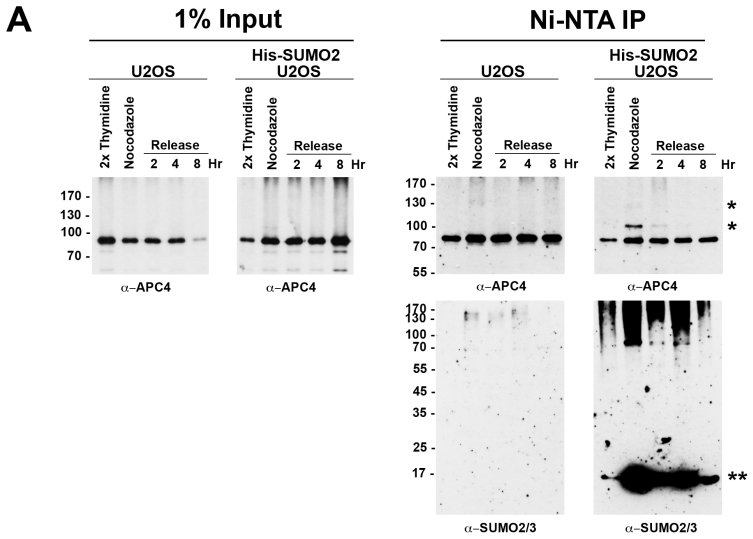
A
1% Input
Ni-NTA IP
U2OS
His-SUMO2 U2OS
2x Thymidine
Nocodazole
Release
2 4 8 Hr
170
130
100
70
55
45
35
25
17
α–APC4
α–SUMO2/3
*
**

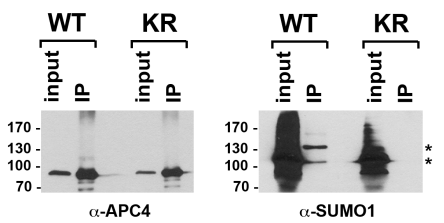
C
WT
KR
input
IP
170
130
100
70
α-APC4
α-SUMO1
*
**

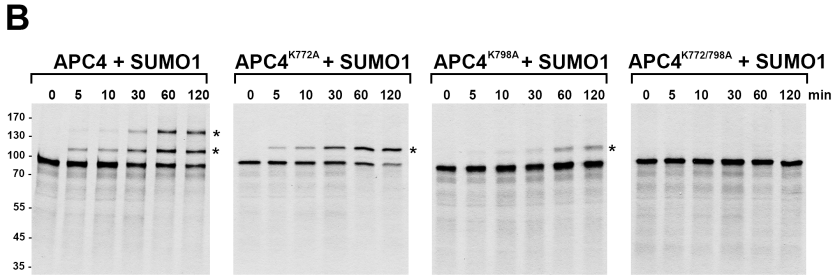
B
APC4 + SUMO1
APC4K772A + SUMO1
APC4K798A + SUMO1
APC4K772/798A + SUMO1
0 5 10 30 60 120 min
170
130
100
70
55
45
35
*

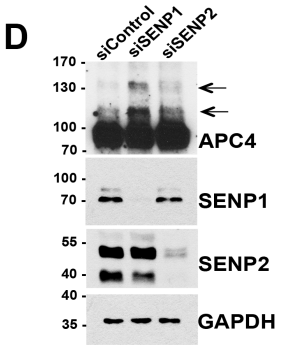
D
siControl
siSENP1
siSENP2
170
130
100
70
55
40
35
APC4
SENP1
SENP2
GAPDH

FIGURE 2-3

APC4 sumoylation is required for normal metaphase to anaphase transition. (A) Cells were treated with or without siRNA to APC4 (Control or siAPC4) for 48 hours followed by 16 hours of timelapse live cell acquisition. siAPC4 treated cells were also induced to express FLAG-APC4 or FLAG-APC4^{KR}. Analysis represents mitotic progression time beginning with nuclear envelope breakdown (NEBD) to anaphase onset. Quantification of mitotic phenotypes is shown. Prolonged metaphase is defined by >60 min in metaphase plate alignment before anaphase onset. Abnormal metaphase is defined by inability to generate a metaphase plate and defects in chromosomal cohesion. n > 100 for each cell line. (B) Cells representative of each mitotic phenotype categorized in (A) are featured with timestamps in min. (C) Mitotic progression beginning with NEBD to metaphase plate alignment and from metaphase plate alignment to anaphase onset was quantified in FLAG-APC4 and FLAG-APC4^{KR} expressing cells. Experiments were performed in triplicate; means are displayed and error bars represent standard deviations. n = 50 for each cell line. Two-tailed t-tests were used to calculate significance: $p = 0.38$ for differences in FLAG-APC4 and FLAG-APC4^{KR} timing from NEBD-metaphase, $p < 0.001$ for differences in FLAG-APC4 and FLAG-APC4^{KR} timing from metaphase

plate alignment to anaphase. (D) Individual timing of metaphase to anaphase progression are displayed for FLAG-APC4 and FLAG-APC4^{KR} expressing cells. n = 215 for each cell line. (E) Representative cells from timelapse acquisition beginning with NEBD to anaphase onset in FLAG-APC4 and FLAG-APC4^{KR} expressing cells with timestamps indicated in min. (F) FLAG-APC4 and (G) FLAG-APC4^{KR} expressing cells were synchronized in S-phase using a double-thymidine arrest and released for various time points. Whole cell lysates were analyzed by immunoblotting for APC4, Cyclin B1, Cdc20 and GAPDH as a loading control. Asterisks (*) indicate sumoylated forms of APC4. (H) Relative protein levels of Cyclin B1 in FLAG-APC4 and FLAG-APC4^{KR} cells were quantitated using ImageJ. Normalized mean values are graphed with standard deviations from three separate experiments.

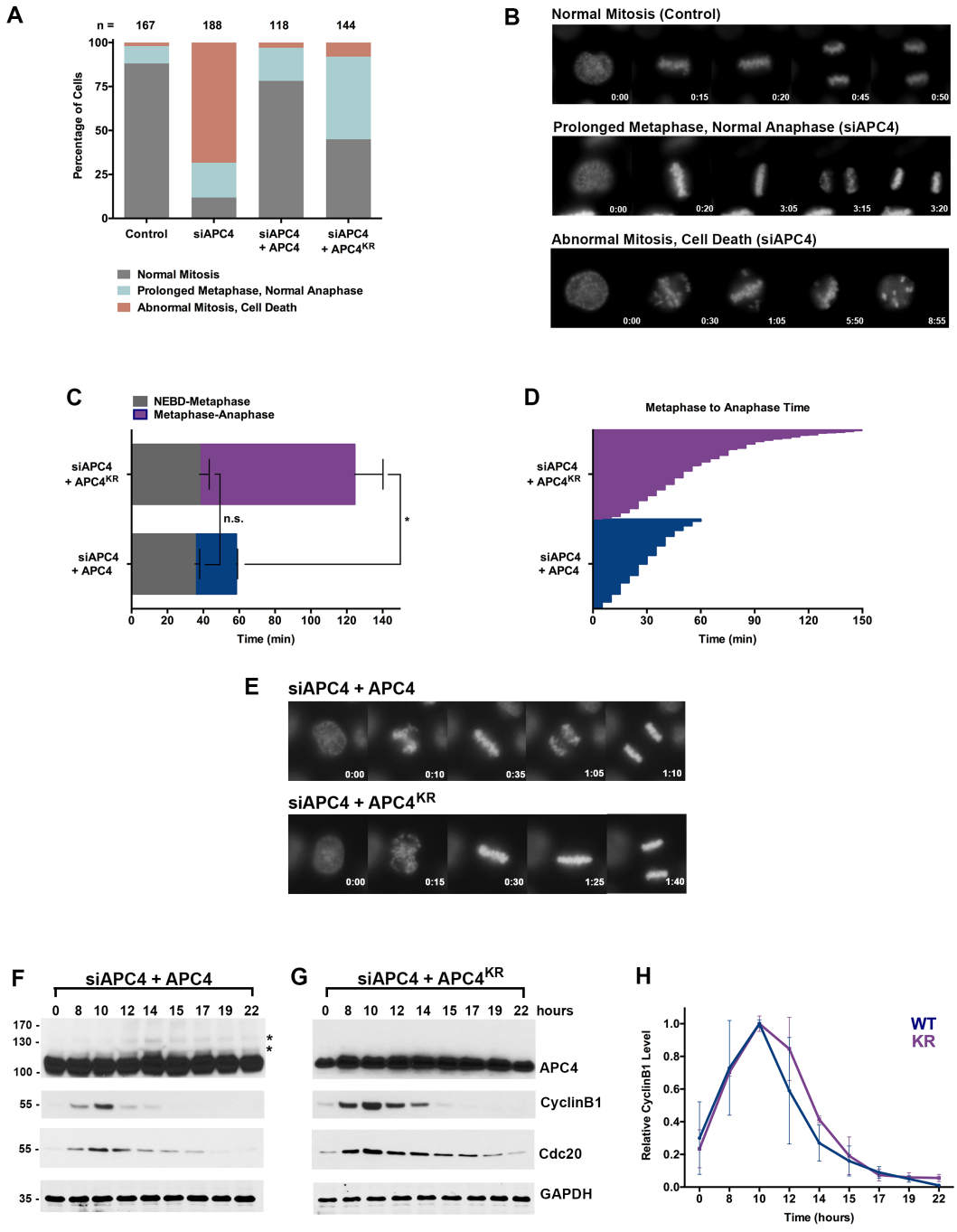
A
n = 167 188 118 144
Percentage of Cells
Control
siAPC4
siAPC4 + APC4
siAPC4 + APC4KR
Normal Mitosis
Prolonged Metaphase, Normal Anaphase
Abnormal Mitosis, Cell Death
B
Normal Mitosis (Control)
Prolonged Metaphase, Normal Anaphase (siAPC4)
Abnormal Mitosis, Cell Death (siAPC4)
C
NEBD-Metaphase
Metaphase-Anaphase
n.s.
Time (min)
D
Metaphase to Anaphase Time
Time (min)
E
siAPC4 + APC4
siAPC4 + APC4KR
F
siAPC4 + APC4
G
siAPC4 + APC4KR
hours
APC4
CyclinB1
Cdc20
GAPDH
H
Relative CyclinB1 Level
Time (hours)
WT
KR

FIGURE 2-4

APC4 sumoylation is well-conserved in mammals and APC4 single SUMO mutant analysis.

(A) Multiple sequence alignments for full length APC4 were compared using Clustal Omega. (B) Constructs coding for FLAG-tagged versions of APC4 sumoylation-deficient mutant containing arginine substitutions at lysines 772 or 798 ($APC4^{772R}$/$APC4^{798R}$) were used to generate stable inducible cell lines in YFP-H2B HeLa cells. (C) Endogenous APC4 was depleted by siRNA, and FLAG-$APC4^{772R}$ or FLAG-$APC4^{798R}$ stable cell lines were induced by doxycycline for 48 h. Immunoblot analysis using APC4 and tubulin specific antibodies reveals that FLAG-$APC4^{772R}$ and FLAG-$APC4^{798R}$ are expressed at near endogenous levels. (D) Cells were treated with or without siRNA to APC4 (Control or siAPC4) for 48 hours followed by 16 hours of timelapse live cell acquisition. Representative cells are featured with timestamps in minutes. (E) Mitotic progression beginning with NEBD to metaphase plate alignment and from metaphase plate alignment to anaphase onset was quantified in FLAG-$APC4^{772R}$ and FLAG-$APC4^{798R}$ expressing cells. Experiments were performed in triplicate; means are displayed and error bars represent standard deviations. $n > 100$ for each cell line. Two-tailed t-tests were used to calculate significance: $p = 0.1551$

for differences in Control vs. and FLAG-APC4^{772R} timing from NEBD-metaphase, p = 0.0724 for differences in Control vs. FLAG-APC4^{798R} timing from NEBD-metaphase; p = 0.0306 for differences in Control vs. FLAG-APC4^{772R} and p = 0.0338 for differences in FLAG-APC4^{798R} timing from metaphase plate alignment to anaphase, respectively. (D) Individual timing of metaphase to anaphase progression are displayed for FLAG-APC4^{772R} and FLAG-APC4^{798R} expressing cells. n = 67 for each cell line.

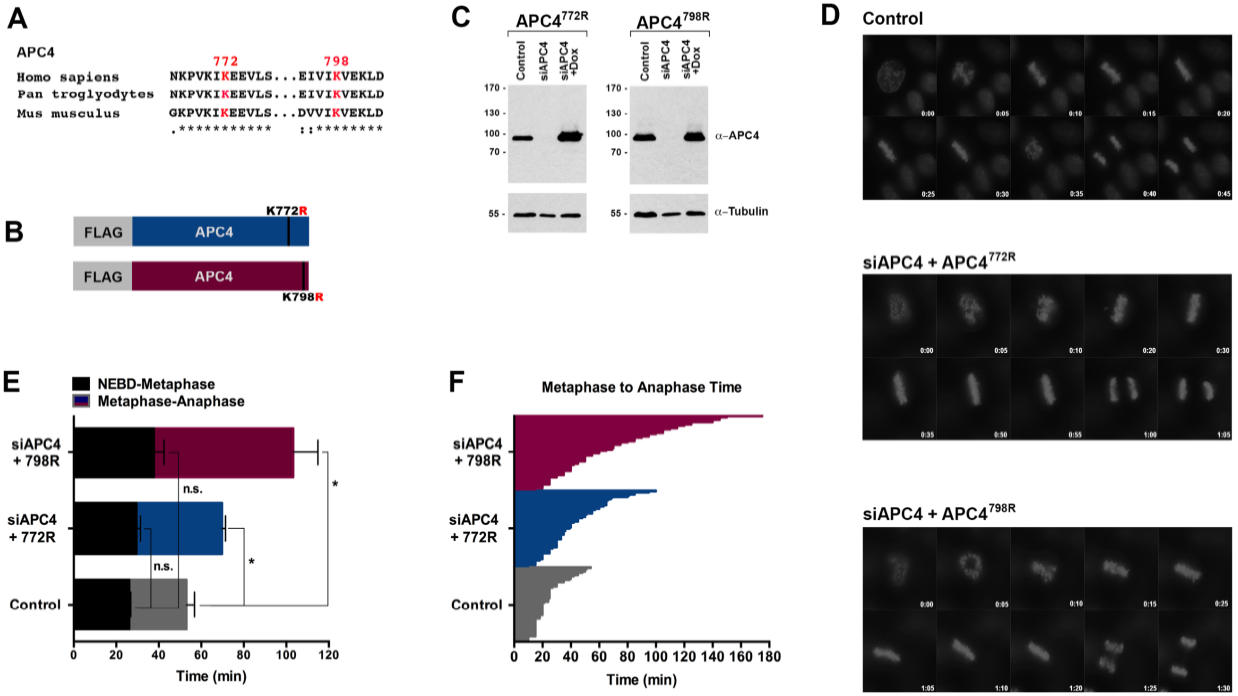
A
APC4
772
798
Homo sapiens NKPVKIKEEVLS...EIVIKVEKLD
Pan troglyodytes NKPVKIKEEVLS...EIVIKVEKLD
Mus musculus GKPVKIKEEVLS...DVVIKVEKLD
B
FLAG
APC4
K772R
K798R
C
APC4772R
APC4798R
Control
siAPC4
siAPC4 +Dox
170
130
100
70
55
α–APC4
α–Tubulin
D
Control
siAPC4 + APC4772R
siAPC4 + APC4798R
E
NEBD-Metaphase
Metaphase-Anaphase
siAPC4 + 798R
siAPC4 + 772R
Control
n.s.
*
Time (min)
F
Metaphase to Anaphase Time
Time (min)

FIGURE 2-5

APC4 sumoylation does not affect APC/C or MCC localization at kinetochores.

(A) Stable inducible cell lines were depleted of endogenous APC4 using siRNA for 48 hours with concomitant induction of FLAG-APC4 or FLAG-APC4^{KR} expression. Cells were stained with FLAG and CREST specific antibodies and analyzed by immunofluorescence microscopy. Boxed regions are magnified to show c-localization at kinetochores during prometaphase and metaphase. (B) Inducible cell lines were treated as in (A) and stained with antibodies specific to Mad1, Mad2, BubR1, and Cdc20 as indicated. Chromatin (colored in teal) was visualized by detection of YFP-H2B expressed in these cell lines.

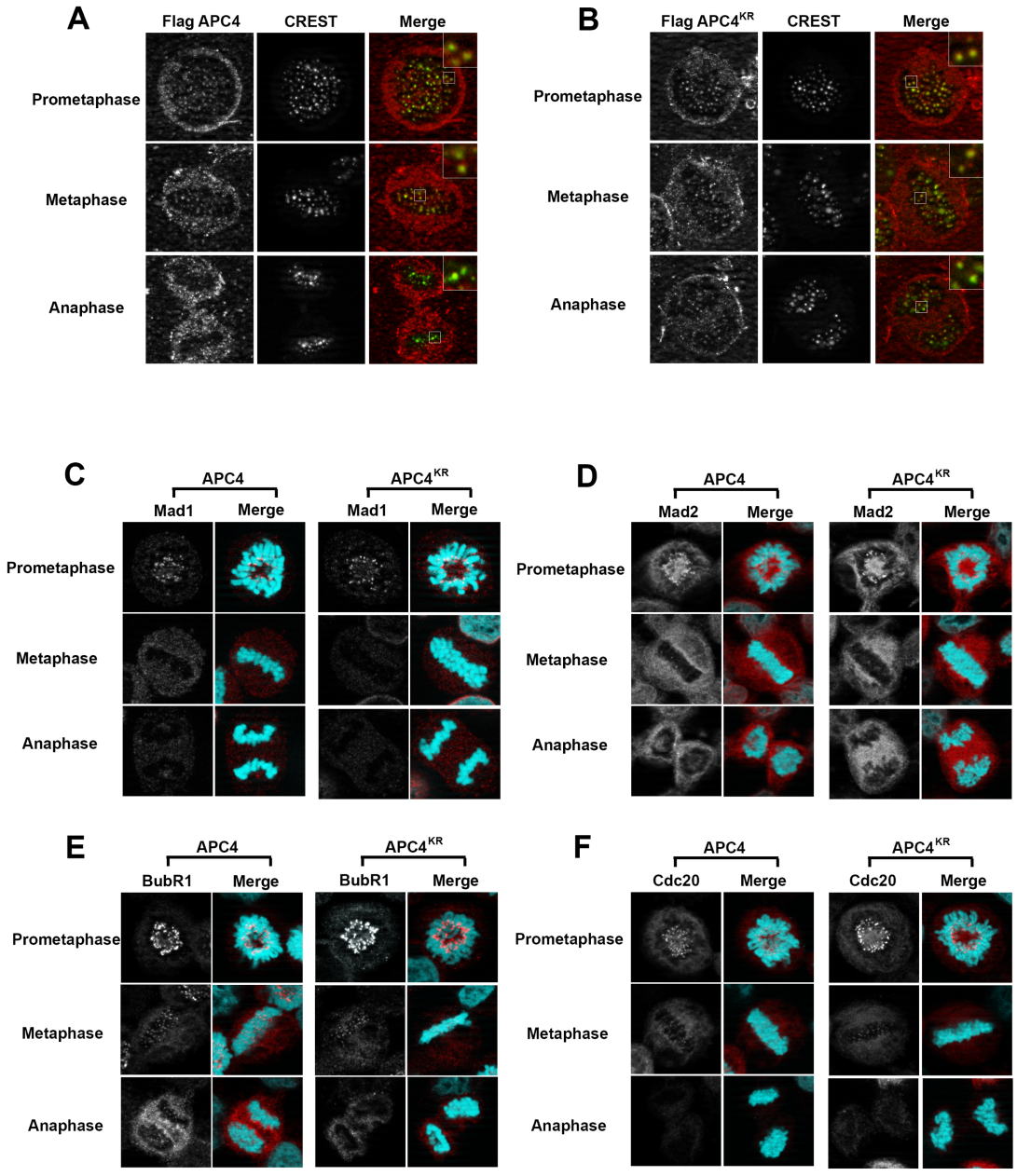
A
Flag APC4
CREST
Merge
Prometaphase
Metaphase
Anaphase
B
Flag APC4KR
CREST
Merge
Prometaphase
Metaphase
Anaphase
C
APC4
APC4KR
Mad1
Merge
Mad1
Merge
Prometaphase
Metaphase
Anaphase
D
APC4
APC4KR
Mad2
Merge
Mad2
Merge
Prometaphase
Metaphase
Anaphase
E
APC4
APC4KR
BubR1
Merge
BubR1
Merge
Prometaphase
Metaphase
Anaphase
F
APC4
APC4KR
Cdc20
Merge
Cdc20
Merge
Prometaphase
Metaphase
Anaphase

FIGURE 2-6

APC4 Sumoylation is critical downstream of Spindle Assembly Checkpoint inactivation

(A) Endogenous APC4 was depleted by siRNA, and FLAG-APC4 or FLAG-APC4^{KR} stable cell lines were induced by doxycycline for 48 h. Immunoblot analysis using APC4 and tubulin specific antibodies reveals that FLAG-APC4 and FLAG-APC4^{KR} are expressed at near endogenous levels. (B) Cells were treated with reversine immediately prior to 4 hr timelapse acquisition, and timing from NEBD to anaphase onset (mitotic exit timing) was collected. Data are representative of 4 independent experiments, n = 23 for each cell line. On average, FLAG-APC4 cells take 48.65 min to mitotic exit (Standard Deviation = SD = 15.99) while reversine treated FLAG-APC4 cells take 34.87 min (SD = 11.00). This difference is significant (p = 0.0014). FLAG-APC4^{KR} cells take 81.48 min to mitotic exit (SD = 30.78) while reversine treated FLAG-APC4^{KR} cells take 78.78 min (SD = 21.41). This difference is not statisitically significant (p = 0.73). Two-tailed t-tests were used to calculate significance. (C-F) Representative cells from timelapse acquisition beginning with NEBD to anaphase onset in cells with or without reversine are shown with timestamps indicated in min.

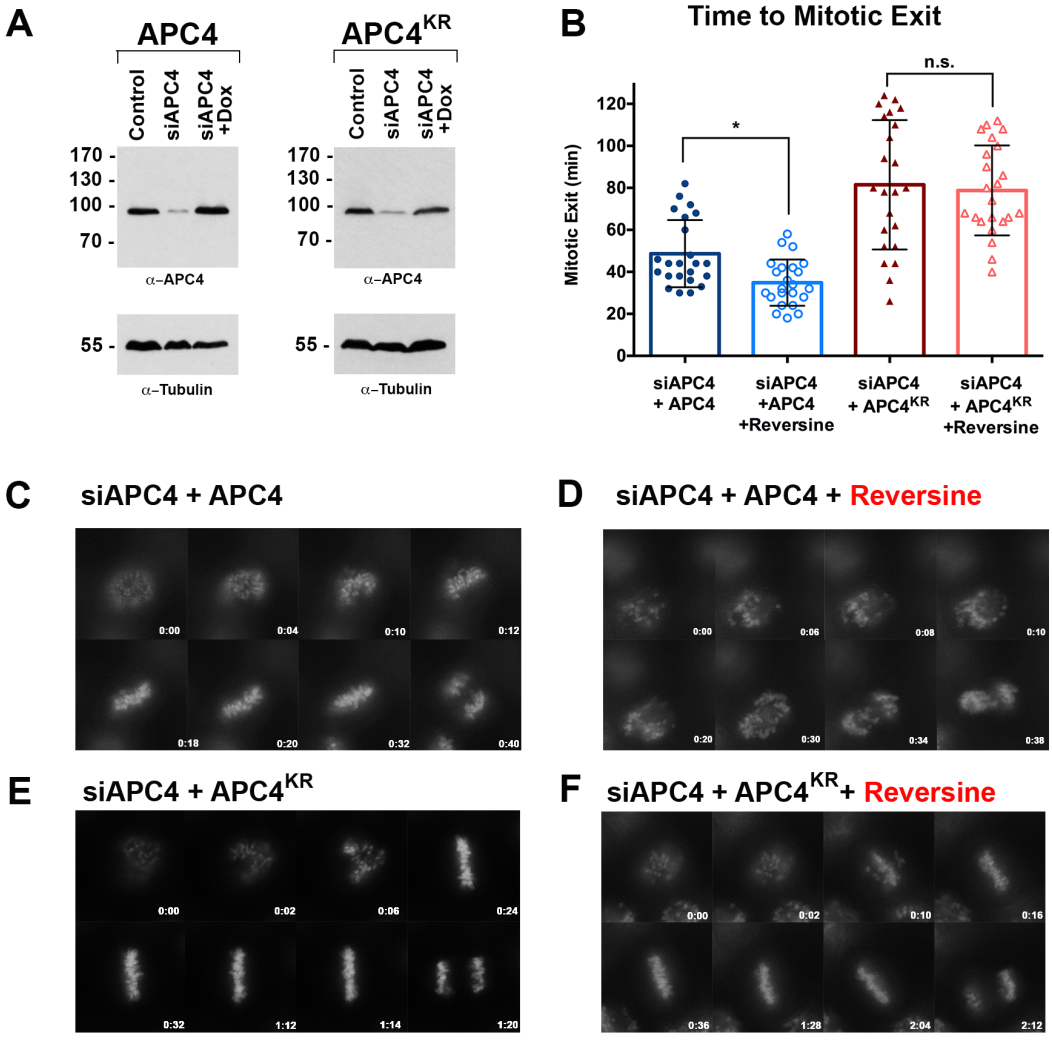
A
APC4
APC4KR
Control
siAPC4
siAPC4 +Dox
170 -
130 -
100 -
70 -
α–APC4
55 -
α–Tubulin
B
Time to Mitotic Exit
Mitotic Exit (min)
n.s.
*
siAPC4 + APC4
siAPC4 +APC4 +Reversine
siAPC4 + APC4KR
siAPC4 + APC4KR +Reversine
C
siAPC4 + APC4
D
siAPC4 + APC4 + Reversine
E
siAPC4 + APC4KR
F
siAPC4 + APC4KR + Reversine

FIGURE 2-7

APC4 sumoylation functions downstream of checkpoint inactivation to affect APC/C activity.

(A) A construct coding for a FLAG-tagged APC4^{KR}-SUMO2 fusion protein (APC4^{KR-S2}) was used to generate stable inducible lines in YFP-H2B HeLa cells. (B) Cells were transfected with or without APC4-targeting siRNAs and cultured in the presence (+Dox) or absence of doxycycline. Endogenous APC4 and FLAG-APC4^{KR-S2} expression levels were analyzed by immunoblot analysis with APC4 and tubulin specific antibodies. (C) Representative cells from timelapse acquisition beginning with NEBD to anaphase onset in control and FLAG-APC4^{KR-S2} expressing cells with timestamps indicated in min. (D) Mitotic timing beginning with NEBD to metaphase plate alignment and from metaphase plate alignment to anaphase onset was quantified in control and FLAG-APC4^{KR-S2} expressing cells. Experiments were performed in triplicate; means are displayed and error bars represent standard deviations. n = 60 for each cell line. Two-tailed t-tests were used to calculate significance: $p = 0.16$ between control and FLAG-APC4^{KR-S2} timing from NEBD-metaphase, $p = 0.35$ for control and FLAG-APC4^{KR-S2} timing from metaphase plate alignment to anaphase. (E) Individual timing of metaphase to anaphase transition times is displayed for

control and FLAG-APC4^{KR-S2} expressing cells. n = 314 for each cell line. (F and G) APC/C was immunopurified from FLAG-APC4 or FLAG-APC4^{KR-S2} expressing cells using FLAG-specific antibodies followed by immunoblot analysis with APC4 or APC2 specific antibodies. (H) *In vitro* ubiquitylation assays were performed using APC/Cs immunopurified from FLAG-APC4 or APC4^{KR-S2} expressing cells. Reactions were incubated with recombinant myc-Cyclin B1 for varying times and analyzed by immunoblotting with anti-myc antibodies (I) Reactions were performed in triplicate and mean relative myc-Cyclin B1 ubiquitylation levels is shown with error bars indicating the standard error of the mean (SEM).

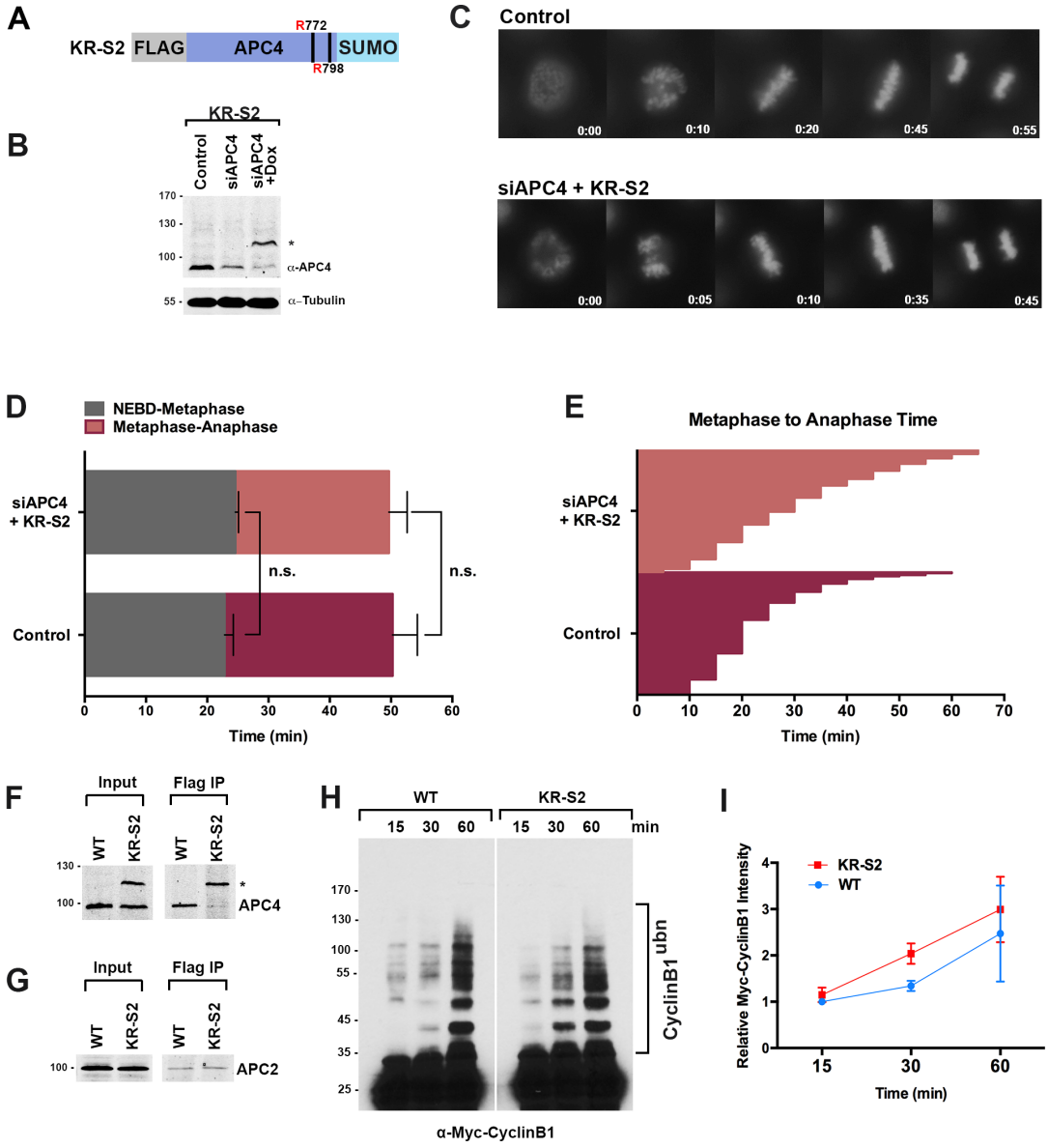
A
KR-S2
FLAG
APC4
SUMO
R772
R798
B
KR-S2
Control
siAPC4
siAPC4 +Dox
170
130
100
55
*
α-APC4
α–Tubulin
C
Control
0:00
0:10
0:20
0:45
0:55
siAPC4 + KR-S2
0:00
0:05
0:10
0:35
0:45
D
NEBD-Metaphase
Metaphase-Anaphase
siAPC4 + KR-S2
Control
n.s.
n.s.
0
10
20
30
40
50
60
Time (min)
E
Metaphase to Anaphase Time
siAPC4 + KR-S2
Control
0
10
20
30
40
50
60
70
Time (min)
F
Input
Flag IP
WT
KR-S2
130
100
*
APC4
G
Input
Flag IP
WT
KR-S2
100
APC2
H
WT
KR-S2
15
30
60
15
30
60
min
170
130
100
55
45
35
25
CyclinB1 ubn
α-Myc-CyclinB1
I
KR-S2
WT
Relative Myc-CyclinB1 Intensity
0
1
2
3
4
15
30
60
Time (min)

FIGURE 2-8

APC2 contains a conserved C-terminal SIM

(A) APC2 (pink) contains a predicted SIM (red) near its C-terminus that is in close proximity to the C-terminus (blue) of APC4 (teal). (PDB ID: 5LCW(Alfieri et al. 2016)). (B) Schematic depicting the APC2 SIM (red) between residues 727-738 and its conservation in mammals. Previously characterized (Brown et al. 2015) α/β and WHB domains extend from residues 549-727 and 735-822, respectively. Alanine substitutes at V728 and L729 were used to generate a SIM Mutant. (C) APC2 and an APC2 SIM mutant were produced in rabbit reticulocyte lysate in the presence of [^{35}S]-methionine. The expressed proteins were incubated with immobilized, recombinant GST or GST-SUMO2 trimer (SUMOx3) and binding was analyzed by SDS-PAGE and autoradiography. (E) Quantitation from 3 independent binding assays. Values from scintillation counting were used to generate relative binding ratios. Means are plotted and bars represent standard deviations. Two-tailed t-tests were performed: $p = 0.04$ for APC2 wild type binding to GST-SUMOx3/GST, $p = 0.08$ for APC2 SIM Mutant binding to GST-SUMOx3/GST.

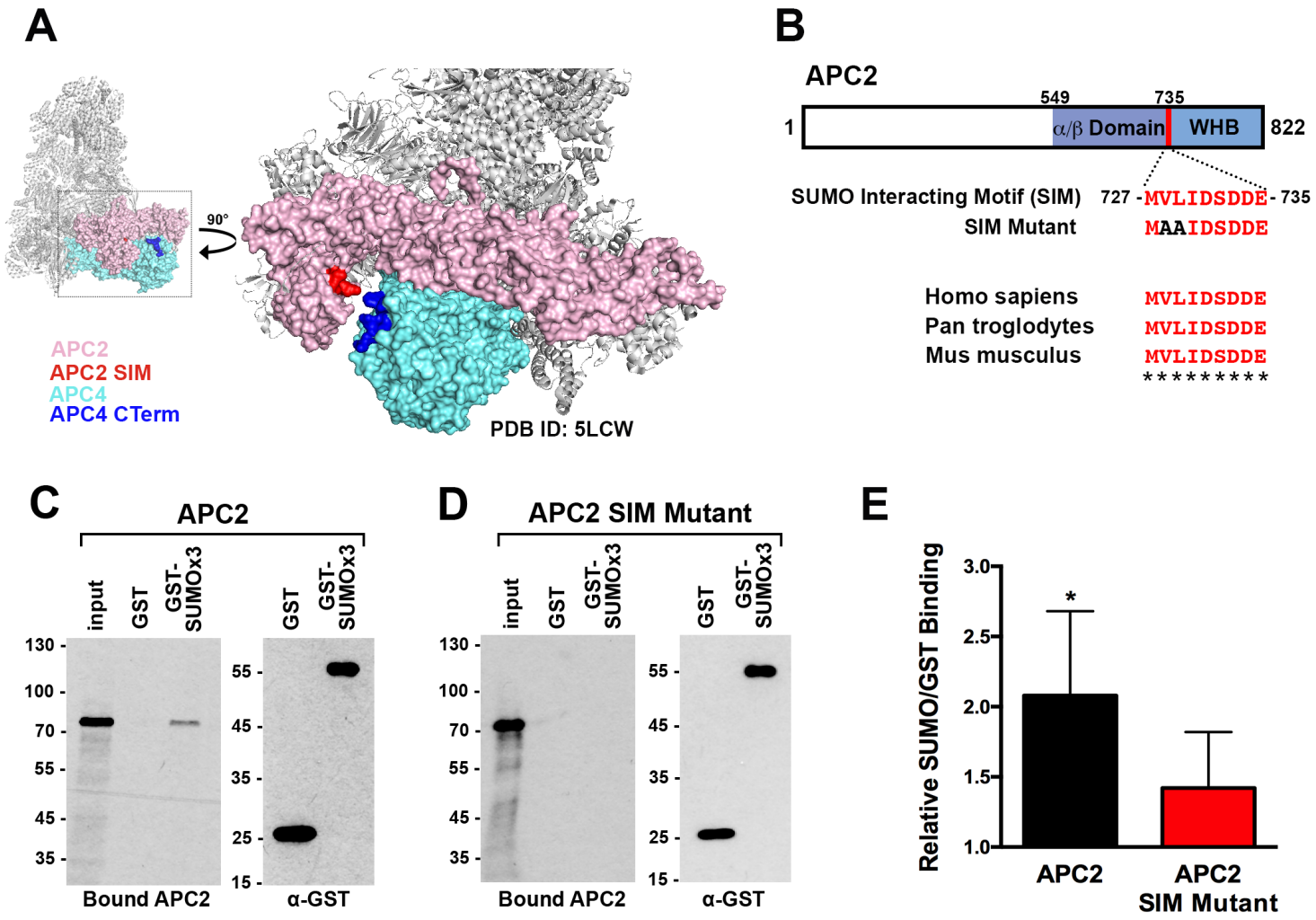
A
90°
APC2
APC2 SIM
APC4
APC4 CTerm
PDB ID: 5LCW
B
APC2
549
735
1
α/β Domain
WHB
822
SUMO Interacting Motif (SIM)
727 - MVLIDSDDE - 735
SIM Mutant
MAAIDSDDE
Homo sapiens MVLIDSDDE
Pan troglodytes MVLIDSDDE
Mus musculus MVLIDSDDE
****
C
APC2
input
GST
GST-SUMOx3
GST
GST-SUMOx3
130
100
70
55
45
35
55
45
35
25
15
Bound APC2
α-GST
D
APC2 SIM Mutant
input
GST
GST-SUMOx3
GST
GST-SUMOx3
130
100
70
55
45
35
55
45
35
25
15
Bound APC2
α-GST
E
Relative SUMO/GST Binding
3.0
2.5
2.0
1.5
1.0
*
APC2
APC2 SIM Mutant

FIGURE 2-9

Characterization of APC2 SIM binding

Truncated constructs of APC2 were generated. (B) *In vitro* binding assays of various APC2 constructs expressing wild type APC2 or a (C) C-terminal SIM Mutant were performed using recombinant GST or a GST-SUMO2 trimer (SUMOx3). (D) Quantitation from 3 independent replicates indicate the relative SUMO/GST binding between APC2 and APC2 SIM Mutant. Values from scintillation counting were used to generate ratios of relative binding. Means are plotted and bars represent standard deviations. Two-tailed t-tests were performed, $p = 0.22$ for APC2 C binding to GST-SUMOx3/GST, $p = 0.75$ for APC2 D binding to GST-SUMOx3/GST, $p = 0.01$ for APC2 E binding to GST-SUMOx3/GST, and $p = 0.18$ for APC2 E SIM Mutant binding to GST-SUMOx3/GST.

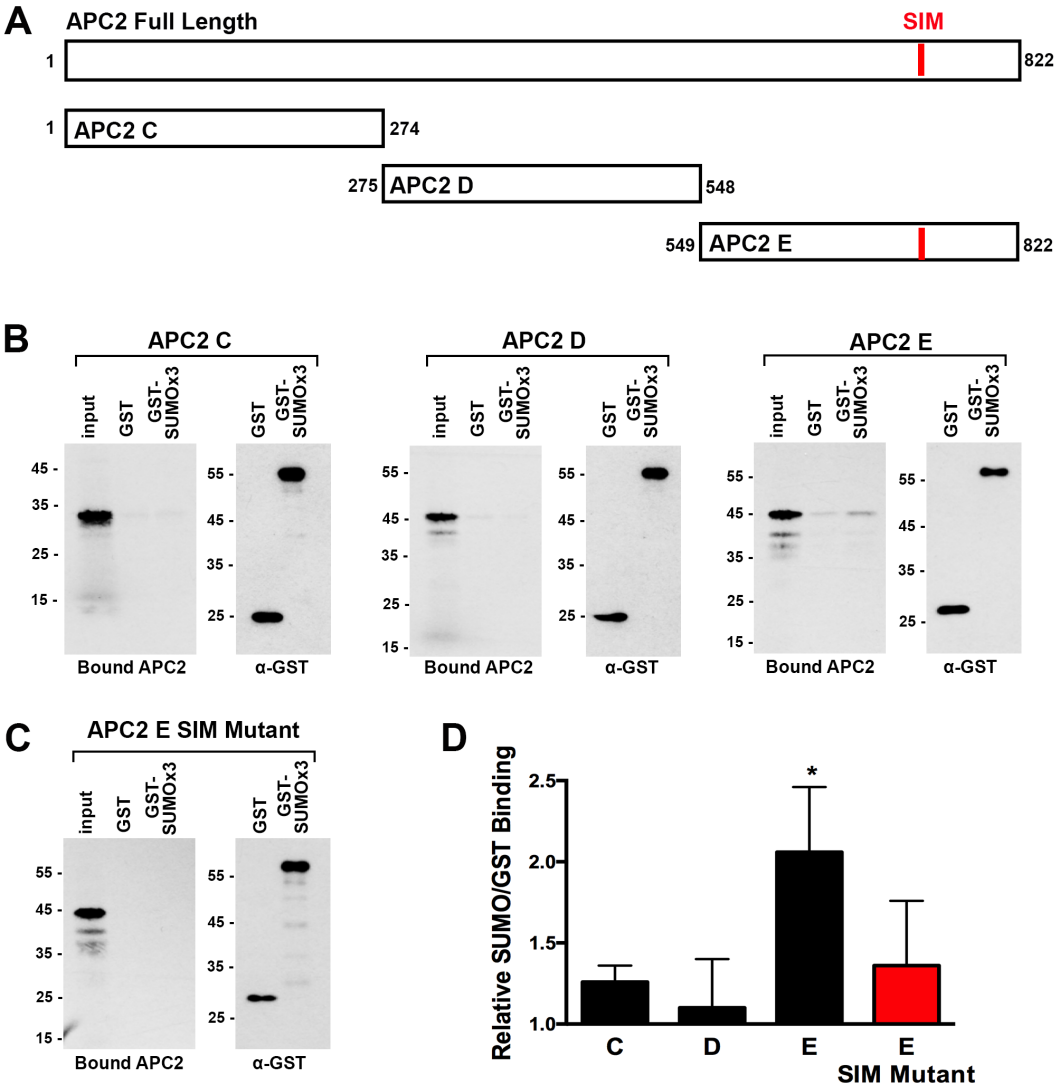
A
APC2 Full Length
SIM
1
822
1
APC2 C
274
275
APC2 D
548
549
APC2 E
822
B
APC2 C
APC2 D
APC2 E
input
GST
GST-SUMOx3
GST
GST-SUMOx3
45
35
25
15
55
45
35
25
Bound APC2
α-GST
C
APC2 E SIM Mutant
D
Relative SUMO/GST Binding
2.5
2.0
1.5
1.0
*
C
D
E
E
SIM Mutant

FIGURE 2-10

The APC2 SIM is required for normal progression from metaphase to anaphase.

(A) Constructs coding for FLAG-tagged versions of wild type APC2 or the SIM mutant ($APC2^{SM}$) were used to generate stable inducible cell lines in YFP-H2B HeLa cells. (B) Cells were transfected with or without APC2-targeting siRNAs (Control or siAPC2) and cultured in the presence (+Dox) or absence of doxycycline. Endogenous APC2, FLAG-APC2 and FLAG-$APC2^{SM}$ expression levels were analyzed by immunoblot analysis with APC2 and tubulin specific antibodies. (C) Mitotic phenotypes observed in cells treated as in (B) are displayed. $n > 130$ for each cell line. (D) Representative cells from timelapse acquisition beginning with NEBD to anaphase onset in FLAG-APC2 and FLAG-$APC2^{SM}$ expressing cells with timestamps indicated in minutes. (F) Mitotic timing beginning with NEBD to metaphase plate alignment and from metaphase plate alignment to anaphase onset was quantified in FLAG-APC2 and FLAG-$APC2^{SM}$ expressing cells. Experiments were performed in triplicate; means are displayed and error bars represent standard deviations. $n = 59$ for each cell line. Two-tailed t-tests were used to calculate significance: $p = 0.912$ between FLAG-APC2 and FLAG-$APC2^{SM}$ timing of NEBD-metaphase, $p <$

0.001 for FLAG-APC2 and FLAG-APC2^{SM} timing from metaphase plate alignment to anaphase. (E) Individual timing of metaphase to anaphase transition times is displayed for FLAG-APC2 and FLAG-APC2^{SM} expressing cells. n = 239 for each cell line.

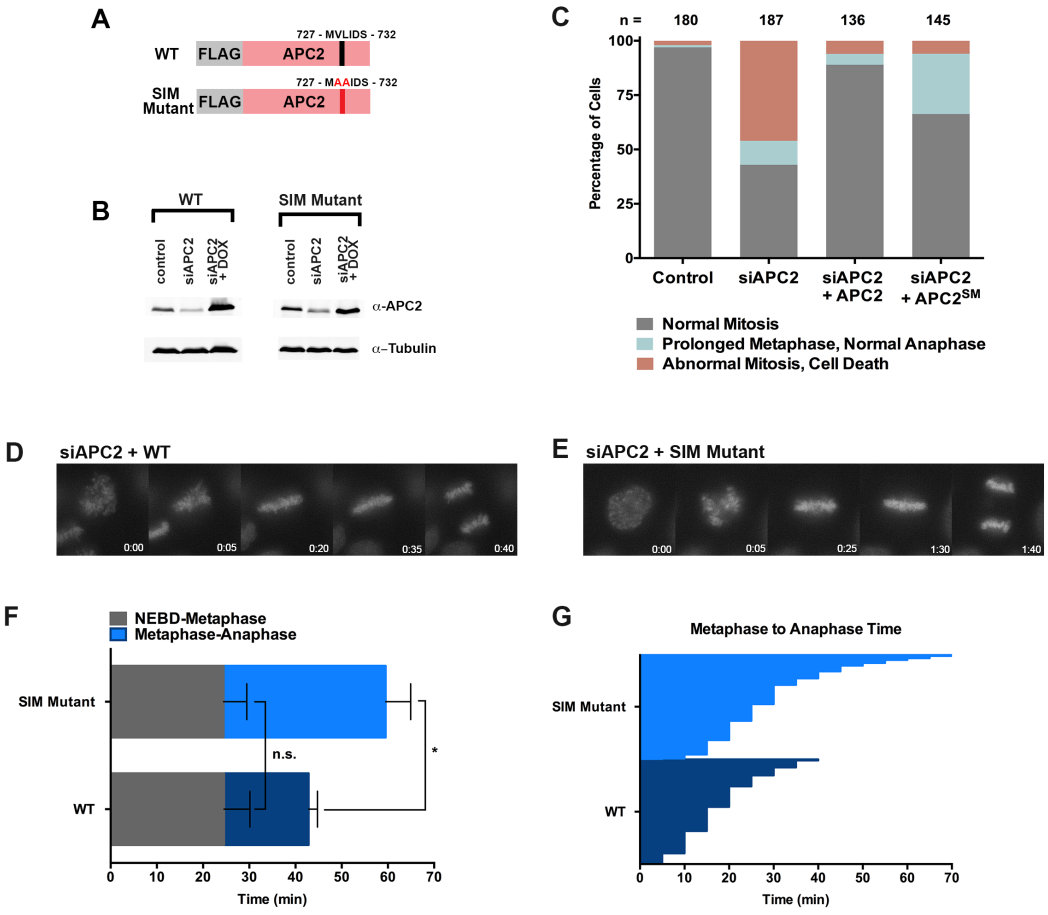
A
WT
FLAG
APC2
727 - MVLIDS - 732
SIM Mutant
FLAG
APC2
727 - MAAIDS - 732
B
WT
SIM Mutant
control
siAPC2
siAPC2 + DOX
α-APC2
α–Tubulin
C
n =
180
187
136
145
Percentage of Cells
100
75
50
25
0
Control
siAPC2
siAPC2 + APC2
siAPC2 + APC2SM
Normal Mitosis
Prolonged Metaphase, Normal Anaphase
Abnormal Mitosis, Cell Death
D
siAPC2 + WT
0:00
0:05
0:20
0:35
0:40
E
siAPC2 + SIM Mutant
0:00
0:05
0:25
1:30
1:40
F
NEBD-Metaphase
Metaphase-Anaphase
SIM Mutant
WT
n.s.
*
0
10
20
30
40
50
60
70
Time (min)
G
Metaphase to Anaphase Time
SIM Mutant
WT
0
10
20
30
40
50
60
70
Time (min)

FIGURE 2-11

SIM binding is required for normal progression from metaphase to anaphase

(A) Constructs coding for FLAG-tagged versions of linear APC4^{KR}SUMO deficient of SIM binding (SUMO2-QFI) was used to generate stable inducible cell lines in YFP-H2B HeLa cells. (B) The crystal structure of SUMO2 (PDB ID: 1WM3 (Huang et al. 2004)) with the SIM binding mutations in the second β-strand (highlighted in yellow) are shown. (C) Cells were transfected with control or APC4-targeting siRNAs (Control or siAPC4) and cultured in the presence (+Dox) or absence of doxycycline. Endogenous APC4 and FLAG-APC4^{KR}SUMO2^{QFI} expression levels were analyzed by immunoblot analysis with APC4 and tubulin specific antibodies. (D) Representative cells from timelapse acquisition beginning with NEBD to anaphase onset in control and (E) FLAG-APC4^{KR}SUMO2^{QFI} expressing cells with timestamps indicated in mins. (F) Mitotic timing beginning with NEBD to metaphase plate alignment and from metaphase plate alignment to anaphase onset was quantified in control and FLAG-APC4^{KR}SUMO2^{QFI} expressing cells. Experiments were performed in triplicate; means are displayed and error bars represent standard deviations (SD). n =101 for each cell line. Two-tailed t-tests were used to calculate

significance: p = 0.097 (not significant) between Control (average = 28.59 min, SD = 2.19) and FLAG-APC^{KR}SUMO2^{QFI} (average = 34.89 min, SD = 1.93) timing of NEBD-metaphase, p = 0.0011 for Control (average = 18.28 min, SD = 1.57) and FLAG-APC4^{KR}SUMO2^{QFI} (average = 53.15 min, SD = 3.85) timing from metaphase plate alignment to anaphase. (E) Individual timing of metaphase to anaphase transition times is displayed for Control and FLAG-APC4^{KR}SUMO2^{QFI} expressing cells. n = 101 for each cell line.

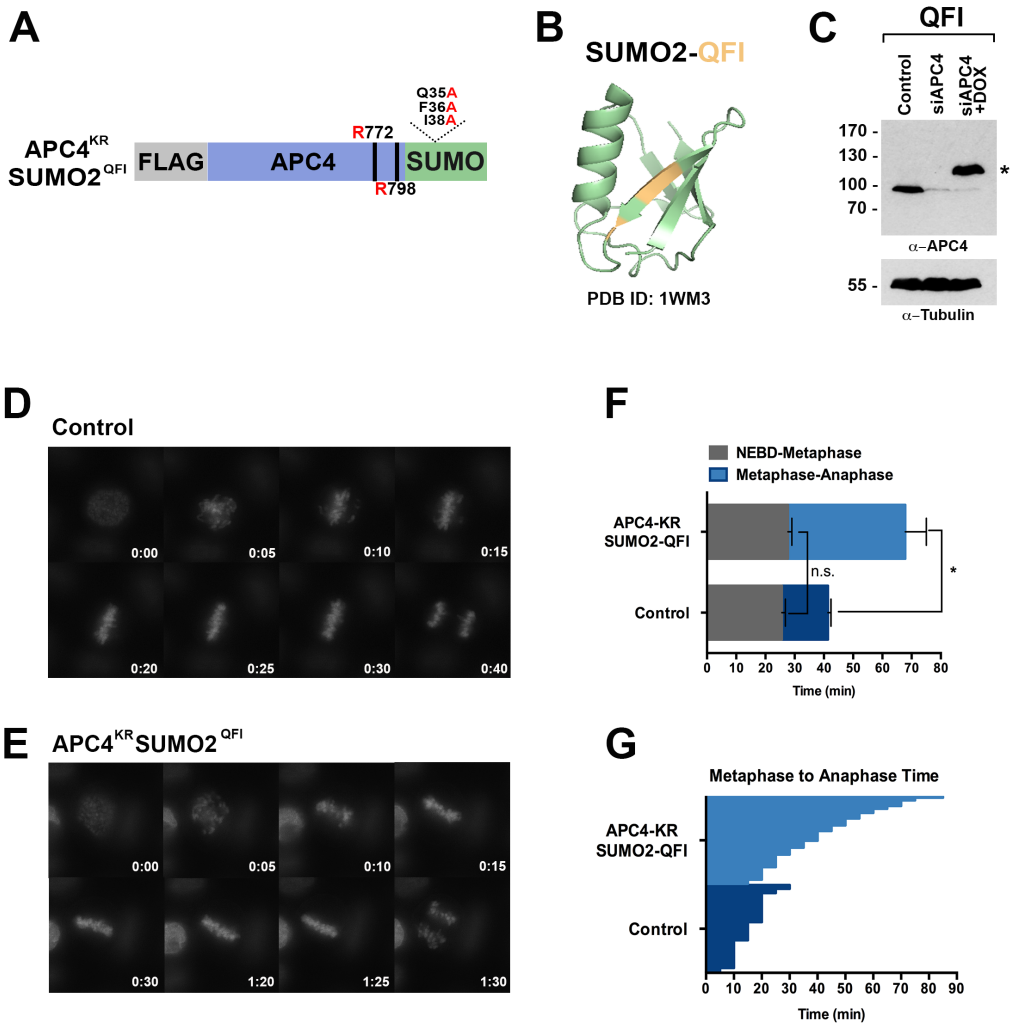
A
APC4KR
SUMO2QFI
FLAG
APC4
SUMO
R772
R798
Q35A
F36A
I38A
B
SUMO2-QFI
PDB ID: 1WM3
C
QFI
Control
siAPC4
siAPC4 +DOX
170 -
130 -
100 -
70 -
*
α–APC4
55 -
α–Tubulin
D
Control
0:00
0:05
0:10
0:15
0:20
0:25
0:30
0:40
E
APC4KRSUMO2QFI
0:00
0:05
0:10
0:15
0:30
1:20
1:25
1:30
F
NEBD-Metaphase
Metaphase-Anaphase
APC4-KR SUMO2-QFI
Control
n.s.
*
0 10 20 30 40 50 60 70 80
Time (min)
G
Metaphase to Anaphase Time
APC4-KR SUMO2-QFI
Control
0 10 20 30 40 50 60 70 80 90
Time (min)

FIGURE 2-12

A model for SUMO-mediated enhancement of APC/C activity involving APC4 sumoylation and APC2 SUMO binding.

(A) Activated APC/C adopts an open conformation competent for sub-optimal E2~Ub interactions. (B) APC4 sumoylation and interactions between SUMO and the APC2 SIM stabilizes a conformation between the APC2-WHB domain and APC11-RING (C). Stabilization of APC2-11 by APC4 sumoylation enhances ubiquitin-charged E2 binding to the APC/C and activity.

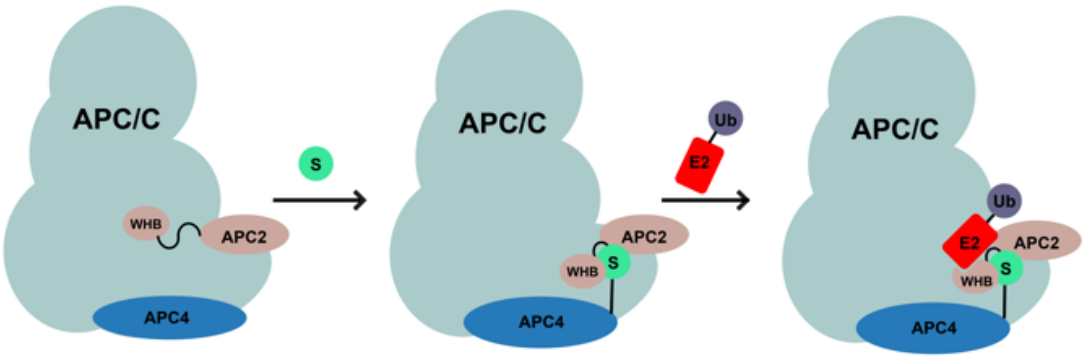

CHAPTER 3:

SPATIALTEMPORAL REGULATION OF SENP1 AFFECTS MITOTIC PROGRESSION

ABSRACT

Cell cycle progression is carefully coordinated so that equivalent copies of replicated DNA are equally divided during mitosis. Aberrations during this process can result in the gain or loss of genetic information, a phenomenon known as aneuploidy. Aneuploidy is one of the key hallmarks of cancer cells, and a fundamental understanding of mitosis will allow us to address strategies to prevent tumorigenesis.

Several regulatory checkpoints during mitosis ensure that sister chromosomes segregate equally. Post-translational modifications such as phosphorylation and ubiquitylation are classic drivers and regulators of the Spindle Assembly Checkpoint (SAC) and the activity of the Anaphase Promoting Complex/Cyclosome (APC/C). Here we present evidence that the SUMO isopeptidase SENP1 has critical roles in regulating the metaphase-anaphase transition. Localization analysis of the sequence elements in the N-terminal domain show that SENP1 is targeted to the nuclear pore complex (NPC) during interphase, and to kinetochores, spindle microtubules, and centromeres during mitosis. Here we also present analysis from proximity-dependent biotin identification (BioID) of SENP1, which validate localization studies. Immunofluorescence analysis of SAC proteins at the NPC during interphase, together with functional assays using timelapse

microscopy, suggest a role for SENP1 activity as a critical determinant of appropriate cell cycle progression.

INTRODUCTION

During the mitotic stage of the cell cycle, equal segregation of duplicated chromosomes must be carefully coordinated in order to maintain genomic integrity. Aberrations in mitosis can result in gains or losses of chromosomes in part or in whole, a condition known as aneuploidy[1]. The ability of aneuploid cells to overcome cellular safeguards and further replicate is a key hallmark of tumorigenesis[2]. Thus, the cellular surveillance mechanisms to ensure the fidelity of chromosome segregation must be exquisitely regulated. While mitosis has been observed for over a hundred years[3], and several key contributions have shaped our current understanding of this essential cellular process, there are yet outstanding questions regarding how events are coordinated, particularly during the metaphase-anaphase transition. Here we demonstrate the importance of regulation by the post-translational modification Small Ubiquitin-related Modifier (SUMO) during mitosis and its role in appropriately timing mitotic progression.

One of the initiating mitotic events is the dissolution of the nuclear membrane, or nuclear envelope breakdown (NEBD). Components of the nuclear membrane reorganize during mitosis, including the disassembly of nuclear pore complexes (NPCs) and nuclear lamina depolarization, which

are both regulated by phosphorylation events[4–6]. Components of the NPC, including the Nup107 complex, Nup358, Rae1, and Tpr function to coordinate kinetochore assembly, recruitment and pre-assembly of mitotic checkpoint protein factors[7–12]. Concurrent with NEBD, chromosomes condense and organize to form a metaphase plate, sister chromosomes become encircled by cohesins, and kinetochores come under attachment with the mitotic spindle. Kinetochores that have not been captured by spindle microtubules are regulated by the Spindle Assembly Checkpoint (SAC)[13], and require multiple inputs from mitotic kinases to coordinate amphitelic attachments[14]. The SAC produces an inhibitory signal consisting of proteins forming the Mitotic Checkpoint Complex (MCC) including BubR1, Bub3, Mad2, and together with the co-activator Cdc20, bind to and inhibit the activity of the Anaphase Promoting Complex/Cyclosome (APC/C)[15,16]. The APC/C is a RING E3 ubiquitin ligase that facilitates the proteolysis of Cyclin B1 and securin, culminating in the segregation of sister chromosomes[17]. Broadly, post-translational modifications by mitotic kinases and the ubiquitin system are indispensable drivers of mitosis. Here we present essential roles for an additional post-translational modification—components of the SUMO pathway—in regulating mitotic progression.

SUMO regulates a variety of cellular events, including transcription, ribosome biogenesis, chromatin remodeling, and chromosome segregation[18–20]. Invertebrates and yeast express a single SUMO, while higher eukaryotes express three functional SUMO isoforms, SUMO1, SUMO2 and SUMO3. SUMO1 is ~45% identical to SUMO2 and SUMO3, with potentially distinct cellular functions, whereas SUMO2 and SUMO3 share ~96% sequence homology and are collectively referred to as SUMO2/3. Like ubiquitin, SUMO is first processed by an isopeptidase to expose a C-terminal di-glycine motif used for conjugation. SUMO is a covalent modification whereby attachment to a substrate is achieved by a sequential enzymatic cascade involving an activating E1 (heterodimer of Aos1/Uba2), a single conjugating E2 (Ubc9), and several ligating E3 enzymes. SUMO modification results in the formation of an isopeptide linkage between the C-terminal glycine of SUMO with the ε-amine of the substrate lysine[18]. The consensus site sequence for SUMO modified substrates is represented by a ψ-K-x-E/D motif, whereby ψ represents a hydrophobic residue, K is the substrate lysine, x is any amino acid, followed by an acidic residue, either glutamic or aspartic acid. SUMO modification can result in redirected localization of substrates, in addition to generating non-covalent interactions between a SUMO modified substrate and a protein containing a SUMO

Interacting Motif (SIM). As a result, sumoylation influences protein activities in a variety of essential cellular processes[21]. Physiologically, perturbations to the SUMO pathway, such as overexpression of the SUMO deconjugating enzymes, have been implicated in a variety of human cancers[22]. Thus, the balanced regulation of SUMO pathway components is critical for human health.

Since its initial discovery, SUMO has been characterized as an essential regulator of mitotic progression. The single SUMO gene identified in *S. cerevisiae*, *SMT3* (Suppressor of Mif Two), emerged from a suppressor screen of *MIF2*, a gene encoding a distant homolog of the mammalian centromere CENP-C protein[21,23]. *SMT3* is essential for mitotic progression, as *smt3* mutants arrest in mitosis. The SUMO homolog in *S. pombe, Pmt3,* also has critical roles in normal chromosome segregation and mitotic progression[24]. Since the identification of sumoylated RanGAP1 in human cells at nuclear pore complexes[25,26], mechanistic roles of the RanGAP1-SUMO complex with the nucleoporin Nup358/RanBP2 have also been shown to coordinate mitotic events[27]. During mitotic initiation, Nup358/RanBP2 functions to integrate nuclear envelope breakdown with kinetochore assembly[10]. During mitosis, Nup358/RanBP2 also functions as a SUMO E3 ligase, and facilitates the SUMO modification of Topoisomerase

IIα at kinetochores[28]. Additional roles for SUMO in regulating mitotic events have emerged, including the decatenation of chromosome arms regulated by Topoisomerase IIα[28,29], kinetochore-microtubule interactions[30–32], and checkpoint signaling[33–35]. Furthermore, recent high-throughput mass spectrometry analyses have diversified the catalog of the SUMO proteome, and the identification of SUMO substrates during mitosis widens the potential for discovering novel regulatory roles[36–38].

At steady state levels, the abundance of the SUMO modified substrate is relatively low, and the regulatory axis of conjugation and deconjugation is mediated in part by SUMO isopeptidases. Several classes of SUMO isopeptidases include the Ulp (UBL-specific protease) family first identified in *S. cerevisiae*[39], the sentrin-specific proteases (SENPs) in humans[40], desumoylating isopeptideses (DeSIs)[41], and ubiquitin-specific protease-like enzyme (USPL1)[42]. All of these proteins function as cysteine proteases. The human SENPs share a conserved C-terminal catalytic domain, but contain divergent N-terminal domains that confer distinct sub-cellular localizations and functions[43]. SENPs are the best studied class of SUMO isopeptidases, and roles for regulating mitotic events have been reported[45]. We have, for example, shown that depletion of SENP1 from cultured mammalian cells results in defects in the timing of mitotic exit[20]. However, the specific

SUMO substrates recognized by SENP1, and the molecular mechanisms regulating its localization and functions in mitosis, remain poorly understood.

Here, we elaborate on the role of SENP1 in regulating the metaphase-anaphase transition. Defects in appropriate timing of the metaphase-anaphase transition in SENP1 depleted cells could be based on several possibilities: (1) inappropriate kinetochore-microtubule capture and appropriate tension during prometaphase, (2) defects in recruitment or accumulation of SAC proteins at kinetochores during prometaphase and metaphase, (3) incomplete inactivation of the SAC, (4) interactions at NPCs during interphase related to the pre-assembly of SAC complexes. By analysis of each of these possibilities, our data suggest that SENP1 depletion results in the accumulation of Mad1 and Mad2 at NPCs during interphase, which ultimately affects the timing of mitotic exit. We further define sequence elements in the N-terminus of SENP1 that direct targeting to components of the NPC during interphase, and to kinetochores, centrosomes, and spindle microtubules during mitosis. Proteomic analysis using proximity-dependent biotin identification (BioID) confirmed interactions of N-terminal SENP1 domains with subunits of the NPC. Finally, functional assays with truncation mutants of SENP1 suggest that

binding interactions with the Nup107 complex are critical for normal mitotic progression. These collective findings lend additional mechanistic insights into roles for SUMO modification during mitosis.

MATERIALS AND METHODS

Cell culture, cell lines, plasmids, and drug treatments

293FT, JW36 HeLa and YFP-H2B HeLa cells (a gift from Andrew Holland, Johns Hopkins University, Baltimore, MD) were maintained at 37°C in a 5% CO_2 atmosphere. Cells were grown in DMEM medium (Gibco) containing 10% fetal bovine serum (Atlanta Biologicals).

GFP-SENP1 constructs were a generous gift from Mary Dasso (National Institute of Health, Bethesda, MD). siRNA oligo-resistant GFP-SENP1 plasmids were generated by PCR-based QuickChange site-directed mutagenesis (Strategene, La Jolla, CA) using the wild-type vector as a template. SENP1 and N-terminal truncation constructs were PCR amplified and inserted into a pmCherry-C2 vector.

293FT and YFP-H2B HeLa cells were used to generate tetracycline-inducible cell lines. Lentiviruses containing a blasticidin-resistant tetracycline inducible plasmid, in addition to hygromycin-resistant Flag-APC4, Flag-APC4^{KR}, or mCherry SENP1 transgenes were incorporated via lentiviral infection as described previously. In brief, 1 μg of lentiviral DNA construct, 800 ng psPAX2 (Addgene, Cambridge, MA, USA), and 200 ng pMD2.G (Addgene) were transfected into 293FT cells using XTremeGene HP (Roche) according to manufacturer's instructions. After 48 h, the viral

supernatant was filtered through a 0.44 μM PVDF membrane and transduced to YFP-H2B HeLa cells in the presence of 8 μg/mL polybrene (Santa Cruz Biotechnology). After 24 h, cells were treated with 10 μg/mL blasticidin to select for the tetracycline inducible cells for 1 week. Selection for stable cell lines was performed with hygromycin B (Roche) at a final concentration of 200 μg/mL for an additional week concomitant with 10 μg/mL blasticidin selection. Individual blasticidin and hygromycin-resistant colonies were isolated with cloning discs (after ~2 weeks) and tested for mCherry SENP1 expression by immunofluorescence microscopy and immunoblot analysis.

Thymidine (Sigma-Aldrich) was dissolved in DMSO and used at a final concentration of 2 mM. To synchronize cells into S phase, cells were cultured in the presence of 2 mM thymidine for 19 h, released in drug-free media for 6 h, and cultured in 2 mM thymidine for 19 h. For mitotic timecourse analysis, cells were released from the double thymidine block and harvested in 2x SDS-sample buffer at indicated timepoints.

To inactivate SAC signaling, 1 μM of the Mps1 kinase inhibitor, Reversine (Cayman Chemical, Ann Arbor, Michigan), was used immediately before timelapse acquisition.

RNAi interference

JW36 HeLa or YFP-H2B HeLa cells were transfected using Lipofectamine RNAiMAX (Invitrogen) and siRNA oligonucleotides at a final concentration of 20 nM for 48 hours and before analysis by immunoblotting, timelapse microscopy, or immunofluorescence microscopy. The following siRNA oligos were used for protein depletion as previously described[41]: scramble control: (5' – CUUCCUCUCUUUCUCUCCCUUGUGA-3'), and SENP1 oligo(b): (5' GCAAAUGGCCAAUGGAGAAAUUCUA-3').

Two oligonucleotides targeting the 3' UTR of APC4 were validated, but oligonucleotide 2 was used for all experiments. APC4 oligonucleotides were purchased from Dharmacon: APC4 Oligo 1: (5' – AGCUUGCCAUUAUUGUGUGUGUAAU – 3'), APC4 Oligo 2: (5' – CAUAGGAGAUGGACUAAGAUGUCUUGG – 3').

Antibody and imaging techniques

For immunoblotting, proteins were separated by SDS-PAGE, transferred onto nitrocellulose membranes, blocked in 5% milk in TS-T, and then probed with the following antibodies diluted in PBS supplemented with 2% BSA and 0.05% NaN_3: Centrin (CEN, mouse, 1:3000, a generous gift from Phil Jordan), Cyclin B1 (mouse, GNS1: sc-245, 1:200, Santa Cruz Laboratories), GAPDH (rabbit, TAB1001, OpenBiosystems, 1:15,000),

mCherry (rabbit, 1:10,000 a generous gift from Jiou Wang), Myc (mouse, 9E10, 1:2000), SENP1 (rabbit, ab108981, 1:10,000, Abcam), SUMO-2/3 (8A2, 1:800), and Tubulin (mouse, DM1A, 1:5000, Sigma-Aldrich. Secondary antibodies conjugated to HRP (Jackson Laboratories) were used at 1:10,000 diluted in 5% milk in TS-T. Immunoblot analysis was performed using either an enzyme-linked chemiluminesence substrate (Luminata Crescendo Western HRP Substrate, EMD Millipore) and developed with film or IR Dye-labeled secondary antibodies (anti rabbit IgG IRDye 800, LI-COR 926-32211) and imaged using the Odyssey infrared imager (LI-COR). Images were processed with Adobe Photoshop CS6.

For SAC co-localization studies using immunofluorescence microscopy, cells were treated with siRNA to SENP1 for 48 hours on glass coverslips. Cells were fixed in 3.5% paraformaldehyde in PBS for 7 min and permeabilized in 0.5% Triton-X 100 in PBS for 20 min at room temperature. For GFP-SENP1 and SAC localization studies, cells were permeabilized using transport buffer (200 mM HEPES pH 6.5, 110 mM potassium acetate, 20 mM magnesium acetate, 1 μg/mL leupeptin, 1 μg/mL pepstatin A, 20 μg/mL aprotinin, 1 mM phenylmethylsulfonyl fluoride (PMSF), and 20 mM N-ethylmaleimide (NEM), and 20 μg/mL digitonin at room temperature for 15 min. Cells were then washed 1x with PBS, and fixed in 2% formaldehyde

at room temperature for 20 mins. After washing with PBS, cells were immunostained at room temperature using respective antibodies.

Immunostaining was performed with the following antibodies diluted in PBS supplemented with 2% BSA: 414 (mouse, 1:2000), BubR1 (rabbit, GeneTex, 1:500), Cdc20 (mouse, p55 CDC(E-7): sc13-162, 1:50), CREST (human, 15-235-0001, Antibodies Inc., 1:100), Hec1 (mouse, BD Transduction 611040, 1:100) Mad1 (mouse, 1:500, Active Motif), followed by secondary antibodies to Alexa Fluor 594 and Alexa Fluor 647 (1:300, Life Technologies, Grand Island, NY). Images were acquired using a Zeiss Observer Z1 fluorescence microscope with a Zeiss Plan-Apochromat 63x objective (numerical aperture 1.40) and Apotome VH optical sectioning grid (Carl Zeiss, Jena, Germany). Images were obtained at room temperature with immersion oil using a Zeiss AxioCam MRm camera and processed using AxioVision Software Release 4.8.2 and Adobe Photoshop CS6.

Fixed and live cell timelapse microscopy

Fixed images were acquired using a Zeiss Observer Z1 fluorescence microscope with a Zeiss Plan-Apochromat 63x objective (numerical aperture 1.40) and Apotome VH optical sectioning grid (Carl Zeiss, Jena, Germany). Images were obtained at room temperature with immersion oil using a Zeiss

AxioCam MRm camera and processed using AxioVision Software Release 4.8.2 and Adobe Photoshop CS6.

For live-cell imaging, cells were cultured in Lab-Tek Chambered #1.0 Borosilicate Coverglass slides (Nunc, Rochester, NY), doxycycline induced and siRNA treated targeting APC4, and then imaged 48 hours post-transfection. Immediately before imaging, cells were switched to pre-warmed CO_2-independent media (Invitrogen) supplemented with 10% FBS. Cells were maintained at 37°C on a Zeiss Observer Z1 fluorescence microscope fitted with an incubation chamber. Images were acquired using a Zeiss EC Plan-Neofluor 40x objective (numerical aperture 1.3) every 5 min for 16 hours (unless otherwise indicated) with a Zeiss AxioCam MRm camera and processed using AxioVision Software Release 4.8.2. Data analysis was performed using Prism 6 for Mac OS X (GraphPad Software, Inc.)

Statistical analysis

Statistical analyses were carried out using Prism 6 for Mac OSX (GraphPad Software, Inc.) with two-tailed student *t* tests. Data with a *P*-value < 0.05 was considered as statistically significant.

RESULTS

SENP1 activity is required for appropriate timing of the metaphase-anaphase transition

We previously reported that SENP1 is critical for normal progression through mitosis[20], but its precise molecular functions are not understood. To more precisely characterize the requirements of SENP1 during mitosis, HeLa cells expressing yellow fluorescent protein (YFP)-tagged histone H2B were used to facilitate live cell imaging. Cells depleted of SENP1 by siRNA for 48 hours were analyzed by timelapse microscopy, which revealed no defects in the timing of nuclear envelope breakdown (NEBD) to metaphase plate alignment compared to control cells (Figure 3-1A-C). On average, control cells spent ~35 minutes while siSENP1 cells spent ~29 minutes transitioning from NEBD-metaphase. In contrast, there was a statistically significant difference in the transition time between metaphase plate alignment and anaphase onset in control cells (~26 minutes) compared to siSENP1 cells (~70 minutes) (Figure 3-1D). Fixed images from timelapse analysis, with time indicated in minutes, show that the prolonged metaphase-anaphase transition observed in SENP1-depleted cells occurs without spindle fatigue or the generation of chromosomal bridges (Figure 3-1A-B).

These observations confirm a critical role for SENP1 during the metaphase-anaphase transition.

Anaphase onset and mitotic exit is dependent on APC/C activity towards specific protein substrates, including securin and Cyclin B1. To evaluate the activity of APC/C under conditions of SENP1 depletion, we analyzed the rate of Cyclin B1 degradation. Cells were treated with control or SENP1 targeting siRNA oligos, synchronized in S-phase using a double thymidine block, and released into drug-free medium. Cell lysates were collected at varying timepoints after release and immunoblotting showed that Cyclin B1 degradation was attenuated in SENP1-depleted cells compared to control cells (Figure 3-1E-F). Immunoblots to SENP1 show protein depletion in cells treated with siRNA across all timepoints, and GAPDH (glyceraldehyde-3-phosphate dehydrogenase) was used as a loading control. The observation that Cyclin B1 degradation is delayed is consistent with the observed mitotic delay and suggests a role for SENP1 in regulating processes that control the metaphase-anaphase transition.

SENP1 depletion does not affect kinetochore-microtubule attachments or perturb SAC signaling

Stable, amphitelic attachments between the kinetochores of sister chromatids and the mitotic spindle are required for chromosome alignment, silencing of the SAC and promotion of timely anaphase onset. To investigate the possibility that SENP1 activity is required during early stages of mitotic chromosome capture and alignment, we evaluated the formation of the bipolar spindle, tension between kinetochores of metaphase aligned sister chromatids, and SAC signaling. Cells were treated with control or SENP1 siRNAs for 48 hours, fixed and co-stained with CREST to identify centromeres and tubulin to mark the mitotic spindle, and analyzed by immunofluorescence microscopy (Figure 3-2A). During metaphase, control and SENP1-depleted cells both form normal amphitelic attachments between the mitotic spindle and kinetochores of sister chromatids. To determine if SENP1 depletion affects tension between kinetochores of metaphase aligned sister chromatids, inter-kinetochore distances were measured (Figure 3-2B). On average, control and SENP1-depleted cells had indistinguishable inter-kinetochore distances, measuring ~0.78-0.79 μm. These findings are consistent with timelapse analysis, whereby early mitotic events leading up to metaphase are indistinguishable between control and SENP1-depleted cells. Immunoblots with antibodies specific for SENP1 show protein

depletion in cells treated with siRNA, and tubulin was used as a loading control (Figure 3-2C).

To evaluate the inhibitory signals generated at prometaphase kinetochores, we evaluated SAC proteins in control and SENP1-depleted cells. Immunofluorescence microscopy analysis was performed using antibodies specific for Cdc20, Mad1, BubR1. Cells were co-stained with anti-CREST antibodies to indicate centromeres. At early prometaphase, localization of SAC proteins at unattached kinetochores was robust in both control and siSENP1 treated cells (Figure 3-2D). Upon metaphase plate alignment, SAC proteins are appropriately released, as fluorescence levels at kinetochores dissipated similarly in both control and siSENP1 treated cells. These data demonstrate that the recruitment and release of SAC proteins at the kinetochore is not affected by SENP1 depletion.

To address whether higher levels of SAC proteins accumulate at kinetochores in SENP1-depleted cells during prometaphase, cells were treated with control or siSENP1 for 48 hours and treated with nocodazole (Figure 3-3). Analysis of Mad1, Mad2, BubR1, and Bub1 levels at kinetochores showed no apparent differences in SENP1-depleted cells compared to control cells. Thus, relative levels and localization of

checkpoint proteins at kinetochores are not affected in SENP1-depleted cells.

SAC inactivation partially rescues the metaphase-anaphase delay in SENP1-depleted cells

To address whether SENP1 activity is required downstream of SAC silencing, we treated control and SENP1-depleted cells (Figure 3-4) with the Mps1 kinase inhibitor, reversine[45]. Progression through mitosis, beginning with nuclear envelope breakdown (NEBD) to anaphase onset was monitored in control or siSENP1 cells for 48 hours followed by 4 hours of timelapse imaging. Immunoblots with antibodies specific to SENP1 and GAPDH as a loading control indicated effective protein depletion following knockdown (Figure 3-4A). Control cells spent ~47 minutes on average in mitosis, while reversine treatment shortened the mitotic duration to ~17 minutes (Figure 3-4B). In contrast, SENP1-depleted cells spent ~105 minutes on average in mitosis and reversine treatment shortened this to ~33 minutes (Figure 3-4B). Fixed images from timelapse acquisition depict random chromosome segregation and catastrophic mitotic exit in control cells treated with reversine (Figure 3-4C). Chromosomes in cells depleted of SENP1, however, align at the metaphase plate just prior to an apparently normal

mitotic exit (Figure 3-8D). These results suggest either incomplete SAC silencing in SENP1-depleted cells or a role for SENP1 downstream of checkpoint inactivation.

SENP1 depletion effects are not dependent on APC/C sumoylation

A regulatory role for sumoylation of APC4 in activation of APC/C and timely mitotic exit was reported in Chapter 2. To determine if the metaphase-anaphase delay observed in SENP1-depleted cells involves enhanced sumoylation of APC4, we analyzed APC4 (wild type) and $APC4^{KR}$ (sumoylation mutant) cells treated with siSENP1 by timelapse microscopy (Figure 3-5). As expected, cells expressing APC4 and treated with siSENP1 exhibited a prolonged metaphase-anaphase transition (~79 min). Furthermore, cells expressing $APC4^{KR}$ and treated with siSENP1 exhibited a similar metaphase-anaphase delay (~81 min), which was significantly greater than the delay in control $APC4^{KR}$ cells (~65.00 min). Thus, the effect of SENP1 depletion on the metaphase-anaphase transition is not dependent on enhanced sumoylation of APC4.

SENP1 depletion affects Mad1 and Mad 2 accumulation at NPCs during interphase

Recent work has demonstrated that pre-assembly of SAC proteins at NPCs during interphase contributes to the total pool of checkpoint proteins present in mitosis and is critical for appropriate mitotic timing and genome maintenance[12,46]. To determine if SENP1 depletion affects recruitment of Mad1 and Mad2 to NPCs during interphase, we analyzed cells by immunofluorescence microscopy (Figure 3-6A). Mad1 levels at NPCs were significantly elevated in SENP1-depleted cells, with an average fluorescence intensity of ~4.8 (units/pixels^2) compared to 3.9 in control cells (Figure 3-6B). Similarly, levels of Mad2 were also significantly higher at NPCs in SENP1-depleted cells compared to control cells, with fluorescence intensities of ~6.8 and (units/pixels^2) ~5.5, respectively (Figure 3-6C). These findings suggest that excess assembly of SAC complexes at NPCs during interphase may contribute to the metaphase-anaphase delay observed in SENP1-depleted cells.

Characterization of determinants of SENP1 localization during different stages of the cell cycle

Based on the finding that Mad1 and Mad2 accumulate at higher levels at NPCs in SENP1 depleted cells, we next analyzed SENP1 targeting signals in SENP1 and interactions with specific NPC subdomains. We previously

demonstrated that SENP1 localizes to NPCs during interphase and to centrosomes, the mitotic spindle, and kinetochores during metaphase[37,39] (Figure 3-7). SENP1 contains a nuclear localization signal (NLS) at amino acids 170-177 and a C-terminal nuclear export signal at amino acids xyz (Figure 3-7A)[47]. Other signals affecting SENP1 localization, however, have not been defined. To further characterize the sequence elements that direct NPC targeting, GFP-SENP1 N-terminal fragments (Figure 3-8A) were expressed in HeLa cells and co-localization with mAb 414 (an NPC marker) was analyzed by immunofluorescence microscopy (Figure 3-8B). Full-length SENP1, and fragments spanning amino acids 154-272 and 273-449 co-localized with NPCs, while fragments spanning amino acids 1-40 and 41-153 localized to the nucleus (Figure 3-8B). These findings reveal two independent NPC-targeting signals in the SENP1 N-terminus, as well as previously unrecognized NLSs within the first 153 amino acids.

To identify signals in SENP1 that direct localization during each stage of mitosis, we expressed GFP-tagged SENP1 and varying SENP1 fragments in HeLa cells and analyzed co-localization with kinetochore (anti-Hec1), centromere (anti-CREST), and centrosome (anti-centrin) markers by immunofluorescene microscopy. Full-length SENP1 showed co-localization with Hec1 during prometaphase, indicating kinetochore recruitment in early

stages of mitosis (Figure 3-9). Consistent with previous findings, full-length SENP1 also localized to centrosomes, kinetochores, and the mitotic spindle during metaphase. GFP-tagged SENP1 fragments 1-41 and 41-153 localized to the mitotic spindle and retained some kinetochore localization, while 154-272 did not localize to mitotic structures (Figure 3-9). Notably, the 273-449 fragment localized to the centromeres, mitotic spindle, and retained some kinetochore localization, albeit to a lesser extent compared to full-length SENP1. Like NPC targeting, these findings demonstrate the contributions of multiple N-terminal domains in localizing SENP1 to mitotic structures.

BioID analysis demonstrates unique NPC interactions with distinct SENP1 N-terminal domains

To assess the interactions of SENP1 with subunits of the NPC, we used the proximity-dependent biotin identification, or BioID, technique essentially as previously described[48] (Figure 3-10A). In brief, a Flag-BirA*-SENP1 fusion protein was inducibly expressed in HeLa cells. BirA* is a biotin conjugating enzyme mutant (BirA R118G) which facilitates the efficient biotinylation of lysine residues in close proximity. Proteins biotinylated by Flag-BirA*-SENP1 were affinity purified using streptavidin and identified using mass spectrometry. Proteins including karyopherins,

nucleoporins, and nuclear lamins were identified (Table 3-1). These data are consistent with the steady state concentration of SENP1 at NPCs[20]. N-terminal fragments of SENP1 were also subjected to BioID analysis. Consistent with the findings that GFP-SENP1$^{1-41}$ and GFP-SENP1$^{41-153}$ did not localize to NPCs (Figure 3-10B), no interactions with nucleoporins were detected with these fragments (Table 3-1). Average spectral counts indicated that full-length SENP1 and fragments 153-272 and 273-449 all interacted with nucleoporins, including the Nup107 complex and Tpr. Interestingly, the 153-272 fragment showed higher than average spectral counts for the Nup107 complex while the 273-449 fragment showed higher than average spectral counts for Tpr, a component of the nuclear basket. Analysis of GFP-SENP1 and GFP-SENP1$^{273-449}$ by fluorescence microscopy showed co-localization with Tpr, consistent with the BioID results (Figure 3-10C). Taken together, these data confirm that sequence elements in the N-terminus of SENP1 specify NPC targeting and demonstrate unique interactions with distinct components of the NPC.

NPC targeting domains of SENP1 are critical for functions in mitosis

To determine if interactions with specific subunits of the NPC are critical for SENP1 function, we generated stable inducible cell lines for

expression of mCherry-tagged SENP1 and SENP1 deletion mutants (Figure 3-11A).

Specifically, mCherry was fused to a truncated SENP1 missing the first 153 amino acids (Δ153), which we predict maintains interactions with the Nup107 complex and Tpr, while a truncation of the first 272 amino acids (Δ272) maintains interactions with Tpr only. To ensure that the truncation mutants did not affect catalytic activity towards SUMO modified substrates, mCherry-SENP1 fragments were transfected into cells together with Myc-tagged SUMO2, and the effects on SUMO conjugation were analyzed by immunoblot analysis (Figure 3-11B-C). Expression of mCherry SENP1 full length (FL), Δ153 and Δ272 all caused global decreases in high molecular weight SUMO2 conjugates, while an mCherry empty vector and a catalytic mutant SENP1^{C603S} do not (Figure 3-11B-C).

The localization of individual truncation mutants was also analyzed by fluorescence microscopy. Consistent with localization studies of GFP-SENP1 fusions, mCherry-SENP1 and SENP1^{C603S} were targeted to the NPCs during interphase, and re-localized to centrosomes, the mitotic spindle, and kinetochores during metaphase (Figure 3-11D-E). mCherry-SENP1$^{\Delta153}$ and mCherry-SENP1$^{\Delta272}$ also retained NPC localization during interphase, and

limited localization at the centrosomes, the mitotic spindle, and kinetochores during metaphase.

To evaluate the functional requirements of SENP1 N-terminal domains for appropriate mitotic progression, we performed rescue experiments using these stable, inducible cell lines. Cells were depleted of endogenous SENP1 for 48 hours with concomitant doxycycline-induced mCherry-SENP1 expression (Figure 3-12A, B). As expected, siSENP1 cells exhibited a prolonged metaphase-anaphase delay compared to control cells (Figure 3-12C-D, fixed images with time indicated in minutes, E-F). Expression of full-length, wild type mCherry-SENP1 rescued the metaphase-anaphase delay, while mCherry-SENP1^{C603S} did not (Figure 3-12C-D, G-H). Importantly, expression of mCherry-SENP1$^{\Delta 153}$ also rescued the metaphase-anaphase delay caused by SENP1 depletion, whereas expression of mCherry-SENP1$^{\Delta 272}$ did not. Thus, our findings reveal that the first 153 amino acids of SENP1 are dispensable for normal metaphase-anaphase transitions, whereas residues from 153-272, which mediate interactions with the Nup107 complex, are critical.

DISCUSSION

During different stages of the cell cycle, proteins in the SUMO pathway localize to unique sub-cellular compartments, with distinct regulatory roles. Over the past several decades, molecular mechanisms by which SUMO modification coordinates cellular processes have been revealed. Functional roles for SUMO deconjugating enzymes, or SENPs, in human cells are diverse and are involved in almost every essential cellular process. SUMO modification of transcription factors has broadly been characterized as inactivating, while de-conjugation by SENP1 have been implicated in activating transcription of innate immune response elements[49]. Additional roles for SENP3 and SENP5 in regulating ribosome biogenesis, SENP6 editing SUMO-ubiquitin hybrid chains, and SENP7 in chromatin remodeling, all indicate an axis of regulation as diverse as SUMO conjugation. Roles for SENPs have also been characterized for mitotic progression, as overexpression of SENP2 causes defects in kinetochore targeting, resulting in chromosome congression defects[50] while SENP6 regulates the assembly of inner kinetochore proteins[51]. Here we further describe a functional requirement of N-terminal SENP1 interactions with components of the NPC that coordinate mitotic checkpoint signaling, to properly coordinate the timing of metaphase to anaphase transitions.

We have expanded our investigation on the functional role of SENP1 during mitosis[20]. Analysis of kinetochore-microtubule interactions in SENP1 depleted cells does not affect SAC recruitment during prometaphase nor release during metaphase from the kinetochore. Inactivation of the SAC by reversine treatment largely rescues the metaphase-anaphase delay observed in SENP1 depleted cells, implicating a functional role for SENP1 in regulating checkpoint signaling. Notably, siSENP1 cells treated with reversine form a metaphase plate and undergo a more normal mitotic progression, with no statistically significant differences in mitotic timing compared to control cells ($p = 0.095$, Figure 3-8D). The absence of catastrophic anaphases in siSENP1 cells is also noted, in addition to the relatively normal mitosis under a condition where SAC is chemically inhibited. This may be due to incomplete SAC silencing by reversine treatment, and while many of the signaling and mechanistic processes of the SAC at the kinetochore have been characterized, it is yet unknown how the "rheostat[52]" of checkpoint signaling is controlled. SENP1 activity may be involved in the fine-tuning process of the "rheostat" and likely affects the activity of a variety of substrates that have potentially opposing roles during mitotic progression.

Here we demonstrate that SENP1 depletion affects targeting and accumulation of Mad1 and Mad2 at the NPCs during interphase. Pre-assembly of SAC complexes during interphase contribute towards inhibitory signals against the APC/C, and increased steady state levels of SAC proteins can contribute towards delayed metaphase-anaphase timing. Whether a soluble fraction of SAC proteins that does not localize at the kinetochore contributes towards inhibiting APC/C activity is yet unknown. SENP1 depletion, resulting in hyper-sumoylation of substrates, may function to recruit or retain Mad1 and Mad2 at the nuclear pore complexes. Indeed, Mad1 has been identified as a SUMO substrate in proteomic studies but has yet to be validated[36]. Whether SENP1 is a regulator of Mad1 SUMO modification, or if novel SUMO-SIM interactions function to retain Mad1 at the nuclear pores are questions of particular future interest. While SENP1 and SENP2 have been previously implicated in regulating the interaction between Mad1 and Mad2 with Tpr[11], neither have been validated as SUMO substrates. Further analysis of the relationship between these proteins will elucidate mechanistic roles for SUMO-mediated checkpoint pre-assembly at the NPC. Whether the pre-assembled checkpoint complexes contribute to inhibitory APC/C signaling localized at kinetochores, or if a soluble kinetochore-independent fraction of inhibitory MCCs are generated to

attenuate APC/C activity, and whether one pool is under regulatory control by SENP1 are all outstanding questions to pursue.

We also performed localization studies using GFP-SENP1 constructs containing N-terminal truncations. Consistent with a previously characterized nuclear localization signal (NLS) at amino acids 171-7, full length SENP1 and truncation mutants containing this NLS localize to the nucleus[47]. Based on our analysis, additional sequences within the first 153 amino acids may be responsible for nuclear targeting of GFP-SENP1$^{1-40}$ and GFP-SENP1$^{41-153}$. Localization analysis was also performed on mitotic cells for GFP-SENP1 and N-terminal truncation mutants. Targeting to the mitotic spindle is conferred by sequences in SENP1 spanning amino acids 1-40, 41-153, and 273-449, while full length GFP-SENP1 also localizes to the centrosomes and at kinetochores. How SENP1 is recruited to these mitotic structures is an area of key interest, as it is yet unknown if SENP1 interacts with specific proteins at the kinetochore. Another possibility for SENP1 targeting is mediated by putative SIM regions in the N-terminus of SENP1 which may direct SENP1 recruitment to SUMO modified substrates at mitotic structures. Whether SENP1 activity is under control of other post-

translational modifications such as phosphorylation to direct specific sub-cellular targeting is also an outstanding question.

In an unbiased approach towards identifying SENP1 interacting proteins in asynchronous cells, we used BioID, a method with sensitivity in capturing non-covalent interactions. Among the categories of proteins interacting with SENP1 are karyopherins, the Nup107-160 complex, FG repeat nucleoporins, and the nuclear lamina. During interphase, two separate targeting domains to NPCs are featured in the N-terminus of SENP1, spanning amino acid residues 153-272 and 273-449. BioID analysis indicates that these domains interact with the nucleoporins Nup107 and Tpr, respectively. Consistent with this finding, other N-terminal fragments that are not targeted to the pore (spanning amino acid residues 1-41 and 41-153) were not identified through BioID analysis (Table 3-1). The association of $SENP1^{153-272}$ with the Nup107 complex together with the interaction of $SENP1^{273-449}$ with Tpr are particularly interesting, as these nucleoporins are known to regulate kinetochore assembly and signaling during mitosis. It is yet unknown how SENP1 interacts with these nucleoporins. Whether the nucleoporins or other binding partners, like Mad1, are SUMO modified – will be an important mechanistic question to address. Furthermore, analysis

using the BirA*-SENP1 system with mitotic cells may reveal additional information regarding unique interactions.

Finally, to investigate the functional requirements of N-terminal sequence domains in SENP1, we generated a system whereby endogenous depletion of SENP1 could be complemented by the expression of inducible transgenes of full length, catalytically mutant (C603S), or N-terminal truncations of SENP1. Endogenous depletion of SENP1 and expression of mCherry SENP1 functionally rescues the metaphase-anaphase delay, while mCherry SENP1^{C603S} does not. This assay was used to evaluate if binding interactions with either the Nup107 complex or Tpr is required for normal mitotic progression. Expression of mCherry SENP1 variants and analysis by timelapse microscopy revealed a functional rescue of the metaphase-anaphase delay in mCherry SENP1$^{\Delta 153}$ which binds to the Nup107 complex. Interestingly, mCherry SENP1$^{\Delta 272}$, which binds to Tpr but not Nup107, does not rescue the metaphase-anaphase delay observed in SENP1 depleted cells. Taken together, these data suggest that SENP1 interactions with Nup107 are critical for normal metaphase-anaphase transition times.

Recent advances in high throughput studies revealing the SUMO proteome have identified thousands of additional proteins that are under regulatory control by the SUMO pathway[36–38,53,54]. Validation and

characterization of these proteins, in addition to proteomic analyses of SENP1 and other SENP isoforms, will further demonstrate the versatility of SUMO modification in regulating mitotic progression. Finally, chemical inhibitors of the SUMO pathway[55,56] have been an area of developing attention. Future work towards the development of specific inhibitors towards individual SENPs will facilitate novel discoveries on how the SUMO pathway affects human health and disease.

REFERENCES

1. Holland & Cleveland. Boveri revisited: chromosomal instability, aneuploidy and tumorigenesis. Nature Reviews Molecular Cell Biology 10, nrm2718 (2009).

2. Hanahan & Weinberg. Hallmarks of Cancer: The Next Generation. Cell 144, 646–674 (2011).

3. Kops, Weaver & Cleveland. On the road to cancer: aneuploidy and the mitotic checkpoint. Nature Reviews Cancer 5, 773–785 (2005).

4. Gerace & Blobel. The nuclear envelope lamina is reversibly depolymerized during mitosis. Cell 19, 277–87 (1980).

5. Heald & McKeon. Mutations of phosphorylation sites in lamin A that prevent nuclear lamina disassembly in mitosis. Cell 61, 579–89 (1990).

6. Macaulay, Meier & Forbes. Differential mitotic phosphorylation of proteins of the nuclear pore complex. Journal of Biological Chemistry 270, 254–262 (1995).

7. Belgareh, Rabut & cell BSO, …. An evolutionarily conserved NPC subcomplex, which redistributes in part to kinetochores in mammalian cells. (2001).

8. Wang, Babu, Harden & JSO, B. The mitotic checkpoint protein hBUB3 and the mRNA export factor hRAE1 interact with GLE2p-binding sequence (GLEBS)-containing proteins. (2001).

9. Babu, Jeganathan, Baker & Biol. Rae1 is an essential mitotic checkpoint regulator that cooperates with Bub3 to prevent chromosome missegregation. (2003).

10. Salina, Enarson, Rattner & Burke. Nup358 integrates nuclear envelope breakdown with kinetochore assembly. The Journal of Cell Biology 162, 991–1001 (2003).

11. Schweizer et al. Spindle assembly checkpoint robustness requires Tpr-mediated regulation of Mad1/Mad2 proteostasis. The Journal of Cell

Biology 203, 883–893 (2013).

12. Rodriguez-Bravo et al. Nuclear Pores Protect Genome Integrity by Assembling a Premitotic and Mad1-Dependent Anaphase Inhibitor. Cell 156, 1017–1031 (2014).

13. Foley & Kapoor. Microtubule attachment and spindle assembly checkpoint signalling at the kinetochore. Nature Reviews Molecular Cell Biology 14, nrm3494 (2012).

14. Lara-Gonzalez, Westhorpe & Taylor. The Spindle Assembly Checkpoint. Current Biology 22, R966–R980 (2012).

15. Musacchio & Salmon. The spindle-assembly checkpoint in space and time. Nature Reviews Molecular Cell Biology 8, 379–393 (2007).

16. Sivakumar & Gorbsky. Spatiotemporal regulation of the anaphase-promoting complex in mitosis. Nature Reviews Molecular Cell Biology 16, nrm3934 (2015).

17. Musacchio. The Molecular Biology of Spindle Assembly Checkpoint Signaling Dynamics. Current Biology 25, R1002–R1018 (2015).

18. Gareau & Lima. The SUMO pathway: emerging mechanisms that shape specificity, conjugation and recognition. Nature Reviews Molecular Cell Biology 11, nrm3011 (2010).

19. Flotho & Melchior. Sumoylation: A Regulatory Protein Modification in Health and Disease. Annual Review of Biochemistry 82, 357–385 (2013).

20. Cubeñas-Potts, Goeres & Matunis. SENP1 and SENP2 affect spatial and temporal control of sumoylation in mitosis. Molecular biology of the cell 24, 3483–95 (2013).

21. Melchior. SUMO-NONCLASSICAL UBIQUITIN. Annual review of cell and developmental biology 591–626 (2000). doi:10.1146/annurev.cellbio.16.1.591

22. Eifler & Vertegaal. SUMOylation-Mediated Regulation of Cell Cycle Progression and Cancer. Trends in Biochemical Sciences 40, 779–793

(2015).

23. Meluh & Koshland. Evidence that the MIF2 gene of Saccharomyces cerevisiae encodes a centromere protein with homology to the mammalian centromere protein CENP-C. Molecular Biology of the Cell 6, 793–807 (1995).

24. Tanaka et al. Characterization of a Fission Yeast SUMO-1 Homologue, Pmt3p, Required for Multiple Nuclear Events, Including the Control of Telomere Length and Chromosome Segregation. Molecular and Cellular Biology 19, 8660–8672 (1999).

25. Matunis, Coutavas & Blobel. A novel ubiquitin-like modification modulates the partitioning of the Ran-GTPase-activating protein RanGAP1 between the cytosol and the nuclear pore complex. The Journal of Cell Biology 135, 1457–1470 (1996).

26. Mahajan, Delphin, Guan, Gerace & Melchior. A Small Ubiquitin-Related Polypeptide Involved in Targeting RanGAP1 to Nuclear Pore Complex Protein RanBP2. Cell 88, 97–107 (1997).

27. Reverter & Lima. Insights into E3 ligase activity revealed by a SUMO–RanGAP1–Ubc9–Nup358 complex. Nature 435, 687–692 (2005).

28. Azuma, Arnaoutov & Dasso. SUMO-2/3 regulates topoisomerase II in mitosis. The Journal of Cell Biology 163, 477–487 (2003).

29. Ryu, Furuta, Kirkpatrick, Gygi & Azuma. PIASy-dependent SUMOylation regulates DNA topoisomerase IIα activity. The Journal of Cell Biology 191, 783–794 (2010).

30. Li et al. SUMOylated NKAP is essential for chromosome alignment by anchoring CENP-E to kinetochores. Nature Communications 7, 12969 (2016).

31. Zhang et al. SUMO-2/3 Modification and Binding Regulate the Association of CENP-E with Kinetochores and Progression through Mitosis. Molecular Cell 29, 729–741 (2008).

32. Yang, Chen & Dai. Sumoylation of Kif18A plays a role in regulating

mitotic progression. BMC Cancer 15, 197 (2015).

33. Restuccia, Yang, Chen, Lu & Dai. Mps1 is SUMO-modified during the cell cycle. Oncotarget 7, 3158–3170 (2015).

34. Ban, Nishida & Urano. Mitotic kinase Aurora-B is regulated by SUMO-2/3 conjugation/deconjugation during mitosis. Genes to Cells 16, 652–669 (2011).

35. Yang et al. BubR1 Is Modified by Sumoylation during Mitotic Progression. Journal of Biological Chemistry 287, 4875–4882 (2012).

36. Schimmel et al. Uncovering SUMOylation Dynamics during Cell-Cycle Progression Reveals FoxM1 as a Key Mitotic SUMO Target Protein. Molecular Cell 53, 1053–1066 (2014).

37. Matic et al. Site-Specific Identification of SUMO-2 Targets in Cells Reveals an Inverted SUMOylation Motif and a Hydrophobic Cluster SUMOylation Motif. Molecular Cell 39, 641–652 (2010).

38. Cubeñas-Potts et al. Identification of SUMO-2/3-modified proteins associated with mitotic chromosomes. Proteomics 15, 763–72 (2015).

39. Li & Hochstrasser. A new protease required for cell-cycle progression in yeast. Nature 398, 18457 (1999).

40. Gong, Millas, Maul & Yeh. Differential Regulation of Sentrinized Proteins by a Novel Sentrin-specific Protease. Journal of Biological Chemistry 275, 3355–3359 (2000).

41. Shin et al. DeSUMOylating isopeptidase: a second class of SUMO protease. EMBO reports 13, 339–346 (2012).

42. Schulz et al. Ubiquitin-specific protease-like 1 (USPL1) is a SUMO isopeptidase with essential, non-catalytic functions. EMBO reports 13, 930–938 (2012).

43. Li & Hochstrasser. The Ulp1 SUMO isopeptidase. The Journal of Cell Biology 160, 1069–1082 (2003).

44. Mukhopadhyay & Dasso. Modification in reverse: the SUMO proteases. Trends in Biochemical Sciences 32, 286–295 (2007).

45. Santaguida, Tighe, D'Alise, Taylor & Musacchio. Dissecting the role of MPS1 in chromosome biorientation and the spindle checkpoint through the small molecule inhibitor reversine. The Journal of Cell Biology 190, 73–87 (2010).

46. Lee, Sterling, Burlingame & McCormick. Tpr directly binds to Mad1 and Mad2 and is important for the Mad1–Mad2-mediated mitotic spindle checkpoint. Genes & Development 22, 2926–2931 (2008).

47. Bailey & O'Hare. Characterization of the Localization and Proteolytic Activity of the SUMO-specific Protease, SENP1. Journal of Biological Chemistry 279, 692–703 (2004).

48. Coyaud et al. BioID-based Identification of Skp Cullin F-box (SCF)β-TrCP1/2 E3 Ligase Substrates. Molecular & Cellular Proteomics 14, 1781–1795 (2015).

49. Nayak, A. & Müller, S. SUMO-specific proteases/isopeptidases: SENPs and beyond. Genome Biology 15, 1–7 (2014).

50. Goeres et al. The SUMO-specific isopeptidase SENP2 associates dynamically with nuclear pore complexes through interactions with karyopherins and the Nup107-160 nucleoporin subcomplex. Molecular Biology of the Cell 22, 4868–4882 (2011).

51. Mukhopadhyay, Arnaoutov & Dasso. The SUMO protease SENP6 is essential for inner kinetochore assembly. The Journal of Cell Biology 188, 681–692 (2010).

52. Collin, Nashchekina, Walker & Pines. The spindle assembly checkpoint works like a rheostat rather than a toggle switch. Nature Cell Biology 15, 1378–1385 (2013).

53. Hendriks & Vertegaal. A comprehensive compilation of SUMO proteomics. Nature Reviews Molecular Cell Biology 17, nrm.2016.81 (2016).

54. Hendriks et al. Uncovering global SUMOylation signaling networks in a site-specific manner. Nature Structural and Molecular Biology 21, nsmb.2890 (2014).

55. Hughes et al. Generation of specific inhibitors of SUMO-1– and SUMO-2/3–mediated protein-protein interactions using Affimer (Adhiron) technology. Sci. Signal. 10, eaaj2005 (2017).

56. He et al. Probing the roles of SUMOylation in cancer cell biology by using a selective SAE inhibitor. Nature Chemical Biology 13, nchembio.2463 (2017).

Figure 3-1

SENP1 is required for normal metaphase-anaphase transition timing.

(A) Cells were treated with control or siRNA to APC4 for 48 hours were imaged by timelapse live cell acquisition for 16 hours. Fixed images from timelapse acquisition of control cells entering mitosis beginning with NEBD at 0:00 (hr:min). (B) siSENP1 cells delay metaphase-anaphase transitions; fixed images from timelapse aquisition. (C) Analysis represents mitotic progression time in minutes, beginning with nuclear envelop breakdown (NEBD) to metaphase, and metaphase to anaphase onset. Data shown are from three replicate experiments. Control and siSENP1 cells spent similar times on average from NEBD to metaphase. (Control 23.86 min ± 0.55, n=140; siSENP1 25.50 min ± 1.18; n=140; average ± SD). (D) siSENP1 cells have a prolonged metaphase-anaphase transition time. (Control, 29.00 ± 0.79 min, n = 140; siSENP170.14 ± 3.71, n=140; average ± SD, $P<0.0001$). (E-F) Cells were treated with control or siSENP1 for 48 hours, followed by a double thymidine block and release into drug-free media. Cells were collected at various timepoints following release and immunoblotting to Cyclin B1, glyceraldehyde-3-phosphate dehydrogenase (GAPDH), and SENP1 was performed.

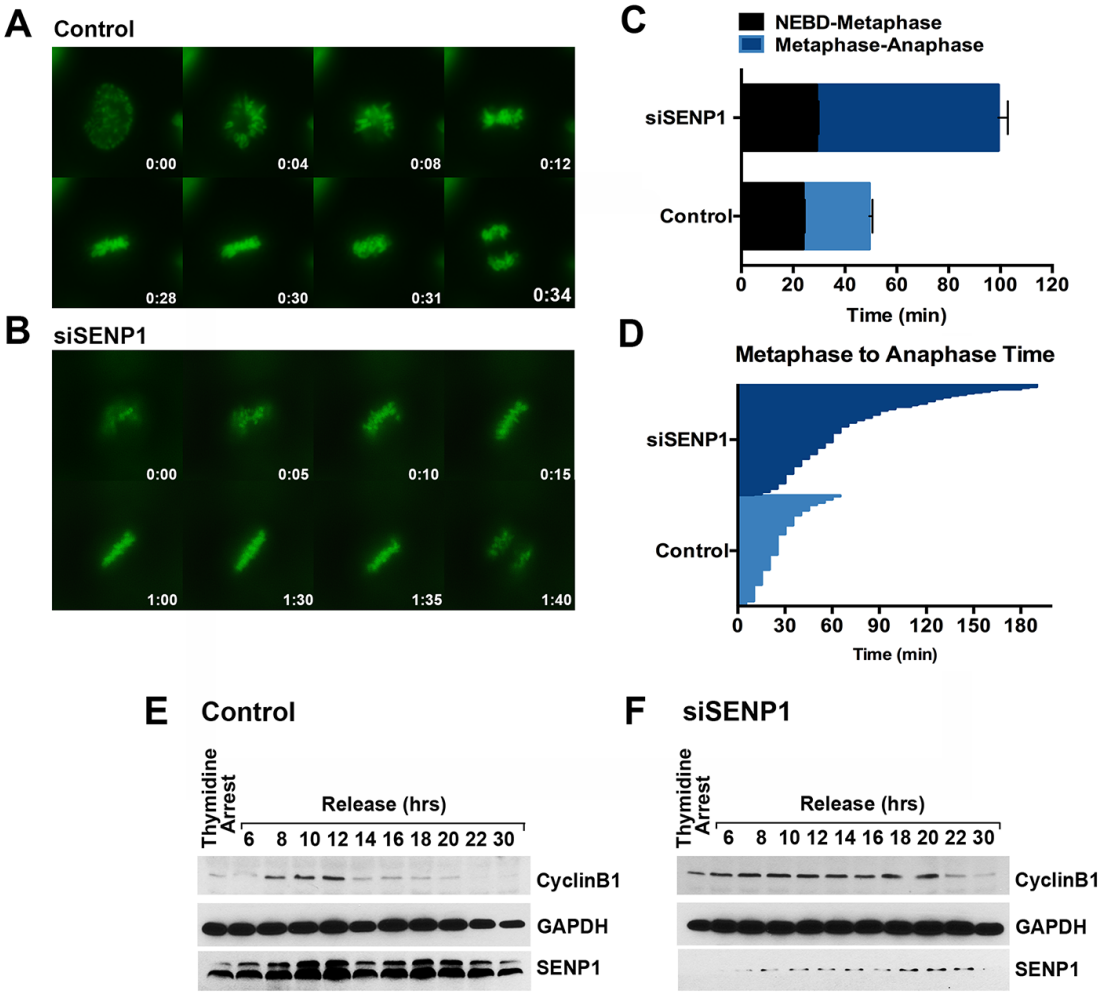
A
Control
0:00
0:04
0:08
0:12
0:28
0:30
0:31
0:34
B
siSENP1
0:00
0:05
0:10
0:15
1:00
1:30
1:35
1:40
C
NEBD-Metaphase
Metaphase-Anaphase
siSENP1
Control
0
20
40
60
80
100
120
Time (min)
D
Metaphase to Anaphase Time
siSENP1
Control
0
30
60
90
120
150
180
Time (min)
E
Control
Thymidine Arrest
Release (hrs)
6 8 10 12 14 16 18 20 22 30
CyclinB1
GAPDH
SENP1
F
siSENP1
Thymidine Arrest
Release (hrs)
6 8 10 12 14 16 18 20 22 30
CyclinB1
GAPDH
SENP1

Figure 3-2

SENP1 depletion does not affect inter-kinetochore distances or SAC protein signaling.

(A) Cells were treated with control or siSENP1 for 48 hours before fixation and immunofluorescence to CREST (red) and tubulin (green) and counterstained with DAPI. Bar, 2 μm. (B) Inter-kinetochore distances were determined (control 0.78 μm ± 0.21, n=463; siSENP1 0.79 μm ± 0.25, n=577. P=0.87). (C) Immunoblots from control or siSENP1 cells with antibodies specific for SENP1 and tubulin as a loading control. (D) Cells were treated with control or siSENP1 for 48 hours before fixation and immunofluorescence to SAC proteins Cdc20, Mad1, and BubR1 (green) with co-immunostaining with CREST (red) and chromatin/DNA counterstained with DAPI. Representative prometaphase and metaphase cells are shown.

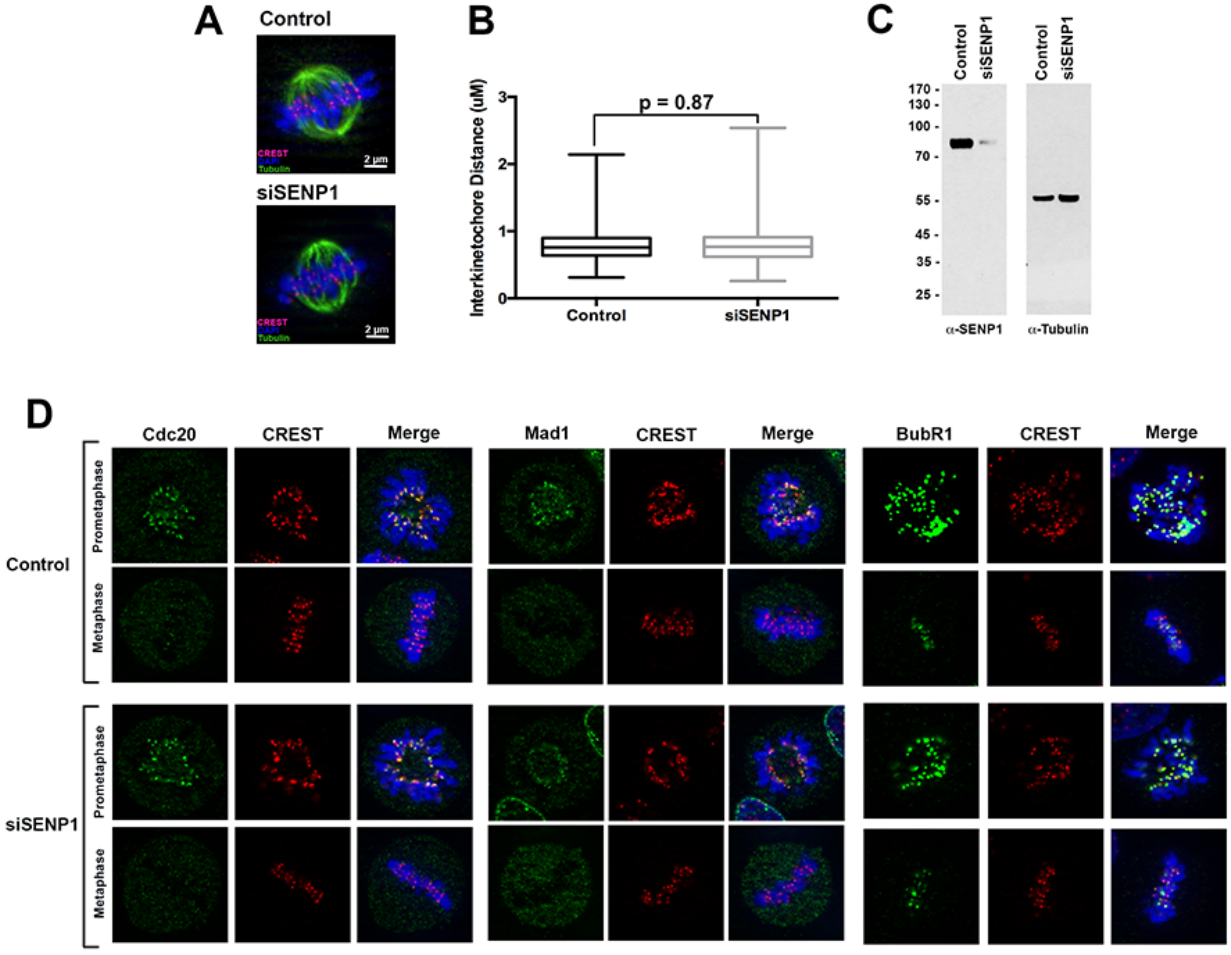
A
Control
CREST
DAPI
Tubulin
2 μm
siSENP1
CREST
DAPI
Tubulin
2 μm
B
Interkinetochore Distance (uM)
p = 0.87
Control
siSENP1
C
Control
siSENP1
Control
siSENP1
170 -
130 -
100 -
70 -
55 -
45 -
35 -
25 -
α-SENP1
α-Tubulin
D
Cdc20
CREST
Merge
Mad1
CREST
Merge
BubR1
CREST
Merge
Control
Prometaphase
Metaphase
siSENP1
Prometaphase
Metaphase

Figure 3-3

SENP1 depleted cells properly localize SAC proteins during prometaphase.

Cells were treated with control or siSENP1 for 48 hours and treated for 12 hours with nocodazole to arrest in prometaphase prior to fixation and immunofluorescence analysis. Antibodies specific to (A) Mad1(B) BubR1 (C) Mad2 or (D) Bub1 used in addition to co-staining with CREST to indicate kinetochores. Chromatin/DNA was counterstained with DAPI.

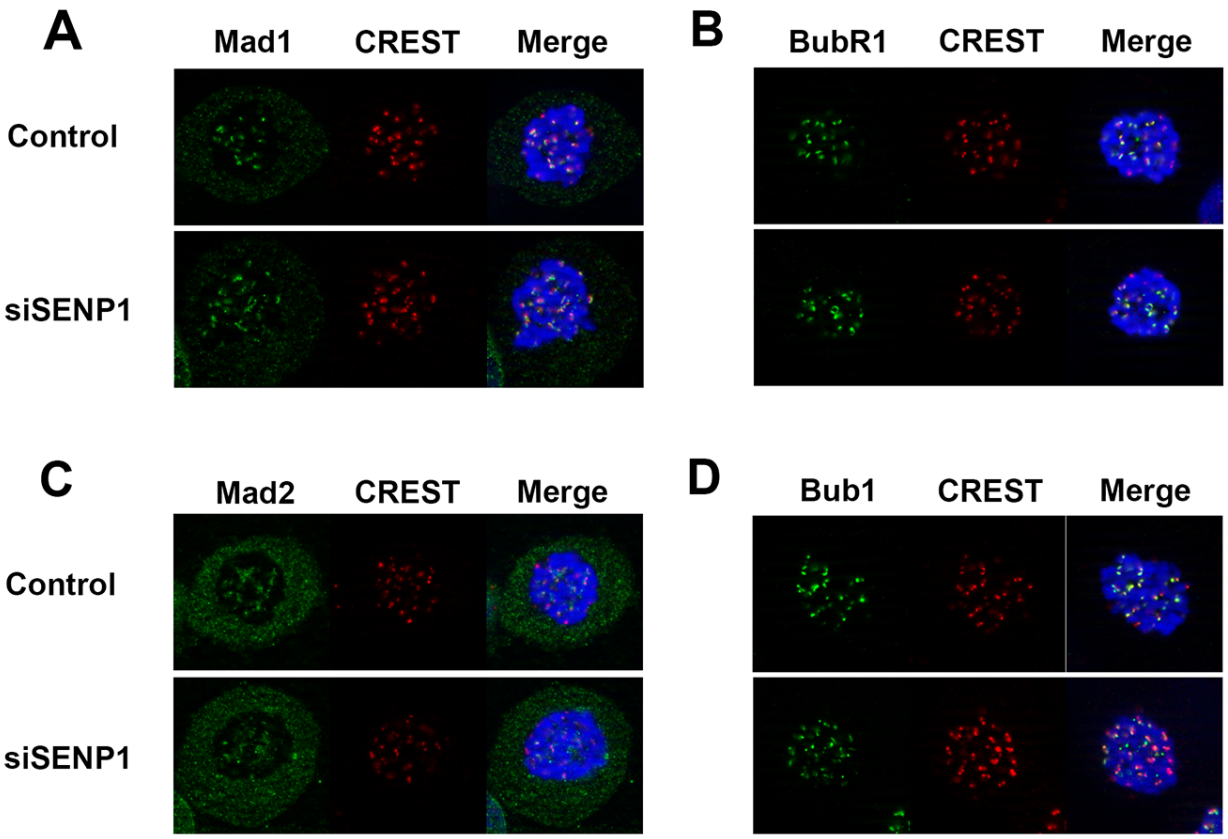
A
Mad1
CREST
Merge
Control
siSENP1
B
BubR1
CREST
Merge
C
Mad2
CREST
Merge
Control
siSENP1
D
Bub1
CREST
Merge

Figure 3-4

Reversine treatment causes catastrophic anaphase in control cells but rescues the metaphase-anaphase delay in SENP1 depleted cells.

(A) HeLa cells were treated with control or siSENP1 for 48 hours. Immunoblotting to SENP1 and GAPDH. (B) siSENP1 cells spent longer total times in mitosis. (control, 46.53 min ± 28.89, n = 17; siSENP1 104.61 ± 37.30, n=31; average ± SD, P=0.095). Control cells treated with reversine spent shorter total times in mitosis compared to control cells. (Control, 46.53 min ± 28.89, n = 17; control + Reversine 17.47 ± 10.75, n=34; average ± SD, P=0.0008). siSENP1 cells treated with reversine spent shorter total times in mitosis compared to siSENP1 cells. (siSENP1 104.61 ± 37.30, n=31; siSENP1 + Reversine 33.45 ± 20.55, n=64; average ± SD, P<0.0001). (C) Fixed images from timelapse microscopy analysis of control cells treated with reversine (time in hr:min). (D) Fixed images from timelapse microscopy analysis of siSENP1 cells treated with reversine (time in hr:min).

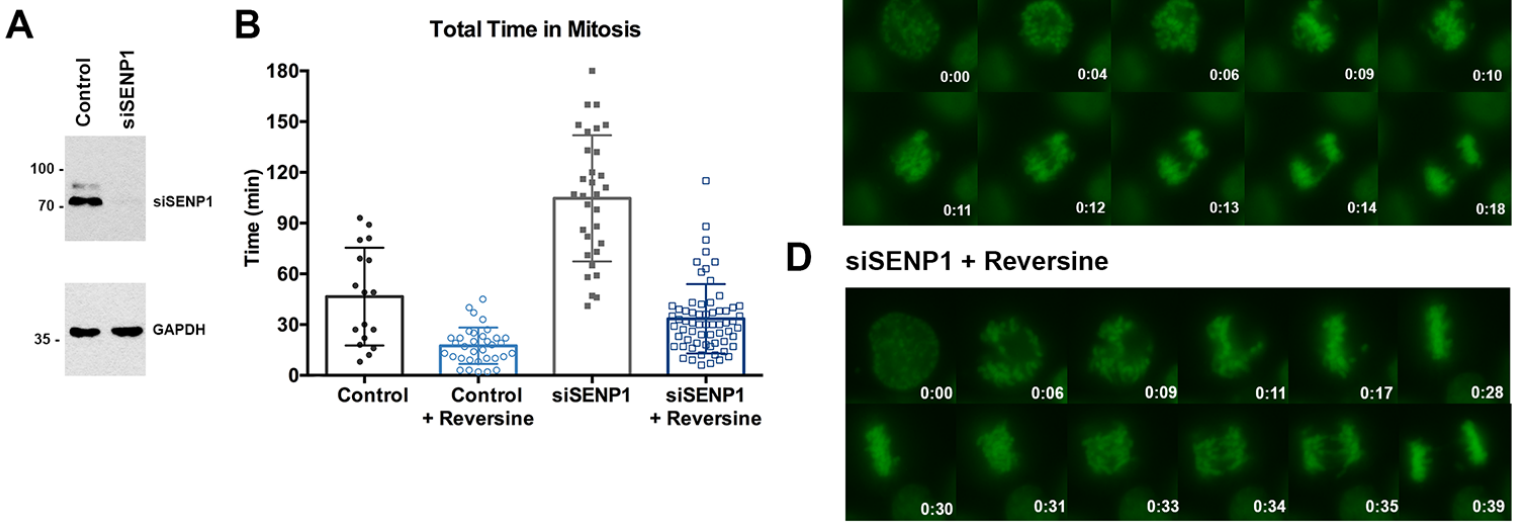
A
Control
siSENP1
100 -
70 -
siSENP1
35 -
GAPDH
B
Total Time in Mitosis
Time (min)
180
150
120
90
60
30
0
Control
Control + Reversine
siSENP1
siSENP1 + Reversine
C
Control + Reversine
0:00
0:04
0:06
0:09
0:10
0:11
0:12
0:13
0:14
0:18
D
siSENP1 + Reversine
0:00
0:06
0:09
0:11
0:17
0:28
0:30
0:31
0:33
0:34
0:35
0:39

Figure 3-5

SENP1 depletion in APC4 and APC4^{KR} cells.

(A) APC4 and APC4^{KR} (SUMO mutant) cells, previously shown to limit the activity of the APC/C were treated with siRNA targeting oligonucleotides to deplete endogenous APC4 with concomitant doxycycline-induced transgene expression. Cells were co-depleted of SENP1. Timelapse imaging analysis shows NEBD-metaphase timing in APC4 + siSENP1, APC4^{KR}, and APC4^{KR} + SENP1 cells (33.24 min ± 1.35, 35.92 min ±1.21, and 34.43 ± 1.41, respectively) and also metaphase-anaphase timing in APC4 + siSENP1, APC4^{KR}, and APC4^{KR} + SENP1 cells (79.49 min ± 4.51, 65.00 min ± 4.72, and 80.67 min ± 3.73, respectively). P-values from two-tailed t-tests are shown. (B) Fixed images from timelapse analysis are shown in hr:min for APC4 cells depleted of SENP1 (C) APC4^{KR} and (D) APC4^{KR} + SENP1 cells.

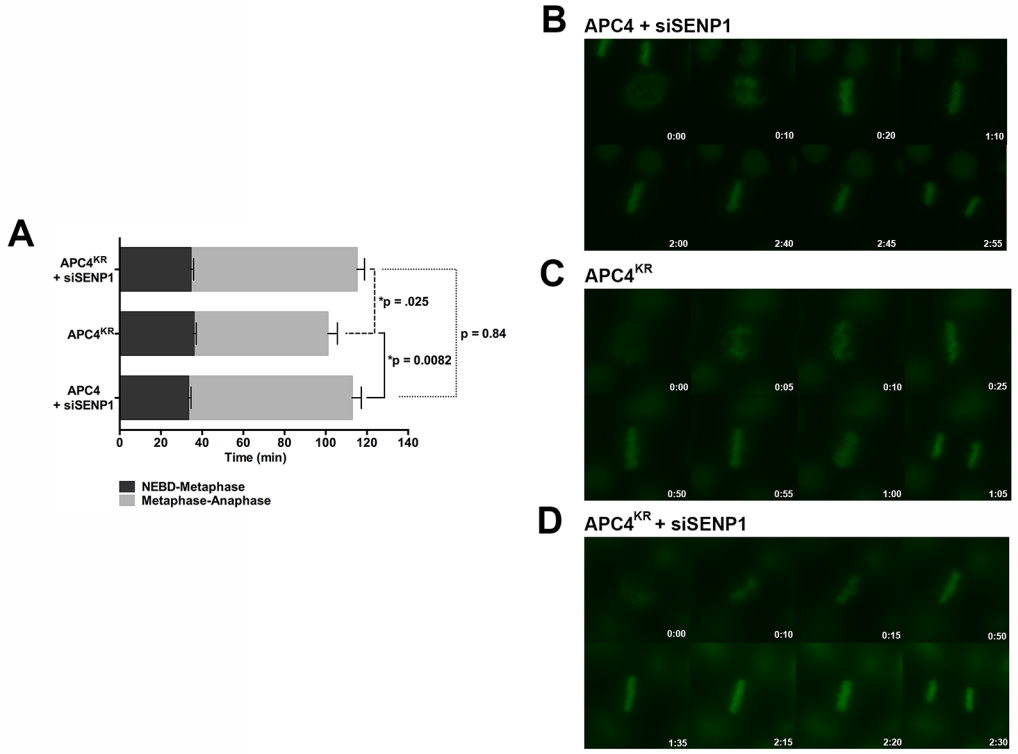
A
APC4KR + siSENP1
APC4KR
APC4 + siSENP1
*p = .025
*p = 0.0082
p = 0.84
0
20
40
60
80
100
120
140
Time (min)
NEBD-Metaphase
Metaphase-Anaphase
B
APC4 + siSENP1
0:00
0:10
0:20
1:10
2:00
2:40
2:45
2:55
C
APC4KR
0:00
0:05
0:10
0:25
0:50
0:55
1:00
1:05
D
APC4KR + siSENP1
0:00
0:10
0:15
0:50
1:35
2:15
2:20
2:30

Figure 3-6

SENP1 depletion results in accumulation of Mad1 and Mad2 at the nuclear pores during interphase.

(A) Cells were treated with control or siSENP1 for 48 hours before fixation and immunofluorescence to Mad1 or Mad2 (green) and chromatin/DNA was counterstained with DAPI. (B) Relative fluorescence density for Mad1 was quantified and normalized to the area of the nuclear periphery in cells treated with a control siRNA or targeting SENP1. Control cells have a relative fluorescence intensity of 3.95 ± 0.52 (n=18) compared to siSENP1 cells 4.86 ± 0.77 (n=20) (P=0.00013). (C) Relative fluorescence intensity for Mad2 was quantified and normalized to the area at the nuclear periphery in cells treated with a control siRNA or targeting SENP1. Control cells have a relative fluorescence intensity of 5.46 ± 1.22 (units/pixel^2) (n=19) compared to siSENP1 cells 6.83 ± 1.69 (n=20) (P=0.0064). (D) Immunoblot of control and siSENP1 cells with antibodies specific for SENP1 and tubulin as a loading control.

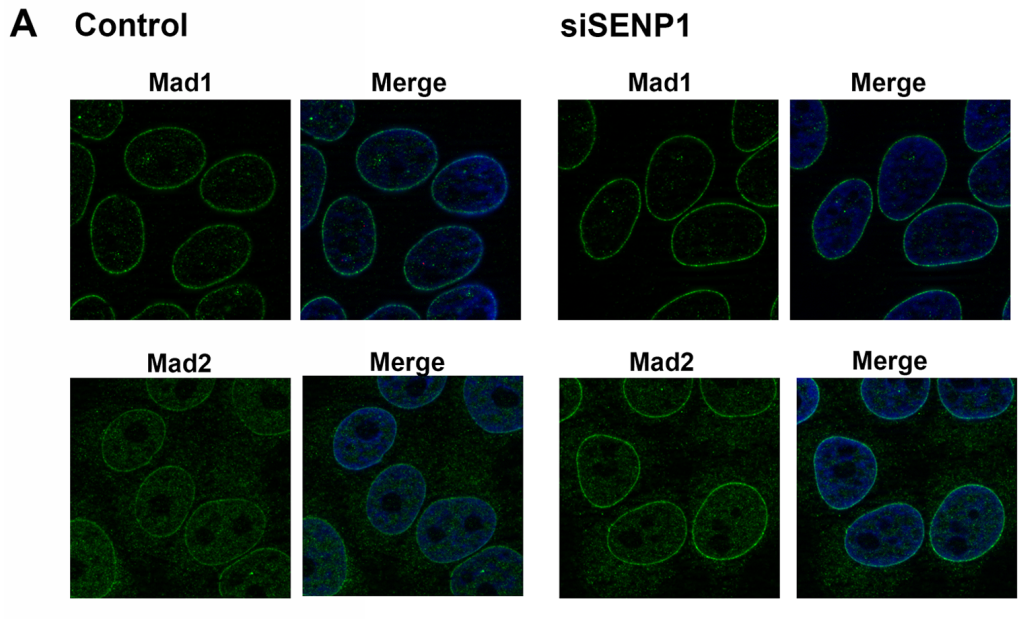
A
Control
siSENP1
Mad1
Merge
Mad1
Merge
Mad2
Merge
Mad2
Merge

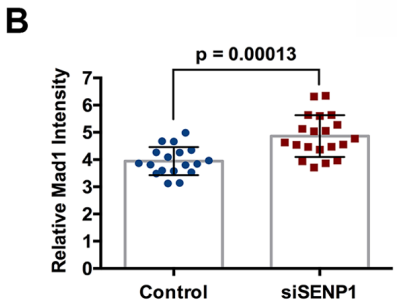
B
p = 0.00013
Relative Mad1 Intensity
0
1
2
3
4
5
6
7
Control
siSENP1

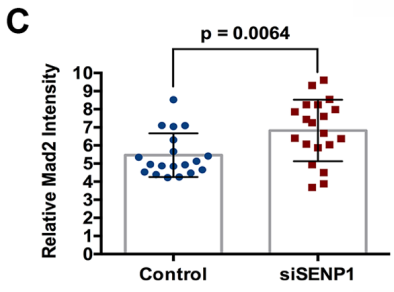
C
p = 0.0064
Relative Mad2 Intensity
0
1
2
3
4
5
6
7
8
9
10
Control
siSENP1

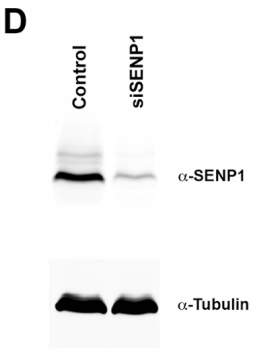
D
Control
siSENP1
α-SENP1
α-Tubulin

Figure 3-7

GFP-SENP1 localizes to unique sub-cellular compartments during the cell cycle.

Asynchronous HeLa cells were transfected with GFP-SENP1 for 48 hours. Immunofluorescence with Hec1 antibody and nuclei/chromosomes counterstained with DAPI in mitotic cells as indicated.

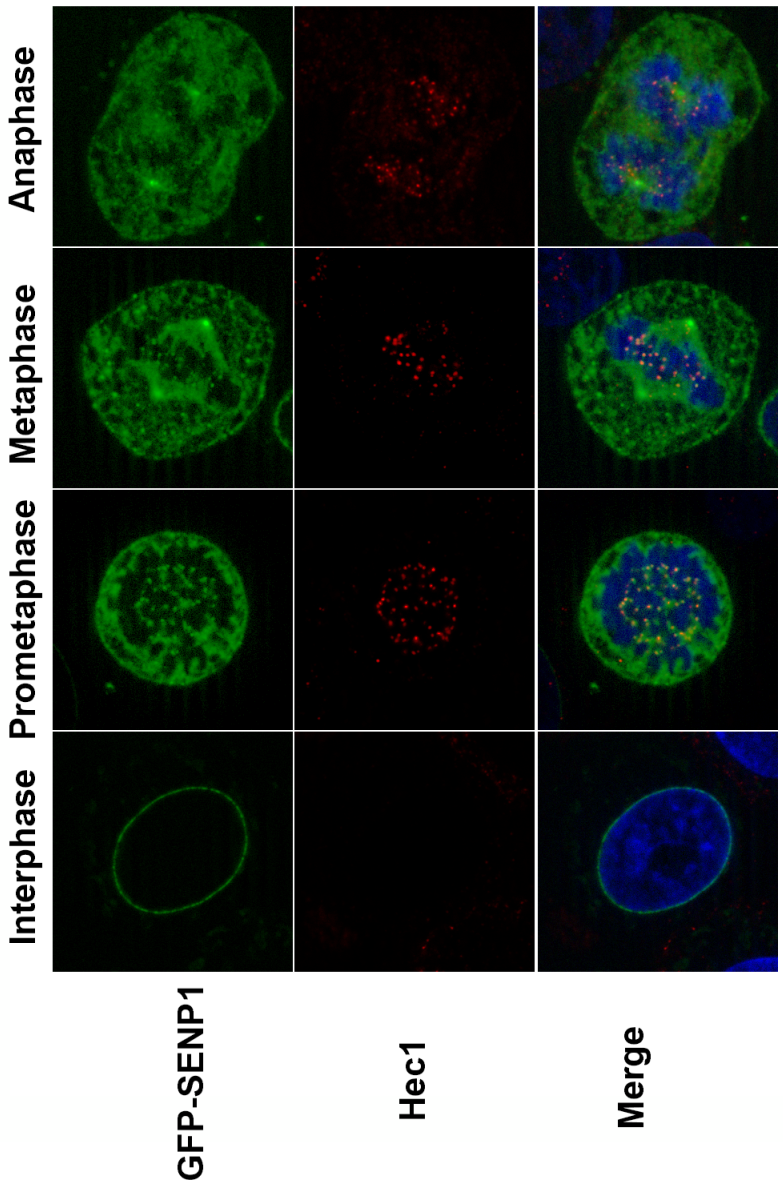
Interphase
Prometaphase
Metaphase
Anaphase
GFP-SENP1
Hec1
Merge

Figure 3-8

SENP1 N-terminal domains localize to the nuclear pore.

(A) SENP1 is a 644 amino acid protein, with a nuclear localization signal sequence (NLS) at amino acids 171-177, a conserved catalytic domain spanning amino acids 419-644, a catalytic cysteine at 603, and a nuclear export signal sequence (NES) at amino acids 633-644. N-terminal GFP fusion constructs were generated for SENP1 1-40, 41-153, 154-272, and amino acids 273-449. (B) GFP-SENP1 constructs were transfected into HeLa cells. Immunofluorescence analysis with the nuclear pore complex marker 414 and counterstaining of chromosomes/DNA with DAPI is shown for various GFP-SENP1 truncations.

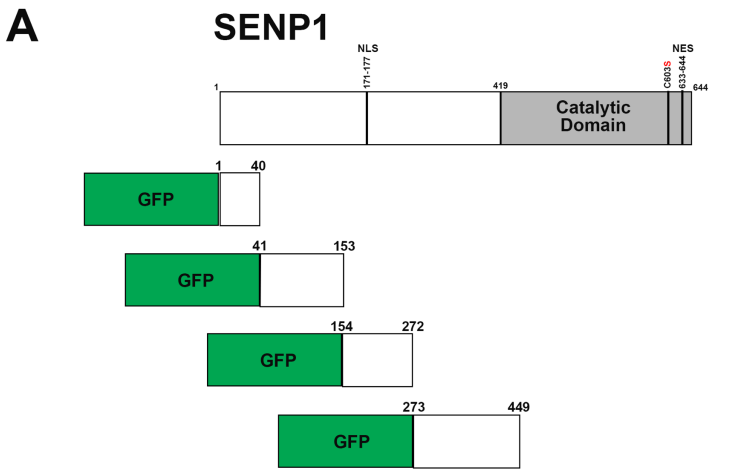
A
SENP1
NLS
171-177
NES
C603S
633-644
1
419
644
Catalytic Domain
1
40
GFP
41
153
GFP
154
272
GFP
273
449
GFP

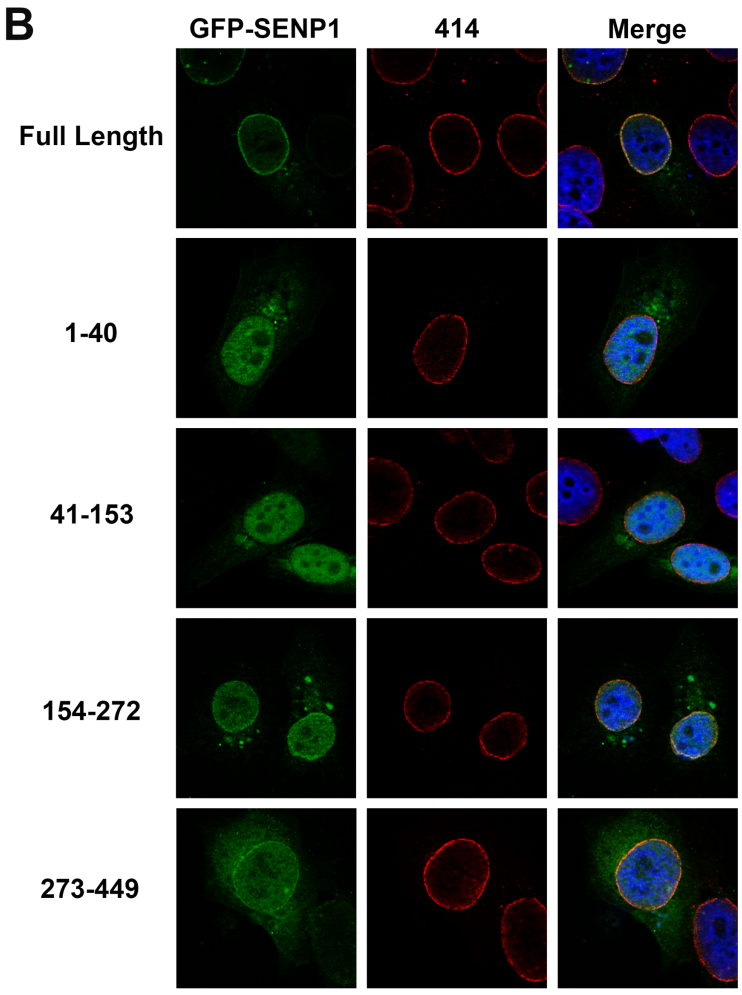
B
GFP-SENP1
414
Merge
Full Length
1-40
41-153
154-272
273-449

Figure 3-9

SENP1 and SENP1 N-terminal domains localize to kinetochores, centromeres, and the mitotic spindle during metaphase.

GFP-SENP1 and various GFP-SENP1 N-terminal truncation constructs were transfected into HeLa cells and analyzed by immunofluorescence with antibodies to (A) centromeres (CEN, red) and (B) kinetochores (CREST, red) and counterstaining with DAPI to indicate chromosomes/DNA.

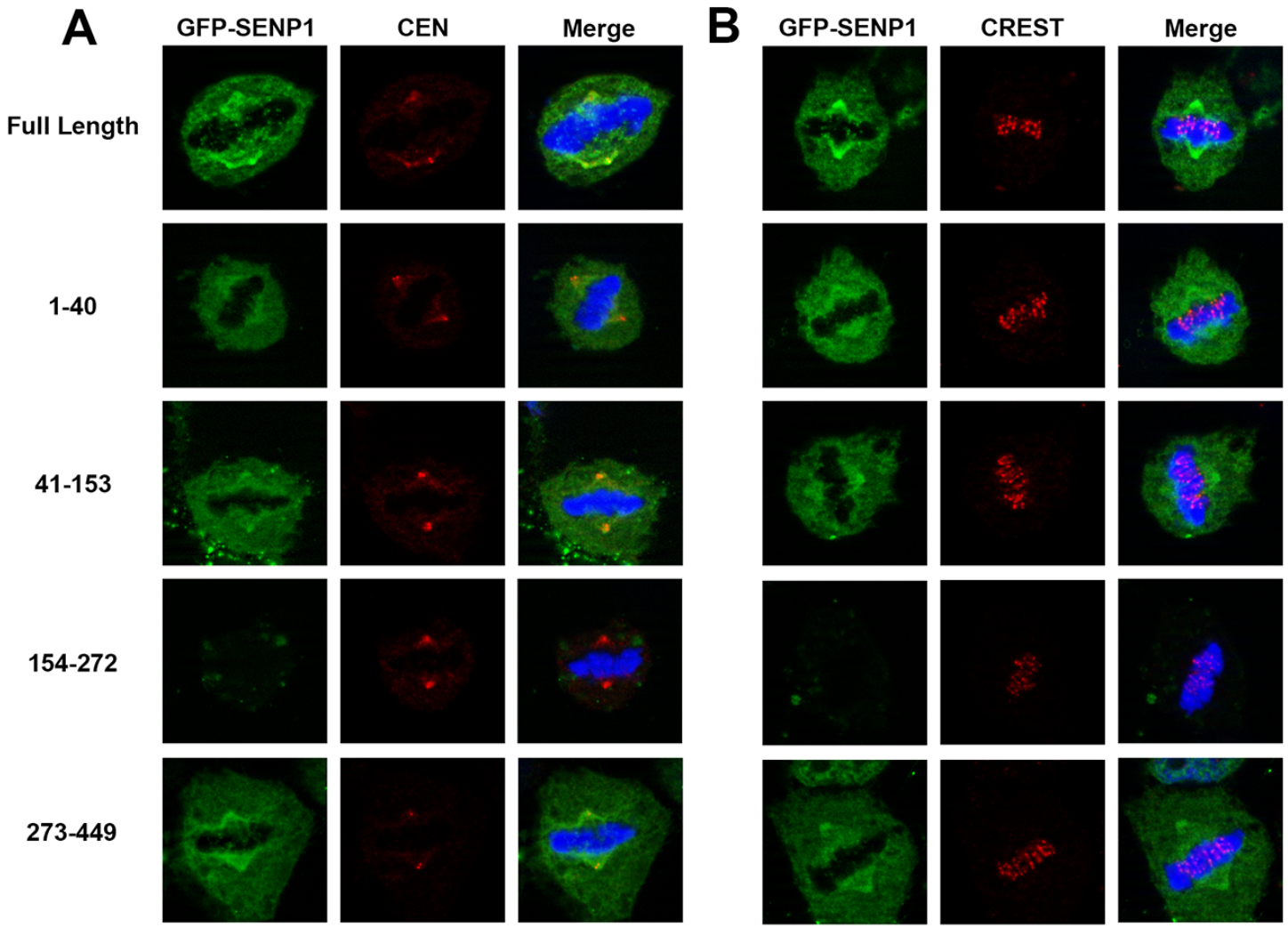
A
GFP-SENP1
CEN
Merge
B
GFP-SENP1
CREST
Merge
Full Length
1-40
41-153
154-272
273-449

Figure 3-10

BirA-SENP1 mass spectrometry analysis reveals unique interactions of SENP1 and SENP1 N-terminal fragments with nucleoporins.

(A) An N-terminal fusion of Flag-BirA with SENP1 was generated and incubated with biotin ligase and HeLa cell lysates. Interactions with the nuclear pore complex were among the substrates identified. Nup160, Nup107-133, Nup153, and Tpr are nucleoporins that compose the nuclear pore complex. Tpr comprises the nuclear basket which resides on the nucleoplasmic face of the pore. (B) Average pectral counts from BirA-SENP1 analysis is shown. GFP-SENP1 full length, GFP-SENP1$^{153-272}$, and GFP-SENP1$^{273-449}$ were used. Gradient grey colors indicate increased frequency of spectra. (C) Cells were transfected with GFP-SENP1 full length and GFP-SENP1$^{273-449}$. Immunofluorescence analysis shows co-localization with the nucleoporin Tpr during interphase. DAPI indicates chromatin/DNA.

A

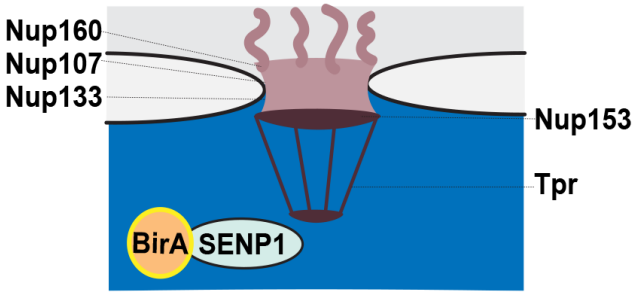

B

	Full Length	153-272	273-449
Nup160	10	14	n.s.
Nup107	27	119	n.s.
Nup133	40	**204**	n.s.
Nup153	176	155	130
Tpr	**283**	138	**287**

C

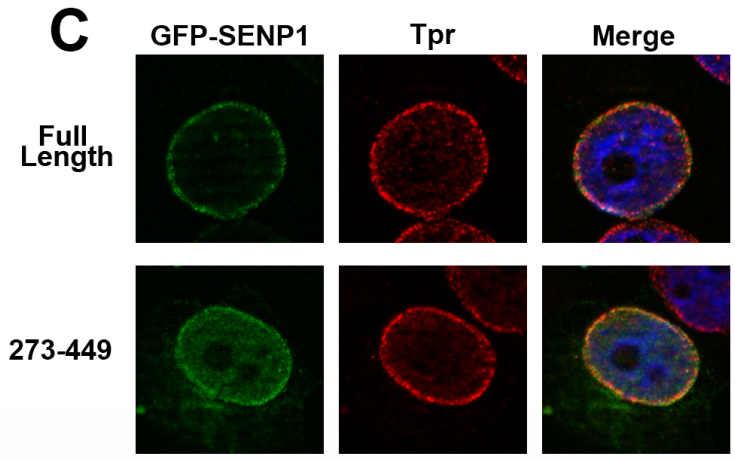

Figure 3-11

mCherry SENP1 constructs are catalytically active towards deconjugating SUMO substrates and localize to unique sub-cellular compartments.

(A) Stable inducible cell lines expressing an N-terminal mCherry fusion to SENP1 full length (mCherry SENP1 FL), SENP1 full length catalytic mutant (mCherry SENP1^{C603S}), and N-terminal truncations (mCherry SENP1$^{\Delta153}$ and mCherry SENP1$^{\Delta272}$) were generated in YFP-H2B HeLa cells. A Nup107 binding domain (amino acids 153-272) and a Tpr binding domain (amino acids 273-449) are indicated. (B) Cells expressing mCherry or mCherry SENP1, or mCherry SENP1 fragments were transfected with myc-SUMO2 to determine catalytic activity. Cell lysates were subjected to immunoblot analysis with antibodies for mCherry and Myc. A non-specific background band migrates at ~57 kDa using the Myc antibody. (D) YFP-H2B HeLa cells with induced expression of mCherry SENP1 FL (E) mCherry SENP1^{C603S} (F) mCherry SENP1$^{\Delta153}$ and (G) mCherry SENP1$^{\Delta272}$ were fixed and imaged in interphase and metaphase.

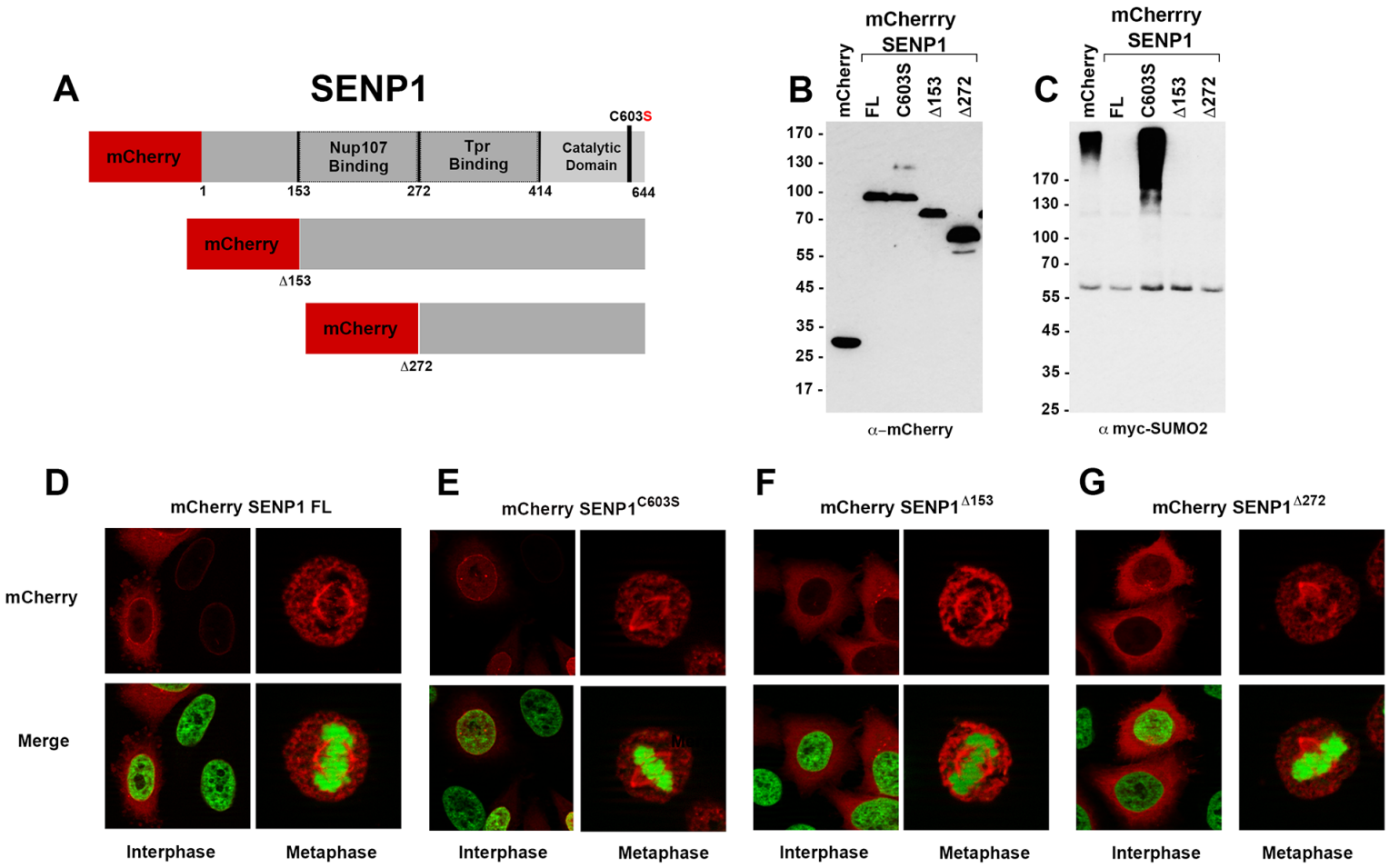
A
SENP1
C603S
mCherry
Nup107 Binding
Tpr Binding
Catalytic Domain
1
153
272
414
644
mCherry
Δ153
mCherry
Δ272
B
mCherrry SENP1
mCherry
FL
C603S
Δ153
Δ272
170
130
100
70
55
45
35
25
17
α–mCherry
C
mCherrry SENP1
mCherry
FL
C603S
Δ153
Δ272
170
130
100
70
55
45
35
25
α myc-SUMO2
D
mCherry SENP1 FL
E
mCherry SENP1C603S
F
mCherry SENP1Δ153
G
mCherry SENP1Δ272
mCherry
Merge
Interphase
Metaphase
Interphase
Metaphase
Interphase
Metaphase
Interphase
Metaphase

Figure 3-12

mCherry SENP1 rescues SENP1 depletion phenotype, N-terminal SENP1 is functionally required for normal metaphase-anaphase transition timing.

(A) Stable inducible HeLa cell lines expressing a constitutive yellow fluorescence protein fused to histone H2B (YFP-H2B) were depleted of endogenous SENP1 by siRNA for 48 hours with (B) concomitant doxycycline induced expression of mCherry SENP1 FL, mCherry $SENP1^{C603S}$, mCherry $SENP1^{\Delta153}$ and mCherry $SENP1^{\Delta272}$ for 48 hours. (C) Total time in mitosis, beginning with nuclear envelope breakdown (NEBD) to metaphase and anaphase was analyzed from three independent replicates of timelapse imaging analysis. Control and siSENP1 cells transition from NEBD-metaphase in 27.29 min ± 0.76 and 30.03 min ± 1.16, respectively (average ± SD, n=60). Cells depleted of SENP1 and induced expression of mCherry SENP1 WT, mCherry $SENP1^{C603S}$, mCherry $SENP1^{\Delta153}$ and mCherry $SENP1^{\Delta272}$ transition from NEBD-metaphase in 27.25 min ± 2.75, 36.49 min ± 2.92, 39.71 min ± 2.03, and 32.28 min ± 2.31, respectively (average ± SD, n=42). (D) Time between metaphase-anaphase was analyzed. Control and siSENP1 cells transition from metaphase-anaphase in 26.14 min ± 2.78 and 76.39 min ± 4.24, respectively (average ± SD). Cells depleted of

SENP1 and induced expression of mCherry SENP1 WT, mCherry SENP1^{C603S}, mCherry SENP1$^{\Delta 153}$ and mCherry SENP1$^{\Delta 272}$ transition from NEBD-metaphase in 35.75 min ± 4.75, 87.44 min ± 14.34, 38.93 min ± 4.59, and 65.22 min ± 7.59, respectively (average ± SD).

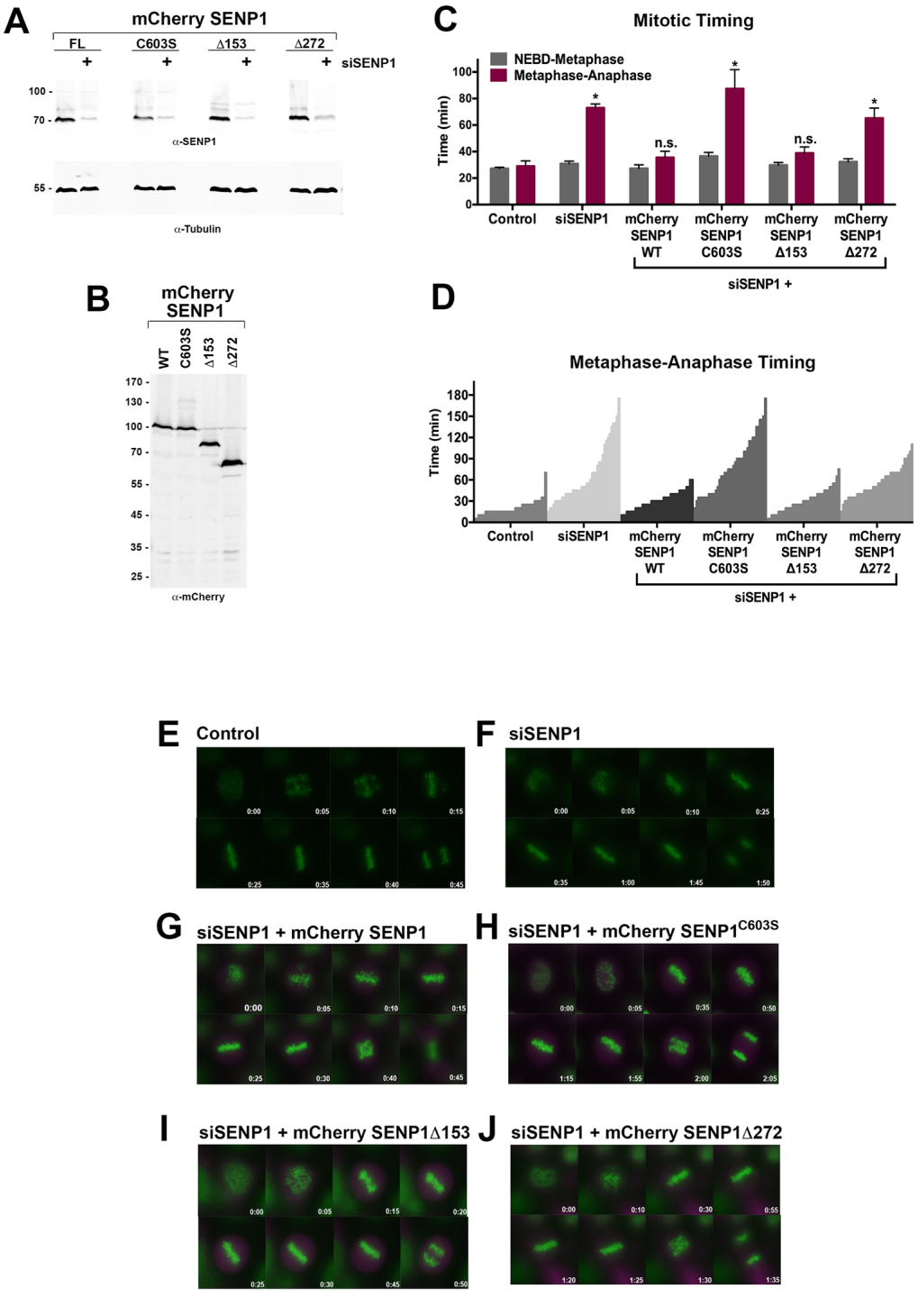
A
mCherry SENP1
FL
C603S
Δ153
Δ272
siSENP1
100 -
70 -
α-SENP1
55 -
α-Tubulin
B
mCherry SENP1
WT
C603S
Δ153
Δ272
170 -
130 -
100 -
70 -
55 -
45 -
35 -
25 -
α-mCherry
C
Mitotic Timing
NEBD-Metaphase
Metaphase-Anaphase
Time (min)
n.s.
Control
siSENP1
mCherry SENP1 WT
mCherry SENP1 C603S
mCherry SENP1 Δ153
mCherry SENP1 Δ272
siSENP1 +
D
Metaphase-Anaphase Timing
Time (min)
E
Control
F
siSENP1
G
siSENP1 + mCherry SENP1
H
siSENP1 + mCherry SENP1C603S
I
siSENP1 + mCherry SENP1Δ153
J
siSENP1 + mCherry SENP1Δ272

Table 3-1

Average spectral counts from Flag-BirA-SENP1 proteomic study

GFP-SENP1		**FL**	**1-40**	**41-153**	**153-272**	**273-449**
Karyopherins	KPNB1	77	23	37	52	32
	KPNA2	24			14	11
Nup107-160	NUP133	40			204	
	NUP107	27			119	
FG Nups	RANBP2	130	20	79	85	44
	NUP153	176		29	155	130
	NUP50	71			25	34
	NUP155	16			12	
	NUP98	17			61	
	AHCTF1	121			62	45
	POM121C	19			34	
Nuclear Lamina	TPR	283	18	60	138	287

APPENDIX:

METHODS TO INVESTIGATE

FUNCTIONAL ROLES OF APC4 SUMO MODIFICATION

INTRODUCTION

We have identified and validated that a subunit of the Anaphase Promoting Complex/Cyclosome (APC/C)—a key regulator of mitotic exit—is SUMO modified during mitosis. To further characterize the functional consequence of APC4 SUMO modification, several approaches were utilized. Through our studies, we confirmed that APC4 sumoylation occurs during mitosis and can be readily SUMO modified using a variety of *in vitro* and *in vivo* approaches. Here, we describe methods used to induce APC4 SUMO modification and conclude with observations regarding the potentially distinct substrates SUMO modified APC4 interacts with.

SENP1 depletion results in enhanced APC4 SUMO modification

We previously observed that APC4 SUMO modification is under the regulatory control of the SUMO isopeptidase SENP1 (Figure 3-2D). To determine the temporal regulation of APC4 SUMO modification during the mitotic stage of the cell cycle, HeLa cells were treated with a control or SENP1 targeting siRNA oligo for 48 hours, followed by a double thymidine block (19 hours in 2 mM thymidine, 6-hour release into drug free media, followed by 19 hours in 2 mM thymidine) to synchronize cells into S phase. Following release into drug-free media, control cells resume cell cycle progression and enter mitosis around 8-10 hours following release, as indicated by immunoblotting to mitotic markers, Cyclin B1 and phosphorylated histone H3 (PH3). Antibodies specific for SENP1 were used to demonstrate protein depletion in siSENP1 cells during the timecourse analysis, and antibodies to glyceraldehyde-3-phosphate dehydrogenase (GAPDH) was used as a loading control (Figure A-1). Notably, APC4 sumoylation levels are higher in cells treated with siSENP1, as indicated by arrows. In control cells, mitotic exit as indicated by decreased Cyclin B1 levels occurs within 12 hours of thymidine release. However, SENP1 depleted cells demonstrate a prolonged mitotic timing, and Cyclin B1 levels are depleted ~22 hours following double thymidine release. These data

suggested that SENP1 depletion, resulting in hyper-sumoylated APC4, may have an effect on mitotic exit. However, we later discovered that constitutive SUMO modification of APC4 did not cause metaphase delays (Figure 3-7). Thus, we conclude that although APC4 is hyper-sumoylated, APC4 is not the molecular target that is responsible for the metaphase-anaphase delay observed in SENP1 knockdown.

In vitro SUMO modification of APC4 immunoprecipitated from stable inducible cell lines

We investigated whether APC/C complexes purified from stable inducible cell lines expressing Flag-APC4 (wild type) or Flag-APC4^{KR} (double SUMO mutant) can be SUMO modified *in vitro*. Stable cell lines were treated with siRNA oligonucleotides to endogenous APC4 and induced with doxycycline for Flag-APC4 or Flag-ACP4^{KR} expression for 48 hours. Cells were lysed using as described in Chapter 2. Cleared lysates were incubated with APC4 antibody (rabbit, A301-176A, 1:2000, Bethyl Laboratories, Inc) conjugated to Protein A AffiPrep Beads (BioRad). *In vitro* sumoylation reactions were performed as described in Chapter 1. Reactions were incubated at 37°C for the indicated times and stopped by addition of 2x SDS-sample buffer and analyzed by SDS-PAGE followed by

immunoblotting. Results demonstrate that APC4 but not APC4^{KR} purified from human cells can be efficiently SUMO modified *in vitro* (Figure A-2).

Characterization of APC4 Sumoylation Through Rapamycin-Mediated Heterodimerization

To control the temporal SUMO modification of APC4, we developed a system to induce heterodimerization between APC4 and the SUMO E2 conjugating enzyme, Ubc9. A derivative of the rapamycin-mediated heterodimerization system[1,2] was used as previously described[3]. This system uses a small, bivalent, cell-permeable compound (AP21967, Ariad Pharmaceuticals, Inc.) to induce dimerization between FKBP (FKBP506 binding protein) and FRB proteins *in vivo*. Induced dimerization between APC4 wild type or APC4^{KR} with induced fusion of the SUMO ligating enzyme Ubc9 would allow us to analyze downstream effects of APC4 sumoylation. Plasmids expressing 3xFlag-APC4-FKBP or 3xFlag-APC4^{KR}-FKBP were co-transfected with FRB-Ubc9-HA (Figure A-3A). Following 18 hours of transfection, 240 nM AP21967 was added to cells. Cells were lysed for analysis by SDS-PAGE and immunoblotting (Figure A-3B) and prepared for immunofluorescence microscopy (Figure A-3C). Immunoblotting using an antibody specific for Flag (M2, 1:2000, Sigma-

Aldrich) indicates that heterodimerization of 3xFlag-APC4-FKBP with FRB-Ubc9-HA efficiently SUMO modified APC4, as indicated by the upshifted band at ~120 kDa (marked by *), while 3xFlag-APC4^{KR}-FKBP did not. Immunoblots specific for HA (mouse, Santa Cruz Biotechnology, Inc.) indicate expression of FRB-Ubc9-HA. Immunofluorescence microscopy analysis shows that upon treatment with heterodimerizer, both 3xFlag-APC4-FKBP and 3xFlag-APC4^{KR}-FKBP localize to the nuclear rim (Figure A-3C). Thus, drug-induced fusion with Ubc9 targets 3xFlag-FKBP-APC4 and 3xFlag-FKBP-APC4^{KR} to the nuclear periphery—likely to nuclear pore complexes. Under certain conditions, Ubc9 is targeted to the nuclear pore[4], and we did not pursue subsequent analysis of APC4 sumoylation using this system due to this dimerization-induced change in localization.

APC4^{SUMO} is not targeted for proteosomal degradation

In the generation of Flag-APC4^{KR}-SUMO2 doxycyline-inducible stable cell lines, we noticed that during single clone selection, induced expression of the SUMO2 fusion cell lines were always lower than Flag-APC4 and Flag-APC4^{KR}. Separate observations during immunopurifications with the single Flag tag were noted and hypothesized to have low affinity for Flag-conjugated Protein A beads. We replaced the single Flag with a

2xStrep sequence (Strep-Tag II sequence was used: WSHPQFEK), which has a high binding affinity to biotin-conjugated beads (Figure A-4). The same observation of low-expressing SUMO2 fusion clones was made with 2xStrep-APC4 cells. Single clones expressing SUMO2 fusion were selected and induced with doxycycline for ~18 hours. To test of the SUMO2 tag was directing Flag-APC4^{KR}-SUMO2 to ubiquitin-mediated proteasomal degradation, cells were treated with 20μM MG132 (proteasome inhibitor) for 4 hours. Cells were lysed and analyzed by SDS-PAGE followed by immunoblotting. As indicated by the asterisk (*), cells treated with MG132 do not accumulate the APC4-SUMO2 fusion in comparison to cells without treatment (Figure A-4). These data suggest that the linear SUMO2 fusion does not get targeted for proteosomal degradation. However, why APC4-SUMO2 is never expressed at high levels is still an outstanding question.

The C-terminus of APC4 Binds to Ube2S *in vitro*

The APC/C has two characterized ubiquitin E2 ligases that bind and interact to catalyze substrate ubiquitylation. UbcH10 and Ube2S[5] are required for efficient catalysis. Interestingly, Ube2S was reported to be critical for the metaphase-anaphase transition, with similar mitotic defects as APC4^{KR} [6]. Furthermore, Ube2S was reported to have a positively charged C-

terminal tail[7] that is functionally required for APC/C activity. Intriguingly, the C-terminus of APC4 contains a stretch of negatively charged residues which reside in close proximity to the SUMO consensus sites (Figure A-5). We hypothesized that SUMO modification of APC4 may interfere with an interaction between the positively charged Ube2S and the negatively charged APC4 C-termini. First, we tested the binding interaction between recombinant Ube2S and APC4 (Figure A-5). Recombinant GST-Ube2S was expressed in pGEX-6P-1 expression vector and transformed into *E. coli* strain BL21. Cultures were grown to an OD = 0.7 and induced with 1 mM IPTG for 16 hours at 20°C. Cells were resuspended in 4°C lysis buffer (40 mM Tris-Hcl pH 8.0, 500 mM NaCl, 1 mM Dtt, 0.4% TNS-100, Roche complete protease inhibitor cocktail, 1 mM PMSF, 100 μM leupeptin, 1μg/mL peptatin A, 20 μg/mL aproptinin, and 10 U/mL benzomase) and sonicated on ice. Insoluble material was removed by centrifugation at 14,000 rpm and supernatants were run over pre-packed glutathione-agarose columns. The C-terminus of APC4, spanning amino acids 554-808 (Figure A-5), was also expressed and purified in pGEX-6P-1 vectors, but the GST tag was cleaved with PreScission Protease, overnight at 4°C. Eluted proteins were further purified using size exclusion on a Superdex 75, in buffer 50 mM Tris-HCl pH 8.0, 150 mM NaCl, 1 mM EDTA, and 1 mM DTT. In

vitro binding assays were performed with 1μM GST only or 1μM GST-Ube2S bound to glutathione agarose. After a blocking reaction containing 2% BSA in assay buffer (20 mM HEPES-KOH pH 7.3, 110 mM potassium acetate, 2 mM magnesium acetate, 0.05% Tween-20), a binding reaction with 1μM APC4 C-Terminus was performed for 3 hours at room temperature. Following several washes with assay buffer, proteins were eluted in 2x Sample Buffer and analyzed by SDS-PAGE followed by immunoblotting. Antibodies specific to GST and APC4 were used. Our results indicate that the C-terminus of APC4 binds to Ube2S (Figure A-5B shows GST- GST-Ube2S inputs, and Figure A-5C shows GST-Ube2S + APC4 binding). These experiments were performed prior to structural studies, which placed Ube2S in close proximity to APC4. Recently, the binding interactions between Ube2S and APC4 have been confirmed. The C-terminal tail of Ube2S is shown to bind to APC4 at amino acids 747-751[8] which is included in our C-terminal fragment but 20 amino acids away from the first SUMO consensus site lysine (772).

Affinity chromatography with Recombinant APC4$^{C\text{-}term}$ with HeLa S3 cell extracts

To take an unbiased approached towards identifying potential substrates that uniquely interact with sumoylated APC4, we immobilized recombinant APC4 and *in vitro* sumoylated APC4 and incubated with HeLa whole cell extracts (Figure A-6). First, recombinant MBP-APC4$^{C\text{-}term}$ was expressed and purified as described above but using amylose resin for affinity purification. *In vitro* sumoylation reactions were performed as described above with 1 μM recombinant SUMO1 and 2 μM of recombinant MBP-APC4 at 37°C for 2 hours. MBP-APC4 or MBP-APC4^{SUMO} was then immobilized onto amylose resin with assay buffer (20 mM HEPES KOH pH 7.0, 110 mM potassium acetate, 2 mM magnesium acetate, and 0.05% Tween-20) for 2 hours at 4°C. HeLa S3 cell lysates were prepared from a 1 L suspension. The cell pellet was lysed by sonication on ice in assay buffer supplemented with a Roche Protease Inhibitor Tablet, phosphatase inhibitor cocktail (PhosStop, Sigma-Aldrich), 1 mM PMSF, and 10 mM NEM. Insoluble material was removed by centrifugation at 70,000 x *g* and filtered through a 0.44 μm PVDF membrane. Total soluble protein concentration was measured by a bicinchoninic assay (BCA) and 100 mg was incubated with either MBP-APC4 or MBP-APC4^{SUMO1} for 1 hour at 4°. After several washes with assay buffer, elutions were performed with 1 M maltose and run on SDS-PAGE followed by silver staining. Compared to MBP-APC4, the

MBP-APC4^{SUMO1} appears to have distinct bands (indicated by asterisks*). Future analysis using full length APC4 may lend insight to the SUMO-specific interactions of APC4, as it is still yet unknown whether APC/C substrate selection is determined by sumoylated APC4.

Concluding Remarks and Future Directions

Our investigation on how the SUMO pathway affects the metaphase-anaphase transition led us to the characterization APC4 sumoylation and the molecular mechanism of how SUMO modification of this subunit stimulates APC/C activity. Here we describe the initial approaches used to generate hyper-sumoylated APC4 *in vitro* and *in vivo*. The findings from these supplementary experiments led us to the body of work described in Chapter 2. Future work on whether APC4 sumoylation perturbs Ube2S binding will be an interesting question to pursue. However, recombinant complexes of APC/C—which is composed of more than 15 subunits in varying stoichiometry—will be a better substrate to use for binding assays. The interactions between two subunits is limiting and does not account for interactions as they occur *in vivo*. Recent methods papers have described a methodology for creating recombinant APC/C, and will be a useful reagent to use in future work[9]. Affinity chromatography using MBP-APC4 and

MBP-APC4^{SUMO1} as bait presents an unbiased direction for the future of this project. It is yet unknown whether SUMO modified APC4 recruits specific substrates to the APC/C, or whether SUMO modified APC4 recruits the APC/C efficiently to kinetochores.

The evolution of this project was influenced by the technological leaps in the field of tomography made in the past decade. The advancements in Cryo-EM tomography have produced structures at atomic resolution of the APC/C[8,10–16]. A snapshot of the structure from 2005 places the coactivator Cdh1 close to the APC2 cullin domain[17] (Figure A-7). In the middle of my PhD, structures at or near atomic resolution re-positioned Cdh1 close to the Tpr repeat regions of APC3 and APC7[15] (Figure A-7). These studies further revealed flexible, disordered regions in APC4 and APC2 that energized us to pursue mechanistic studies. Of note, the C-terminal sumoylation consensus site lysines are in a disordered region that is not resolved in any of the current structures. We hypothesize that SUMO modification of APC4 stabilizes this C-terminal domain, limiting the degrees of freedom for both the APC2 cullin domain as proposed in our model (Figure 2-8) and the C-terminal tail of APC4. Finally, inhibitors of the APC/C for cancer therapeutics are currently in development[13,18]. It is of

particular interest to determine if the sumoylation site on APC4 is a unique druggable target.

REFERENCES

1. Brown *et al.* A mammalian protein targeted by G1-arresting rapamycin–receptor complex. *Nature* **369,** 369756a0 (1994).

2. Sabatini, Erdjument-Bromage, Lui, Tempst & Snyder. RAFT1: A mammalian protein that binds to FKBP12 in a rapamycin-dependent fashion and is homologous to yeast TORs. *Cell* **78,** 35–43 (1994).

3. Zhu *et al.* Small Ubiquitin-related Modifier (SUMO) Binding Determines Substrate Recognition and Paralog-selective SUMO Modification. *Journal of Biological Chemistry* **283,** 29405–29415 (2008).

4. Werner, Flotho & Melchior. The RanBP2/RanGAP1*SUMO1/Ubc9 Complex Is a Multisubunit SUMO E3 Ligase. *Molecular Cell* **46,** 287–298 (2012).

5. Wu *et al.* UBE2S drives elongation of K11-linked ubiquitin chains by the Anaphase-Promoting Complex. *Proceedings of the National Academy of Sciences* **107,** 1355–1360 (2010).

6. Kelly, Wickliffe, Song, Fedrigo & Rape. Ubiquitin Chain Elongation Requires E3-Dependent Tracking of the Emerging Conjugate. *Molecular Cell* **56,** 232–245 (2014).

7. Williamson *et al.* Identification of a physiological E2 module for the human anaphase-promoting complex. *Proceedings of the National Academy of Sciences* **106,** 18213–18218 (2009).

8. Brown *et al.* Dual RING E3 Architectures Regulate Multiubiquitination and Ubiquitin Chain Elongation by APC/C. *Cell* **165,** 1440–1453 (2016).

9. Weissmann *et al.* biGBac enables rapid gene assembly for the expression of large multisubunit protein complexes. *Proceedings of the National Academy of Sciences* **113,** E2564–E2569 (2016).

10. Yamaguchi *et al.* Cryo-EM of Mitotic Checkpoint Complex-Bound APC/C Reveals Reciprocal and Conformational Regulation of Ubiquitin Ligation. *Molecular Cell* **63,** 593–607 (2016).

11. Qiao *et al.* Mechanism of APC/CCDC20 activation by mitotic phosphorylation. *Proceedings of the National Academy of Sciences* **113,** E2570–E2578 (2016).

12. Brown *et al.* RING E3 mechanism for ubiquitin ligation to a disordered substrate visualized for human anaphase-promoting complex. *Proceedings of the National Academy of Sciences* **112,** 5272–5279 (2015).

13. Alfieri *et al.* Molecular basis of APC/C regulation by the spindle assembly checkpoint. *Nature* **536,** 431–436 (2016).

14. Zhang *et al.* Molecular mechanism of APC/C activation by mitotic phosphorylation. *Nature* **533,** 260–264 (2016).

15. Chang, Zhang, Yang, McLaughlin & Barford. Atomic structure of the APC/C and its mechanism of protein ubiquitination. *Nature* **522,** 450–454 (2015).

16. Fujimitsu, Grimaldi & Yamano. Cyclin-dependent kinase 1–dependent activation of APC/C ubiquitin ligase. *Science* **352,** 1121–1124 (2016).

17. Dube *et al.* Localization of the Coactivator Cdh1 and the Cullin Subunit Apc2 in a Cryo-Electron Microscopy Model of Vertebrate APC/C. *Molecular Cell* **20,** 867–879 (2005).

18. Zeng *et al.* Pharmacologic Inhibition of the Anaphase-Promoting Complex Induces A Spindle Checkpoint-Dependent Mitotic Arrest in the Absence of Spindle Damage. *Cancer Cell* **18,** 382–395 (2010).

Figure A-1

SENP1 depletion results in enhanced APC4 SUMO modification

HeLa cells were treated with either a control or SENP1 siRNA targeting oligo for 48 hours, followed by a double thymidine block (using 2 mM Thymidine). Cells were released and harvested at indicated timepoints and analyzed by immunoblotting using antibodies specific for APC4, Cyclin B1, Phosphorylated Histone H3 (PH3), SENP1, and GAPDH as a loading control. Arrows indicate sumoylated forms of APC4.

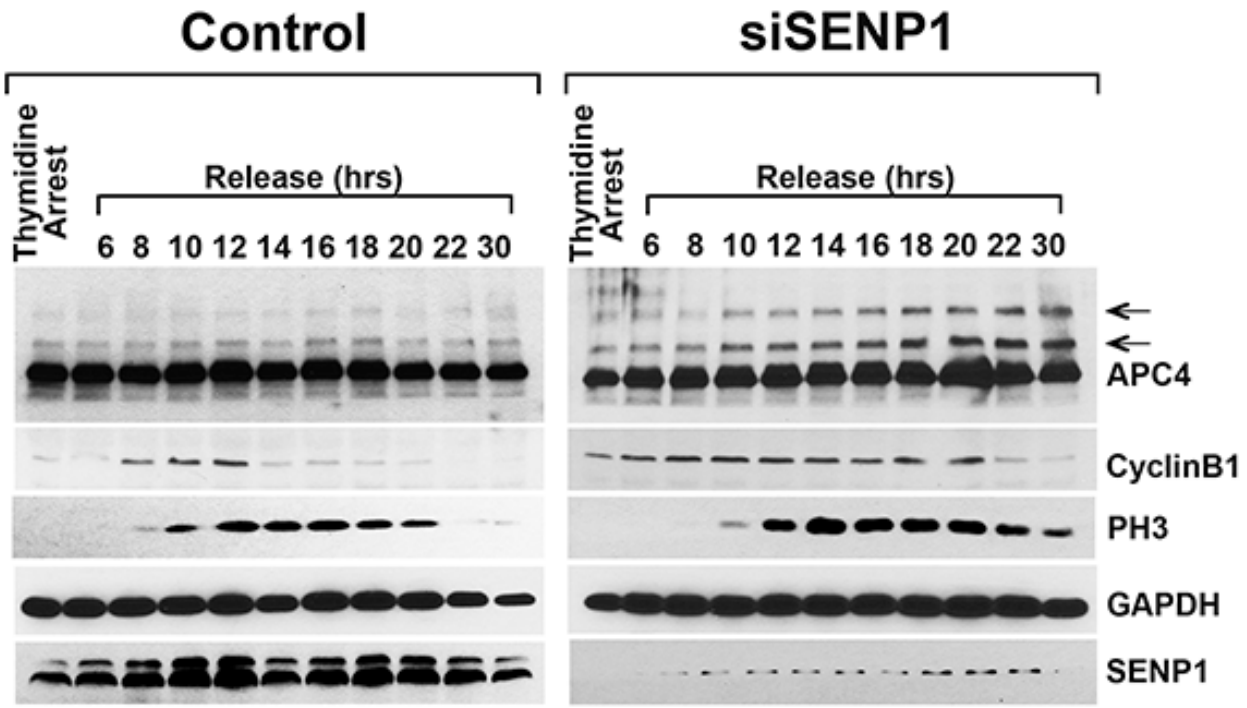
Control
siSENP1
Thymidine Arrest
Release (hrs)
6 8 10 12 14 16 18 20 22 30
APC4
CyclinB1
PH3
GAPDH
SENP1

Figure A-2

***In vitro* SUMO modification of APC4 immunoprecipitated from stable inducible cell lines**

Stable inducible cell lines expressing APC4 or APC4^{KR} were induced for 48 hours using doxycycline, with concomitant depletion of endogenous APC4 using an siRNA targeting oligo to the 3'UTR of APC4. Cells were lysed and APC4 was immunoprecipitated using GαDDDK antibody (Bethyl, 2 μg antibody for 1 mg cell lysate, based on BCA quantification) conjugated to Protein A AffiPrep beads (BioRad). *In vitro* sumoylation reactions were performed using recombinant SUMO E1 and SUMO E2 enzymes, and SUMO-1 or SUMO-2 protein at 37°. Reactions were stopped at indicated timepoints using 2x Sample Buffer and immunoblotting was performed using an antibody specific for APC4. Asterisks indicate SUMO modified forms of APC4.

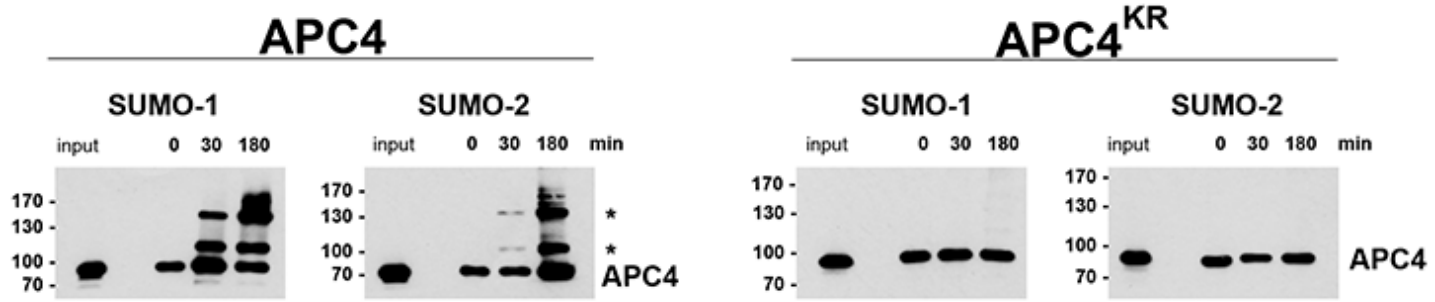
APC4
SUMO-1
SUMO-2
input
0
30
180
min
170
130
100
70
*
*
APC4
APC4KR
SUMO-1
SUMO-2
input
0
30
180
min
170
130
100
70
APC4

Figure A-3

Characterization of APC4 Sumoylation Through Rapamycin-Mediated Heterodimerization

(A) A plasmid expressing 3xFlag-APC4 wild type (WT) or double SUMO mutant (KR) with a linear FKBP tag was co-expressed with a plasmid expressing FRB-Ubc9-HA in HeLa cells using Lipofectamine 2000 reagent according to manufacturer's protocols (Thermo Fisher Scientific). (B) Following 24 hours of transfection, heterodimerization reagent was added. Following 48 hours of transfection and 24 hours of heterodimerization, cells were harvested using 2x Sample Buffer, and analyzed using SDS-PAGE followed by immunblotting analysis with antibodies specific for Flag (Flag M2, 1:2000, Sigma) and HA (rabbit, Y-11, 1:1000, Santa Cruz). (C-F) Immunofluorescence analysis of cells expressing 3xFlag-APC4 WT or KR and FRB-Ubc-HA in the absence or presence of heterodimerizer was performed following fixation with 2% formaldehyde and permeabilization with 0.2% TNX-100. Antibodies specific for Flag (M2, 1:400, Sigma), HA (rabbit, Y-11, 1:300, Santa Cruz), and counterstaining with DAPI to visualize chromatin was performed.

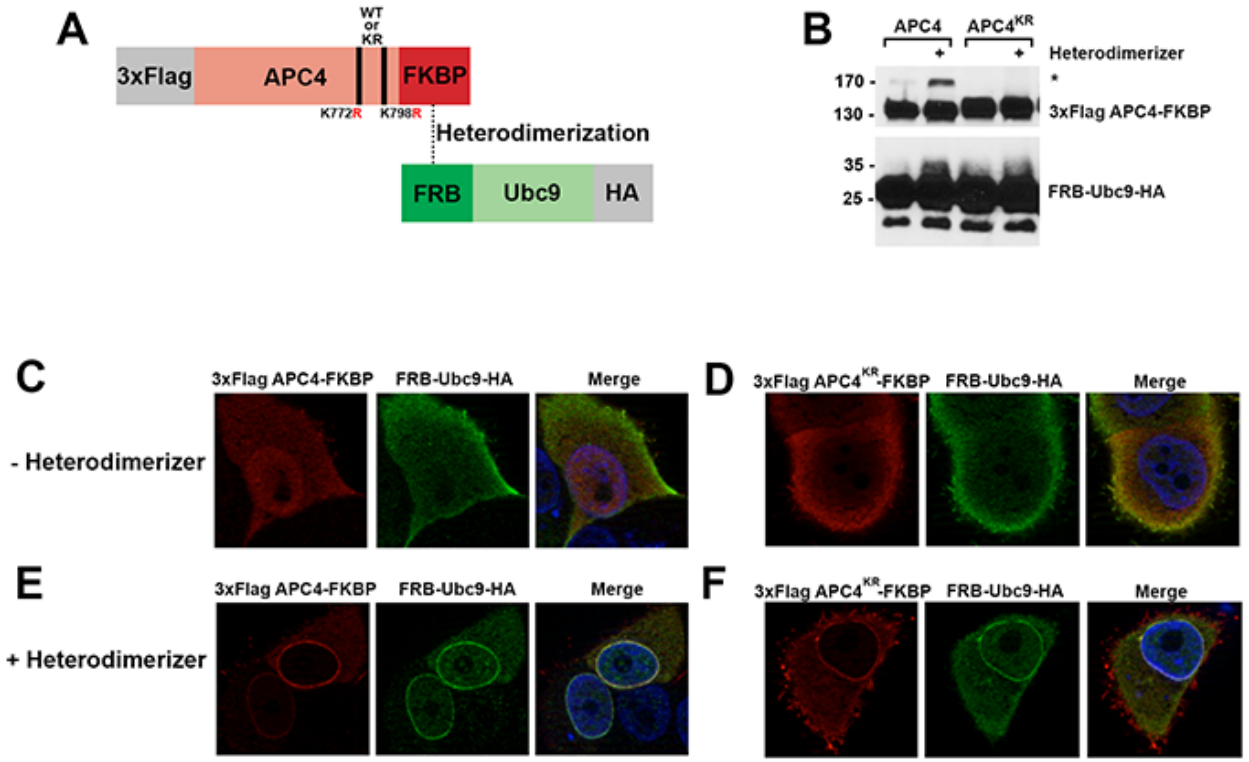
A
WT or KR
3xFlag
APC4
FKBP
K772R
K798R
Heterodimerization
FRB
Ubc9
HA
B
APC4
APC4KR
+
+
Heterodimerizer
170 -
130 -
*
3xFlag APC4-FKBP
35 -
25 -
FRB-Ubc9-HA
C
3xFlag APC4-FKBP
FRB-Ubc9-HA
Merge
- Heterodimerizer
D
3xFlag APC4KR-FKBP
FRB-Ubc9-HA
Merge
E
3xFlag APC4-FKBP
FRB-Ubc9-HA
Merge
+ Heterodimerizer
F
3xFlag APC4KR-FKBP
FRB-Ubc9-HA
Merge

Figure A-4

APC4^{SUMO} is not targeted for proteosomal degradation

Stable inducible cell lines expressing N-terminal 1xFlag or 2xStrep tags followed by APC4^{KR}-SUMO2 were treated with doxycycline to induce transgene expression for 48 hours. Following 24 hours of doxycycline induction, cells were treated with 4 μM MG132 to inhibit proteasome activity and to monitor protein stability. Cells were lysed in 2x Sample Buffer and analyzed by SDS-PAGE followed by immunoblotting with an antibody specific for APC4. Asterisk indicates induction of APC4$^{KR\text{-}SUMO2}$.

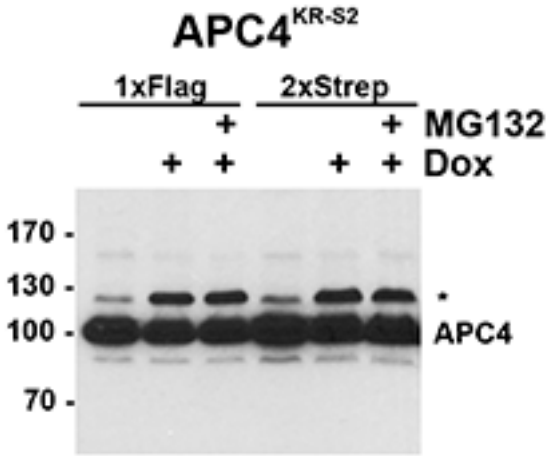

Figure A-5

The C-terminus of APC4 binds to Ube2S *in vitro*

(A) Recombinant proteins were expressed and induced in *E. coli*. A linear fusion of GST-Ube2S (full length) contains a stretch of positively charged amino acid residues (indicated by K – lysine – highlighted in blue) in the C-terminal end. The C-terminus of APC4, including amino acids 554-808, was expressed and purified from *E. coli*. A C-terminal domain contains a stretch of negatively charged amino acid residues (indicated by D and E – aspartic and glutamic acids – highlighted in pink). (B) *In vitro* binding assays were performed using GST-Ube2S or GST as a positive control immobilized on glutathione beads (Pierce). Binding reactions with recombinant C-terminal APC4 were analyzed by SDS-PAGE followed by immunoblotting with antibodies specific for GST (mouse, 1:500, SC-138, Santa Cruz Biotechnology) and (C) APC4 (rabbit, 1:2000, Bethyl).

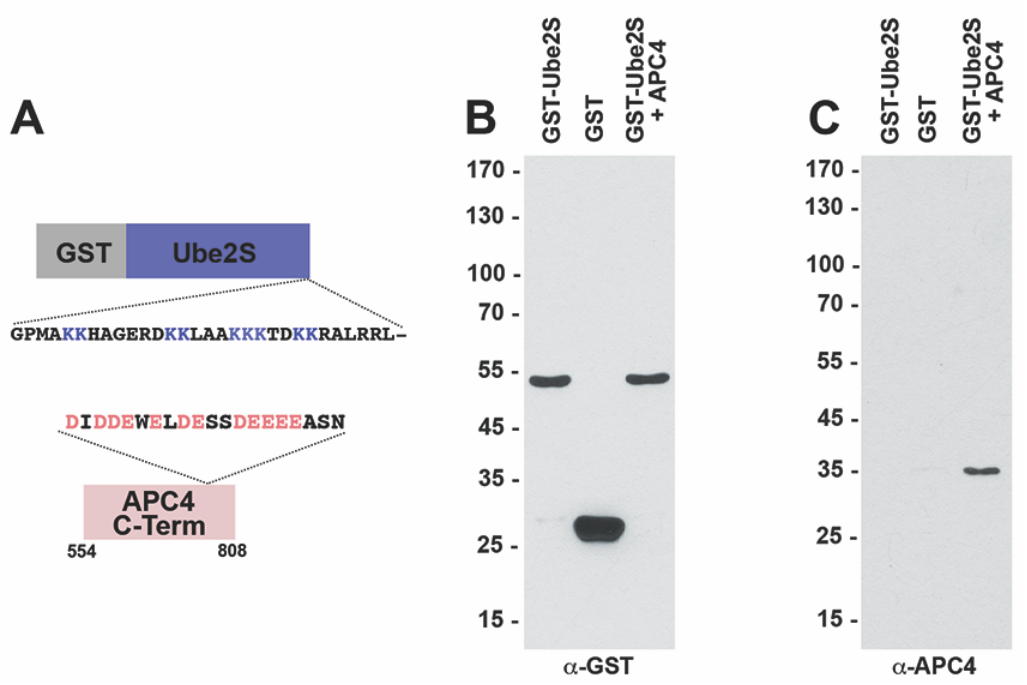
A
GST
Ube2S
GPMAKKHAGERDKKLAAKKKTDKKRALRRL–
DIDDEWELDESSDEEEEASN
APC4
C-Term
554
808
B
GST-Ube2S
GST
GST-Ube2S
+ APC4
170 -
130 -
100 -
70 -
55 -
45 -
35 -
25 -
15 -
α-GST
C
GST-Ube2S
GST
GST-Ube2S
+ APC4
170 -
130 -
100 -
70 -
55 -
45 -
35 -
25 -
15 -
α-APC4

Figure A-6

Affinity chromatography with recombinant APC4$^{C\text{-}term}$ with HeLa S3 cell extracts

Recombinant MBP-APC4 (C-terminal amino acids 554-808) were expressed and purified in *E. coli*. MBP-APC4 was SUMO modified using recombinant SUMO E1 and E2 enzymes and recombinant SUMO1 protein. MBP-APC4 or MBP-APC4^{SUMO1} was immobilized onto amylose resin (New England Biolabs) for *in vitro* binding reactions with 1 mg of total protein (determined by BCA) extracted from HeLa S3 cells. MBP-APC4 or MBP-APC4^{SUMO1} was eluted using 1 M maltose and proteins were analyzed by SDS-PAGE followed by silver staining. Asterisks indicate potentially different proteins that bind differently to MBP-APC4 or MBP-APC4^{SUMO1}.

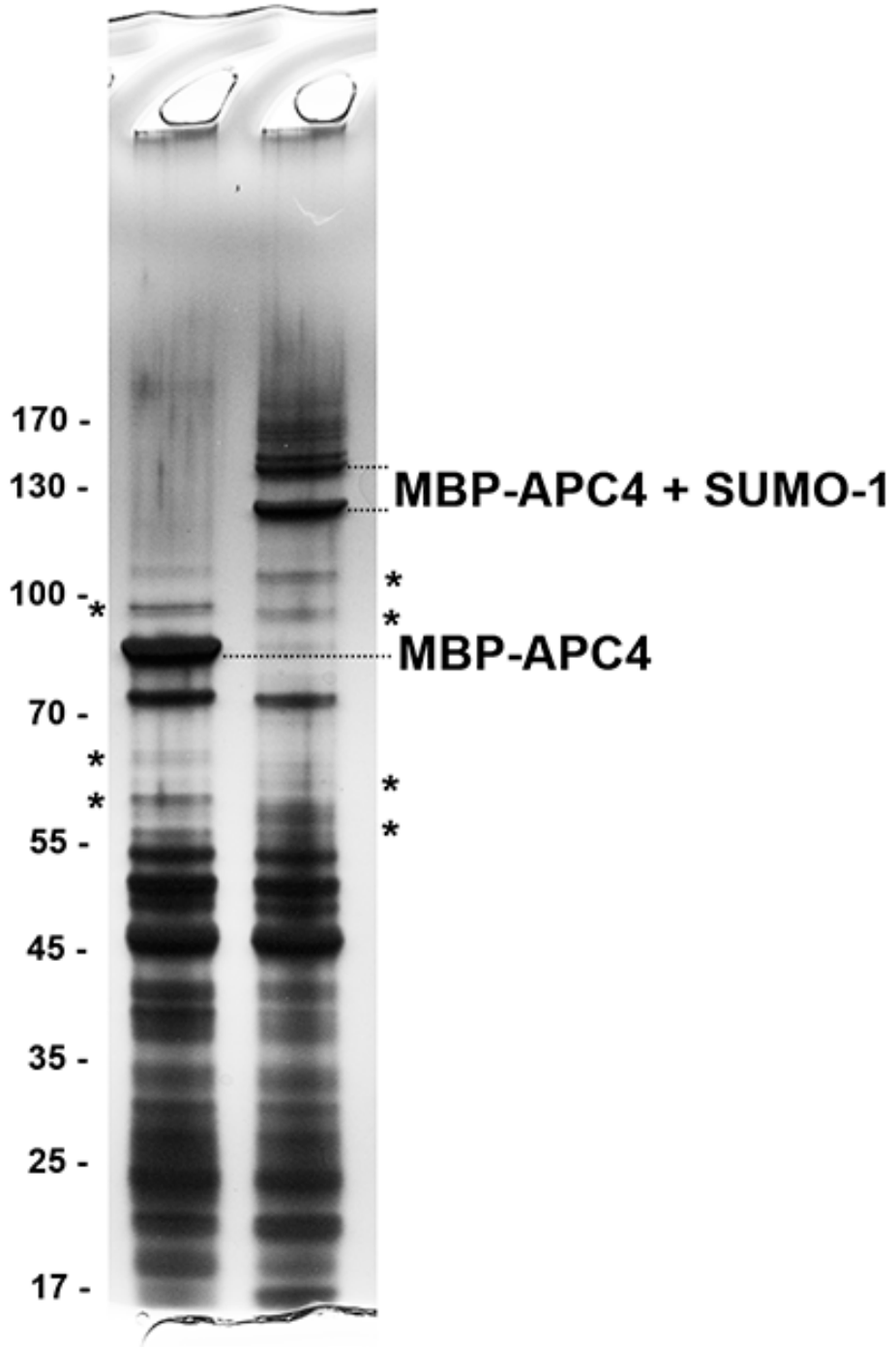
170 -
130 -
100 -
70 -
55 -
45 -
35 -
25 -
17 -
MBP-APC4 + SUMO-1
MBP-APC4
*
*
*
*
*
*
*
*

Figure A-7

Analysis of Cryo-EM strucutres of the APC/C

Cryo-EM structures of the APC/C solved by Dube et al. in 2005 and Chang et al. in 2015 show the advances in resolution achieved over time in the field of tomography.

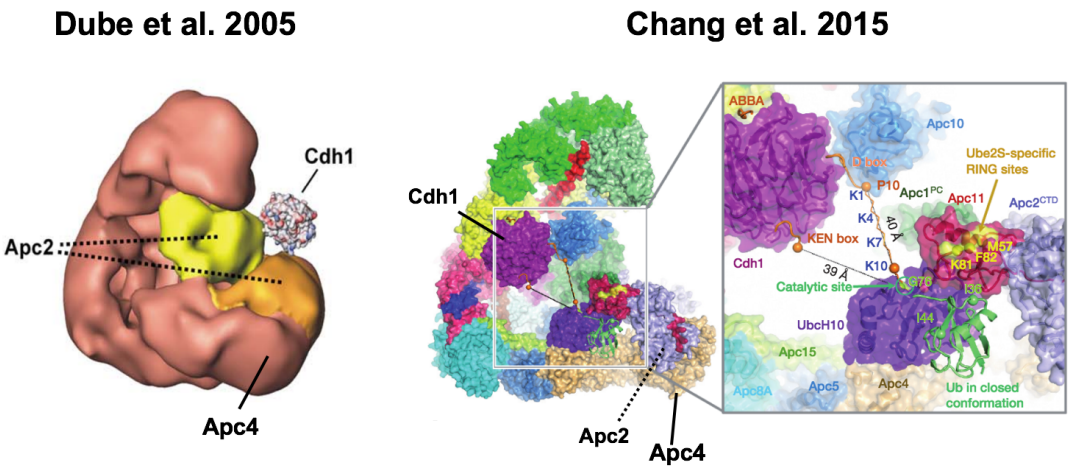

OVERVIEW AND FUTURE DIRECTIONS

Mitosis is an essential cellular process that is coordinated by several axes of regulation. At the onset of nuclear envelope breakdown, a robust signaling cascade is initiated, involving the activity of mitotic kinases like Cdk1 so that appropriate alignment and amphitelic microtubule-kinetochore interactions are achieved. Unattached kinetochores generate the Spindle Assembly Checkpoint (SAC), a "wait anaphase" signal to inhibit the activity of the Anaphase Promoting Complex/Cyclosome (APC/C). The metaphase-anaphase transition is a time when SAC signaling is attenuated and the activity of the APC/C is stimulated to ubiquitylate substrates like Cyclin B1 and securin. Precisely how the "rheostat[3]" in the mitotic cell receives inputs from the SAC to "tune up" inhibitory signals against APC/C activity is still an unanswered question.

Chapter 2 describes one mechanism of how the activity of the APC/C is stimulated through the SUMO modification of the APC4 subunit. SUMO modification of APC4 facilitates novel non-covalent interactions with the SIM (SUMO interacting Motif) in the cullin subunit APC2 of the APC/C. Based on our model, this SUMO-SIM interaction stabilizes a conformation of the APC/C that limits the degrees of flexibility in APC2, and positions this catalytic subunit towards optimal configurations for binding the

ubiquitin-charged E2 enzyme, UbcH10. Binding of the ubiquitin-charged E2 to the APC/C is a critical step that is followed by the efficient transfer of ubiquitin to substrates so that mitotic exit can be correctly achieved. We propose that SUMO modification of APC4 thus stimulates UbcH10-dependent catalysis of the APC/C.

We have identified that the second E2 enzyme that cooperates with the APC/C, Ube2S, binds to the C-terminus of APC4. Future work on characterizing the mechanistic effects of APC4 sumoylation on Ube2S is of particular interest. Furthermore, it is still unknown how the inhibitory mitotic checkpoint complex (MCC) generated by the SAC is disassembled or released from the APC/C. Although the APC15[2] subunit and the activity of AAA-ATPase[3] have been implicated, it is compelling to consider the role of SUMO in this process. The APC/C adopts a distinct conformation upon MCC binding and release, and whether the sumoylation of APC4 contributes to this process is a key area of inquiry. Expression and purification of recombinant complexes of the APC/C will be valuable in biochemical assays to address these questions. Recent papers have described a methodology for creating recombinant APC/C, which will be a useful reagent to use in future work[1]. Our cellular assays demonstrate that a single SUMO fusion is sufficient for restoring normal metaphase-anaphase transitions, thus a

recombinant APC/C complex can include a linear SUMO fusion to the C-terminus of APC4.

The evolution of this project was influenced by the technological leaps in the field of tomography made in the past decade. The advancements in Cryo-EM tomography have produced structures at atomic resolution of the APC/C[5–10]. A snapshot of the structure from 2005 places the coactivator Cdh1 close to the APC2 cullin domain[11] (Figure A-7). In the middle of my PhD, structures at or near atomic resolution re-positioned Cdh1 close to the Tpr repeat regions of APC3 and APC7[12] (Figure A-7). These studies further revealed flexible, disordered regions in APC4 and APC2 that energized us to pursue mechanistic studies. Of note, the C-terminal sumoylation consensus site lysines are in a disordered region that is not resolved in any of the current structures. Whether SUMO medication of APC4 stabilizes this disordered region, and the verification of interactions with the SIM in APC2 is of key future interest. Furthermore, inhibitors of the APC/C for cancer therapeutics are currently in development[13,14]. It is of particular interest to determine if the sumoylation site on APC4 is a unique druggable target. Structural studies using cryo-EM will be one approach towards addressing these outstanding questions.

It is yet an unknown whether SUMO modification can also recruit specific substrates to the APC/C for ordered ubiquitylation and protein degradation. In an unbiased approach towards addressing whether sumoylated APC4 has unique affinities to soluble proteins, affinity chromatography using MBP-APC4 and MBP-APC4^{SUMO1} as bait with whole cell lysates was performed (Figure A6). Analysis from this experiment suggests that the SUMO-modified C-terminal tail of APC4 interacts with distinct proteins compared to unmodified APC4, and identification and characterization of these proteins will be an interesting avenue to pursue.

Chapter 3 proposes another mechanism of how the SUMO pathway "tunes up" inhibitory SAC signaling. First, we demonstrate that localization of the SUMO isopeptidase SENP1 to the nuclear pore complex during interphase is regulated by specific N-terminal sequences. Characterization by immunofluresence microscopy, supported by BioID analysis, indicate that SENP1$^{153-272}$ interacts with the Nup107 complex and SENP1$^{274-449}$ interacts with the Tpr subunit at the nuclear pore. Functional assays suggest that SENP1 interactions with Nup107 are required for normal mitotic exit, as SENP1 depletion results in delays during the metaphase-anaphase transition. SENP1 depletion also results in the accumulation of the SAC proteins Mad1 and Mad2 at the nuclear pore during interphase. This pre-assembled

checkpoint complex has been implicated in regulating mitotic timing[15]. Whether a distinct, soluble pool of checkpoint complexes are generated during interphase to fine tune APC/C activity is an area of future investigation. Gel filtration of whole cell lysates that separate soluble pre-assembled checkpoint complexes in control or SENP1 depleted cells is a key first step in pursuit of this mechanistic study.

SUMO modification is conserved from yeast to humans. While lower eukaryotes only express a single SUMO paralog, vertebrates express several SUMO isoforms[16]. Genetic knockouts of individual SUMO genes in mice demonstrate that SUMO1 and SUMO3 are dispensable, while SUMO2 is not[17,18]. This is due in part to the relative level of SUMO expression in mice; *Sumo3* mRNA only accounts for 2% of total *Sumo* mRNA in E7.5 and E8.5 mouse embryos, while *Sumo2* accounts for 80% of total *Sumo* mRNA[18]. Whether the relative expression levels of SUMO2 and SUMO3 in human cells is similar is yet unknown.

Broadly, work over the past decade has shed significant insights into how SUMO2/3 regulate mitotic progression, as discussed in Chapter 1 of this thesis. High throughput proteomic studies have already identified thousands of SUMO substrates, including those uniquely regulated during mitosis[19,20]. Of the thousands of SUMO substrates identified, a relatively

small fraction has been validated, and many defined molecular mechanisms support a model of sumoylation as "molecular Velcro[21]." However, future endeavors focused on additional SUMO substrates may lead to novel discoveries and new models of how sumoylation regulates cellular functions.

The APC/C is a molecular machine that is highly conserved in all eukaryotes, and the APC2 and APC4 subunits are also highly conserved. However, the sumoylation sites on the APC4 subunit of the APC/C are only conserved in vertebrates (Figure 3-4A). Interestingly, the SIM motif in the APC2 subunit are also only conserved in vertebrates (Figure 3-8B). This suggests that sumoylation of the APC4 subunit co-evolved with a receptor for SUMO, in the form of a SIM in the APC2 subunit. While work from this thesis suggests that SUMO modification of APC4 is critical for catalytic activity of the APC/C through non-covalent interactions with the cullin subunit, APC2, it is interesting to consider whether there are additional functional roles for sumoylated APC4. Specifically, whether the assembly of the APC/C, a multi-subunit E3 ligase, requires SUMO modification is an intriguing question to consider. The catalytic APC2/11 module has been previously shown to dissociate from the rest of the core APC/C under conditions of high salt or acidic pH[22]. Whether the entire catalytic arm is dynamically associating and dissociating from the APC/C is yet an

unanswered question, and whether SUMO modification of APC4 – which comprises part of the stable platform domain of the APC/C – is an intriguing question to consider. Finally, why eukaryotes require additional regulatory features in the mitotic apparatus, including additional kinases and components of the SUMO pathway, is an over-arching question. Perhaps the complexity of mitosis in vertebrates, or the requirement of mitotic fidelity to maintain longer lifespans in high order organisms, necessitates additional levels of regulation by post-translational modifications. Taken together, the vignettes of APC4 sumoylation in regulating metaphase-anaphase transitions, and the regulatory role of the SUMO pathway in regulating mitotic progression in human cells presented in this thesis, provide a glimpse of how higher order eukaryotes have adapted to this complex process.

REFERENCES

1. Collin, Nashchekina, Walker & Pines. The spindle assembly checkpoint works like a rheostat rather than a toggle switch. Nature Cell Biology 15, 1378–1385 (2013).

2. Mansfeld, Collin, Collins, Choudhary & Pines. APC15 drives the turnover of MCC-CDC20 to make the spindle assembly checkpoint responsive to kinetochore attachment. Nature Cell Biology 13, ncb2347 (2011).

3. Eytan et al. Disassembly of mitotic checkpoint complexes by the joint action of the AAA-ATPase TRIP13 and p31comet. Proceedings of the National Academy of Sciences 111, 12019–12024 (2014).

4. Weissmann et al. biGBac enables rapid gene assembly for the expression of large multisubunit protein complexes. Proceedings of the National Academy of Sciences 113, E2564–E2569 (2016).

5. Yamaguchi et al. Cryo-EM of Mitotic Checkpoint Complex-Bound APC/C Reveals Reciprocal and Conformational Regulation of Ubiquitin Ligation. Molecular Cell 63, 593–607 (2016).

6. Fujimitsu, Grimaldi & Yamano. Cyclin-dependent kinase 1–dependent activation of APC/C ubiquitin ligase. Science 352, 1121–1124 (2016).

7. Brown et al. Dual RING E3 Architectures Regulate Multiubiquitination and Ubiquitin Chain Elongation by APC/C. Cell 165, 1440–1453 (2016).

8. Alfieri et al. Molecular basis of APC/C regulation by the spindle assembly checkpoint. Nature 536, 431–436 (2016).

9. Zhang et al. Molecular mechanism of APC/C activation by mitotic phosphorylation. Nature 533, 260–264 (2016).

10. Qiao et al. Mechanism of APC/CCDC20 activation by mitotic phosphorylation. Proceedings of the National Academy of Sciences 113, E2570–E2578 (2016).

11. Dube et al. Localization of the Coactivator Cdh1 and the Cullin Subunit Apc2 in a Cryo-Electron Microscopy Model of Vertebrate APC/C. Molecular Cell 20, 867–879 (2005).

12. Chang, Zhang, Yang, McLaughlin & Barford. Atomic structure of the APC/C and its mechanism of protein ubiquitination. Nature 522, 450–454 (2015).

13. Zeng et al. Pharmacologic Inhibition of the Anaphase-Promoting Complex Induces A Spindle Checkpoint-Dependent Mitotic Arrest in the Absence of Spindle Damage. Cancer Cell 18, 382–395 (2010).

14. Lange et al. Defective sister chromatid cohesion is synthetically lethal with impaired APC/C function. Nature Communications 6, 8399 (2015).

15. Rodriguez-Bravo et al. Nuclear Pores Protect Genome Integrity by Assembling a Premitotic and Mad1-Dependent Anaphase Inhibitor. Cell 156, 1017–1031 (2014).

16. Melchior & Melchior. SUMO-NONCLASSICAL UBIQUITIN. Annual Review of Cell and Developmental Biology (2000). doi:10.1146/annurev.cellbio.16.1.591

17. Zhang et al. Sumo-1 Function Is Dispensable in Normal Mouse Development. Molecular and Cellular Biology 5381–5390 (2008). doi:10.1128/MCB.00651-08

18. Wang et al. SUMO2 is essential while SUMO3 is dispensable for mouse embryonic development. EMBO reports 878–885 (2014). doi:10.15252/embr.201438534

19. Schimmel et al. Uncovering SUMOylation Dynamics during Cell-Cycle Progression Reveals FoxM1 as a Key Mitotic SUMO Target Protein. Molecular Cell 53, 1053–1066 (2014).

20. Cubeñas-Potts et al. Identification of SUMO-2/3-modified proteins associated with mitotic chromosomes. Proteomics 15, 763–72 (2015).

21. Newman et al. A high throughput mutagenic analysis of yeast sumo

structure and function. PLOS Genetics 13, e1006612 (2017).

22. Vodermaier, Gieffers, Maurer-Stroh, Eisenhaber & Peters. TPR Subunits of the Anaphase-Promoting Complex Mediate Binding to the Activator Protein CDH1. Current Biology 13, 1459–1468 (2003).

Christine C. Lee

Department of Biochemistry & Molecular Biology
Johns Hopkins Bloomberg School of Public Health
615 N. Wolfe St. W8104-2, Baltimore, MD 21205
e-mail: clee217@jhu.edu / yourchristinelee@gmail.com
cell: (704) 661-5555

Education

Johns Hopkins University **Ph.D., December 2017**
Department of Biochemistry & Molecular Biology
Michael J. Matunis, Ph.D., Advisor..
Thesis: *Characterization of the SUMO Pathway in Regulating Mitotic Progression*

University of Chicago **B.A., May 2009**
Department of Public Policy Studies
Thesis: *Tuberculosis Public Health Policy in the United States*

Research Experience

Graduate Student, Johns Hopkins Bloomberg School of Public Health 2012-2017
Department of Biochemistry & Molecular Biology
Advisor: Michael J., Matunis, Ph.D.
Characterized a molecular mechanism by which SUMO modification of a ubiquitin E3 ligase, known as the Anaphase Promoting Complex/Cyclosome, regulates mitotic exit in human cancer cells.

Research Technician, University of Chicago Medical Center 2009-2012
Department of Pathology, Clinical Chemistry Research Laboratories
Advisor: K.T. Jerry Yeo, Ph.D., DABCC, FACB
Performed method development and validation for a clinical pharmacogenetics program. This study validated a rapid chip-based genotyping platform for detecting polymorphisms in the CYP2C19 gene, known to affect differential drug metabolism in patients from diverse ethnic backgrounds. Created, managed, and executed IRB protocols for clinical trials. Supported method development for detecting pheromones using LC-MS/MS.

Jeff Metcalf Fellow, The Field Museum 2008
Pritzker Laboratory for Molecular Systematics & Evolution
Advisors: Kentaro Hosaka, Ph.D., Gregory Mueller, Ph.D.
Performed nucleotide sequencing analysis of specimens collected from over 30 countries of model fungal ectomycorrhizal genus *Laccaria*. These data were used for molecular dating analysis and estimating diversification rates in the genus.

Fellowships, Honors, and Awards

2017	Frederik B. Bang Award, Johns Hopkins Bloomberg School of Public Health
2016-2017	Elsa Orent Keiles Fellowship, Johns Hopkins Bloomberg School of Public Health
2016	First Place, Sweren Student Book Collecting Contest, Johns Hopkins University
2012-2015	National Institutes of Health Training Grant: T32 CA009110-038
2011	American Association of Clinical Chemistry Educational Grant; Atlanta, GA
2008	Jeff Metcalf Fellowship; The Field Museum of Natural History; Chicago, IL

Publications

Peer Reviewed Manuscripts

1. **Lee C**, Li B, Yu H, Matunis MJ. Sumoylation Promotes Optimal APC/C Activation and Timely Anaphase. *Under revision at eLife.*
2. Cubeñas-Potts C, Srikumar T, **Lee C**, Osula O, Subramonian D, Zhang SC, Cotter RJ, Raught B, Matunis MJ. Identification of SUMO-2/3 modified proteins associated with mitotic chromosomes. *Proteomics.* 2015 Feb;15(4):763-72.
3. Leung EKY, Sheu FYB, **Lee CC**, Gay T, Ourada S, Yeo KTJ. Clinical Evaluation of the Enterprise Point of Care for Blood Gas Electrolytes and Metabolites. *Point of Care*. 2013 Sept;12:127-133.
4. Westerhoff M, Hovan L, **Lee c**, Hart J. Effects of dropping the requirement for goblet cells from the diagnosis of Barrett's esophagus. *Clin Gastroenterol Heptal.* 2012 Nov;10(11)1232-6.
5. Babic N, Zibrat S, Gordon IO, **Lee CC**, Yeo KT. Effect of blood collection tubes on the incidence of artefactual hyperkalemia on patient samples from an outreach clinic. *Clin Chim Acta*. 2012 Oct 9;413(12-20):1454-8.
6. **Lee CC**, McMillin GA, Babic N, Melis R, Yeo KT. Evaluation of a CYP2C19 genotype panel on the GenMark eSensor platform and the comparison to the Autogenomics Infiniti and Luminex CYP2C19 panels. *Clin Chim Acta*. 2011 May 12;412:1133-7.

News and Reviews

7. **Lee CC,** Matunis MK. Resolving chromatin bridges with SIMs, SUMOs, and PICH. *Cell cycle*. 2016 Oct;15(19):2547-48.

Contributor, *ASBMB Today*

8. **Lee C.** (2016, Dec) "Metformin reverses metabolic memory in a diabetes model."
9. **Lee C.** (2016, Apr.) "TREM2 defects linked to neurodegeneration."
10. **Lee C.** (2015, Oct.) "Actions of iron-dependent dioxygenases."

Presentations

Invited Talks

1. 2017 ASCB Mid-Atlantic Mitosis Meeting, *National Institutes of Health, Bethesda, MD.*
2. 2015 Mid-Atlantic Mitosis Meeting, *National Institutes of Health, Bethesda, MD.*
3. 2014 Mid-Atlantic Mitosis Meeting, *National Institutes of Health, Bethesda, MD.*

Poster Presentations

1. 2016 Cell Cycle Meeting, Cold Spring Harbor Laboratories, NY. **Lee C**, Matunis MJ. Characterizing the role of the SUMO protease, SENP1, during mitosis.

2. 2014 Nuclear Organization and Function Meeting, Cold Spring Harbor Laboratories, NY. **Lee C**, Cubeñas-Potts C, Raught B, Matunis MJ. Control of the Spindle Assembly Checkpoint by the SUMO Protease, SENP1.
3. 2013 American Association of Clinical Chemistry Annual Meeting, *Houston, TX*. Yi X, Leung EK, Kern DW, McClintock MK, **Lee CC**, Yeo KTJ. Development of an LC-MS/MS method for the quantitation of serum Androsta-4, 16, -dien-3-one
4. 2013 American Association of Clinical Chemistry Annual Meeting, *Houston, TX.* Leung EK, Krastins B, Lopez MF, Yi X, **Lee CC**, Grogan R, Angelos P, Kaplan EL, Yeo KTJ. Use of coupled mass spectrometric immunoassay-selective reaction monitoring (MSIA-SRM) to measure PTH and variants during intraoperative parathyroidectomy.
5. 2012 American Association of Clinical Chemistry Annual Meeting, *Anaheim, CA*. **Lee C**, Angelos P, Kaplan EL, Zibrat SJ, Toney L, Helke J, Babic N, Yeo KTJ. Clinical Impacts of Differences in Intra-Operative Parathyroid Hormone Assays.
6. 2011 American Association of Clinical Chemistry Annual Meeting, *Atlanta, GA*. **Lee CC**, McMillin GA, Babic N, Melis R, Yeo KT. Evaluation of a CYP2C19 genotype panel on the GenMark eSensor platform and the comparison to the Autogenomics Infiniti and Luminex CYP2C19 panels.

Teaching & Leadership Experience

Journal Club Coordinator
2016-2017
Johns Hopkins Bloomberg School of Public Health,
Dept. of Biochemistry & Molecular Biology

Teaching Assistant, Principles of Cell Biology
2015-2017
Johns Hopkins Bloomberg School of Public Health
Dept. of Biochemistry & Molecular Biology

Instructor, Collaborative Learning in Chemistry
2007-2009
University of Chicago
Dept. of Chemistry

Skills

Laboratory skills in biochemistry, molecular, and cell biology: Recombinant Protein Purification, PCR, Western Analysis, Gel Electrophoresis, Molecular Cloning, Immunopurification, Fixed Cell Immunofluresence Microscopy, Timelapse Live Cell Microscopy, Lentiviral Transduction

Experienced using: Adobe Illustrator, Adobe Photoshop, MS Office Suite, PyMOL